AD NUMBER
AD903922
LIMITATION CHANGES
TO: **Approved for public release; distribution is unlimited.**
FROM: **Distribution authorized to U.S. Gov't. agencies only; Test and Evaluation; OCT 1972. Other requests shall be referred to Air Force Armament Lab., Eglin AFB, FL.**
AUTHORITY
AFATL ltr 23 Jan 1976

AEDC-TR-72-146
AFATL-TR-72-193

Cy 2

SEPARATION CHARACTERISTICS OF SIX STORES FROM THE A-7D AIRCRAFT AT MACH NUMBERS FROM 0.325 TO 0.814

Willard E. Summers

ARO, Inc.

October 1972

PROPULSION WIND TUNNEL FACILITY
ARNOLD ENGINEERING DEVELOPMENT CENTER
AIR FORCE SYSTEMS COMMAND
ARNOLD AIR FORCE STATION, TENNESSEE

Prope[illegible] Force
[illegible]
F40600-73-C-0004

NOTICES

When U. S. Government drawings specifications, or other data are used for any purpose other than a definitely related Government procurement operation, the Government thereby incurs no responsibility nor any obligation whatsoever, and the fact that the Government may have formulated, furnished, or in any way supplied the said drawings, specifications, or other data, is not to be regarded by implication or otherwise, or in any manner licensing the holder or any other person or corporation, or conveying any rights or permission to manufacture, use, or sell any patented invention that may in any way be related thereto.

Qualified users may obtain copies of this report from the Defense Documentation Center.

References to named commercial products in this report are not to be considered in any sense as an endorsement of the product by the United States Air Force or the Government.

SEPARATION CHARACTERISTICS OF SIX STORES FROM THE A-7D AIRCRAFT AT MACH NUMBERS FROM 0.325 TO 0.814

Willard E. Summers
ARO, Inc.

FOREWORD

The work reported herein was sponsored by the Air Force Armament Laboratory (DLGC/Lt S. C. Braud), Air Force Systems Command (AFSC), under Program Element 27121F, System 337A.

The test results presented were obtained by ARO, Inc. (a subsidiary of Sverdrup & Parcel and Associates, Inc.), contract operator of the Arnold Engineering Development Center (AEDC), AFSC, Arnold Air Force Station, Tennessee, under Contract F40600-73-C-0004. The test was conducted from June 21 to 27, 1972, under ARO Project No. PA033. The manuscript was submitted for publication on July 28, 1972.

This technical report has been reviewed and is approved.

L. R. KISSLING
Lt Colonel, USAF
Chief Air Force Test Director, PWT
Directorate of Test

A. L. COAPMAN
Colonel, USAF
Director of Test

ABSTRACT

Wind tunnel captive trajectory tests were conducted in the Aerodynamic Wind Tunnel (4T) to investigate the separation characteristics of six stores from the wing pylons and racks of the A-7D aircraft. The stores tested represented possible combinations of munitions to be carried by the A-7D when performing search and rescue missions. Separation trajectory data were obtained for the loaded and expended SUU-23/A gun pod, CBU-12A/A, CBU-46/A, LAU-3/A, LAU-68A/A, and the expended CBU-30/A. Trajectories were obtained at Mach numbers from 0.325 to 0.814 with aircraft angle of attack corresponding to level flight at 4000-ft altitude. For selected configurations, data were obtained to assess the influence of changes in the applied ejector forces during separation from the MAU-12B/A pylon rack. The stores separated without contacting the aircraft with only two exceptions. Store-to-pylon contact occurred for the expended SUU-23/A at one Mach number/ejector force combination, and the expended LAU-3/A contacted the triple ejection rack for one configuration at one Mach number.

CONTENTS

APPENDIXES

I. ILLUSTRATIONS

Figure

Figure Page

II. TABLES

NOMENCLATURE

BL	Aircraft buttock line from plane of symmetry, in., model scale
b	Store reference dimension, ft, full scale
C_A	Store axial-force coefficient, axial force/$q_\infty S$
C_ℓ	Store rolling-moment coefficient, rolling moment/$q_\infty Sb$
C_{ℓ_p}	Store roll-damping derivative, $dC_\ell/d(pb/2V_\infty)$
C_m	Store pitching-moment coefficient, referenced to the store cg, pitching moment/$q_\infty Sb$
C_{m_q}	Store pitch-damping derivative, $dC_m/d(qb/2V_\infty)$
C_n	Store yawing-moment coefficient, referenced to the store cg, yawing moment/$q_\infty Sb$
C_{n_r}	Store yaw-damping derivative, $dC_n/d(rb/2V_\infty)$
FS	Aircraft fuselage station, in., model scale

F_Z	TER ejector force, lb
F_{Z_1}	Pylon forward ejector force, lb
F_{Z_2}	Pylon aft ejector force, lb
H	Pressure altitude, ft
I_{xx}	Full-scale moment of inertia about the store X_B axis, slug-ft^2
I_{yy}	Full-scale moment of inertia about the store Y_B axis, slug-ft^2
I_{zz}	Full-scale moment of inertia about the store Z_B axis, slug-ft^2
M_∞	Free-stream Mach number
$\overline{m}$	Full-scale store mass, slugs
p	Store angular velocity about the X_B axis, radians/sec
p_∞	Free-stream static pressure, psfa
q	Store angular velocity about the Y_B axis, radians/sec
q_∞	Free-stream dynamic pressure, psf
r	Store angular velocity about the Z_B axis, radians/sec
S	Store reference area, ft^2, full scale
t	Real trajectory time from initiation of trajectory, sec
V_∞	Free-stream velocity, ft/sec
WL	Aircraft waterline from reference horizontal plane, in., model scale
X	Separation distance of the store cg parallel to the flight axis system X_F direction, ft, full scale measured from the prelaunch position
X_{cg}	Full-scale cg location, ft, from nose of store
X_L	Ejector piston location relative to the store cg, positive forward of store cg, ft, full scale
X_{L_1}	Forward ejector piston location relative to the store cg, positive forward of store cg, ft, full scale

X_{L_2} Aft ejector piston location relative to the store cg, positive forward of store cg, ft, full scale

Y Separation distance of the store cg parallel to the flight axis system Y_F direction, ft, full scale measured from the prelaunch position

Z Separation distance of the store cg parallel to the flight-axis system Z_F direction, ft, full scale measured from the prelaunch position

Z_{cg} Full-scale cg location relative to the store lower surface for the CBU-30/A store only, ft. The cg for all other stores was on the store longitudinal axis.

ZE Ejector stroke length, ft, full scale

α Parent-aircraft model angle of attack relative to the free-stream velocity vector, deg

θ Angle between the store longitudinal axis and its projection in the X_F-Y_F plane, positive when store nose is raised as seen by pilot, deg

ψ Angle between the projection of the store longitudinal axis in the X_F-Y_F plane and the X_F axis, positive when the store nose is to the right as seen by the pilot, deg

FLIGHT-AXIS SYSTEM COORDINATES

Directions

X_F Parallel to the free-stream wind vector, positive direction is forward as seen by the pilot

Y_F Perpendicular to the X_F and Z_F directions, positive direction is to the right as seen by the pilot

Z_F In the aircraft plane of symmetry, perpendicular to the free-stream wind vector, positive direction is downward

The flight-axis system origin is coincident with the aircraft cg and remains fixed with respect to the parent aircraft during store separation. The X_F, Y_F, and Z_F coordinate axes do not rotate with respect to the initial flight direction and attitude.

STORE BODY-AXIS SYSTEM COORDINATES

Directions

X_B Parallel to the store longitudinal axis, positive direction is upstream in the prelaunch position

Y_B Perpendicular to the store longitudinal axis, and parallel to the flight-axis system X_F-Y_F plane when the store is at zero roll angle, positive direction is to the right looking upstream when the store is at zero yaw and roll angles

Z_B Perpendicular to both the X_B and Y_B axes, positive direction is downward as seen by the pilot when the store is at zero pitch and roll angles

The store body-axis system origin is coincident with the store cg and moves with the store during separation from the parent airplane. The X_B, Y_B, and Z_B coordinate axes rotate with the store in pitch, yaw and roll so that mass moments of inertia about the three axes are not time-varying quantities.

SECTION I
INTRODUCTION

Included in the possible mission capabilities of the A-7D aircraft is its use in support of search and rescue operations. During these missions, the external munitions carried can be significantly different from those carried for other support and interdiction missions. The purpose of the present test was to investigate separation characteristics of some external stores that might be carried by the A-7D when performing in the search and rescue role.

Separation trajectory data were obtained for the loaded and expended SUU-23/A gun pod, CBU-12A/A, CBU-46/A, LAU-3/A, and LAU-68A/A and for the expended CBU-30/A. Trajectories were obtained to assess the influence on store separation resulting from changes in Mach number, adjacent store loadings, and ejector forces.

Testing was accomplished in the Aerodynamic Wind Tunnel (4T) using 0.05-scale models of the A-7D aircraft and the stores. The A-7D model was mounted on the main tunnel support system, and the store models were mounted on the captive trajectory support (CTS). Separation trajectories were obtained from the wing pylons or racks of the A-7D at conditions simulating level flight at Mach numbers from 0.325 to 0.814 at 4000-ft altitude.

SECTION II
APPARATUS

2.1 TEST FACILITY

The Aerodynamic Wind Tunnel (4T) is a closed-loop, continuous-flow, variable-density tunnel in which the Mach number can be varied from 0.1 to 1.3. At all Mach numbers, the stagnation pressure can be varied from 300 to 3700 psfa. The test section is 4 ft square and 12.5 ft long with perforated, variable porosity (0.5- to 10-percent open) walls. It is completely enclosed in a plenum chamber from which the air can be evacuated, allowing part of the tunnel airflow to be removed through the perforated walls of the test section.

For store separation testing, two separate and independent support systems are used to support the models. The parent aircraft model is inverted in the test section and supported by an offset sting attached to the main pitch sector. The store model is supported by the CTS which extends down from the tunnel top wall and provides store movement (six degrees of freedom) independent of the parent-aircraft model. An isometric drawing of a typical store separation installation is shown in Fig. 1 (Appendix I).

Also shown in Fig. 1 is a block diagram of the computer control loop used during captive trajectory testing. The analog system and the digital computer work are an integrated unit and, utilizing required input information, control the store movement during a trajectory. Store positioning is accomplished by use of six individual d-c electric motors. Maximum translational travel of the CTS is ±15 in. from the tunnel centerline in the lateral and vertical directions and 36 in. in the axial direction. Maximum angular

displacements are ±45 deg in pitch and yaw and ±360 deg in roll. A more complete description of the test facility can be found in the Test Facilities Handbook.[1] A schematic showing the test section details and the location of the models in the tunnel is shown in Fig. 2.

2.2 TEST ARTICLES

The test articles used were 0.05-scale models of the stores and the A-7D aircraft (including pylons, racks, and dummy models used for configuration loading). The A-7D model was geometrically similar to the full-scale airplane except for some modifications incident to the wind tunnel installation and CTS operation. A sketch of the A-7D model showing basic dimensions and location of the wing pylon stations is shown in Fig. 3. Dimensions of the wing pylons are presented in Fig. 4. When installed on the aircraft, all pylon surfaces for store and rack mounting are at a 3-deg nose down attitude with respect to the aircraft waterline. Triple ejection rack (TER) and multiple ejection rack (MER) details are shown in Figs. 5 and 6, respectively. These racks were mounted on the pylons at a position corresponding to the 30-in. lug attachment. Details of the dummy MK-82 snakeye and 300-gal fuel tank models (used for configuration loading) are presented in Figs. 7 and 8.

Details and dimensions of the SUU-23/A, CBU-12A/A and CBU-46/A, LAU-3/A, CBU-30/A, and LAU-68A/A are shown in Figs. 9 through 13, respectively. These models were geometrically similar to the full-scale stores except for slight modifications to the SUU-23/A, expended LAU-3/A, and expended LAU-68A/A necesssary to allow for attachment to the internal balance. The aft fairing of the SUU-23/A was truncated; flow-through rocket tube simulation was not possible for the expended LAU-3/A; and the rocket tubes were partially blocked for the expended LAU-68A/A. Except as noted in Figs. 9 through 13, geometry of the dummy models was the same as for the sting-mounted models.

The A-7D aircraft model was inverted in the tunnel and attached by an offset sting to the main sting-support system. Store models were mounted on an internal strain-gage balance that was attached to the CTS system. A photograph showing a typical A-7D CTS installation in the tunnel is shown in Fig. 14.

2.3 INSTRUMENTATION

Three internal strain-gage balances were used during the test. A 0.75-in.-diam, 6-component balance was used for tests with the SUU-23/A; a 0.16-in.-diam, 4-component balance was used for tests with the LAU-68A/A; and a 0.40-in. diam, 6-component balance was used for tests with the CBU-12A/A, CBU-46/A, CBU-30/A, and LAU-3/A. Translational and angular positions of the store models were obtained from the CTS analog outputs. The aircraft angle of attack was set using the main sting support and digital readout system.

---

[1] Test Facilities Handbook (Ninth Edition). "Propulsion Wind Tunnel Facility, Vol. 4." Arnold Engineering Development Center, July 1971.

The pylons and racks were instrumented with spring-loaded plungers (touch wires) which were electrically connected to give a visual indication on the control console when the store contacted the touch wire at the carriage position. The CTS system was also electrically connected to automatically stop the CTS movement if the store model or CTS contacted the aircraft model, aircraft support sting, or the test section walls.

SECTION III
TEST DESCRIPTION

3.1 TEST CONDITIONS

Separation trajectory data were obtained at Mach numbers from 0.325 to 0.814. Tunnel dynamic pressure ranged from 250 psf at $M_\infty = 0.325$ to 500 psf for $M_\infty \geq 0.489$, and tunnel stagnation temperature was maintained near 110°F.

Tunnel conditions were held constant at the desired Mach number and stagnation pressure while data for each trajectory were obtained. In general, termination of the trajectories resulted from store sting-to-aircraft contact or reaching a CTS travel limit.

3.2 TRAJECTORY DATA ACQUISITION

To obtain a trajectory, test conditions were established in the tunnel, and the parent model was positioned at the desired angle of attack. The store model was then oriented to a position corresponding to the store carriage location. After the store was set at the desired initial position, operational control of the CTS was switched to the digital computer which controlled the store movement during the trajectory through commands to the CTS analog system (see block diagram, Fig. 1). Data from the wind tunnel, consisting of measured model forces and moments, wind tunnel operating conditions, and CTS rig positions, were input to the digital computer for use in the full-scale trajectory calculations.

The digital computer was programmed to solve the six-degree-of-freedom equations to calculate the angular and linear displacements of the store relative to the parent aircraft pylon. In general, the program involves using the last two successive measured values of each static aerodynamic coefficient to predict the magnitude of the coefficients over the next time interval of the trajectory. These predicted values are used to calculate the new position and attitude of the store at the end of the time interval. The CTS is then commanded to move the store model to this new position, and the aerodynamic loads are measured. If these new measurements agree with the predicted values, the process is continued over another time interval of the same magnitude. If the measured and predicted values do not agree within the desired precision, the calculation is repeated over a time interval one-half the previous value. This process is repeated until a complete trajectory has been obtained.

In applying the wind tunnel data to the calculations of the full-scale store trajectories, the measured forces and moments are reduced to coefficient form and then applied with proper full-scale store dimensions and flight dynamic pressure. Dynamic pressure was calculated using a flight velocity equal to the free-stream velocity component plus the components of store velocity relative to the aircraft and a density corresponding to the simulated altitude.

The initial portion of each launch trajectory incorporated simulated ejector forces in addition to the measured aerodynamic forces acting on the store. For all trajectories, the ejector force was simulated using a constant force applied throughout the time interval when the ejector piston was extending to its maximum stroke. Identification of the ejector forces used for the stores is presented in Table I (Appendix II). The ejector forces were considered to act perpendicular to the rack or pylon mounting surface. The locations of the applied ejector forces and other full-scale store parameters used in the trajectory calculations are listed in Table II.

3.3 CORRECTIONS

Balance, sting, and support deflections caused by the aerodynamic loads on the store models were accounted for in the data reduction program to calculate the true store-model angles. Corrections were also made for model weight tares to calculate the net aerodynamic forces on the store model.

3.4 PRECISION OF DATA

The trajectory data are subject to error resulting from uncertainties in tunnel conditions, balance measurements, extrapolation tolerances, and CTS positioning control. Maximum error in the CTS position control was ±0.05 in. for translational settings and ±0.15 deg for angular displacements in pitch and yaw. Extrapolation tolerances were ±0.1 for all aerodynamic coefficients. Based on a 95-percent confidence level, and ignoring bias errors, the uncertainties in the full-scale trajectory data resulting from balance precision limitations were calculated and are presented in Table III.

Some trajectories were repeated during the test, and a review of these data (for the loaded and expended SUU-23/A and loaded LAU-3/A) shows that the differences in the repeat data are less than the uncertainties quoted in Table III.

Estimated uncertainty in setting Mach number was ±0.003, and the uncertainty in aircraft model angle of attack was estimated to be ±0.1 deg.

SECTION IV
RESULTS AND DISCUSSION

Separation trajectory data were obtained for the SUU-23/A, CBU-12A/A, CBU-46/A, LAU-3/A, CBU-30/A, and LAU-68A/A stores when ejected from the A-7D aircraft. Data showing the linear displacements of the store cg relative to the carriage position and the angular displacements relative to the flight-axis coordinate system are presented as functions of full-scale trajectory time. Positive X, Y, and Z displacements (as seen by the pilot) are forward, to the right and down, respectively. Positive changes in θ and ψ (as seen by the pilot) are nose-up and nose-right, respectively. Identification of the simulated ejector forces used during the test is given in Table I, and full-scale store parameters used in the trajectory calculations are presented in Table II. Note that the axial-force coefficient was an input parameter for the LAU-68A/A stores. This was necessary because the internal balance used during the LAU-68A/A testing did not have an axial-force gage. The axial-force coefficients used were estimated from existing data on similar models.

Aircraft wing loading configurations are identified in Table IV. Identification of the TER and MER stations used in Table IV is given in Fig. 15.

Termination of the trajectories was generally a result of the store-support sting contacting the aircraft wing on the CTS reaching a travel limit. In some cases, as noted, termination of the trajectories resulted from the separating store contacting the TER or pylon.

4.1 SUU-23/A DATA

Separation trajectory data were obtained for both the loaded and expended SUU-23/A gun pod and are presented in Figs. 16 and 17, respectively. These data show the trajectories for the store at Mach number/angle of attack combinations representing level flight at a simulated altitude of 4000 ft. The loaded store experienced a nose-down pitch motion at all Mach numbers, with nose-down pitch increasing with increasing Mach number. At the lower Mach numbers, the expended store trajectories indicate a nose-up pitch, with nose-down pitch occurring at the higher Mach numbers (M_∞ = 0.569 or above).

The presence of adjacent stores produced little effect on the store translation and pitch motions (comparing configurations 1L and 1R). However, some effect is noted in yaw at the higher Mach numbers.

Effects on the trajectories resulting from changes in the ejector force are shown in Figs. 18 and 19 for the loaded and expended SUU-23/A, respectively. The effect of applying force at both ejector pistons (ejector force 2 and 4) was to increase the store vertical translation and produce a positive change in the pitch rate.

Possible store-to-aircraft contact occurred for only one of the trajectories presented in Figs. 16 through 19. Apparent store-to-pylon contact occurred for the expended store at M_∞ = 0.569 with ejector force 2 (Fig. 19).

4.2 CBU-12A/A AND CBU-46/A DATA

Trajectory data were obtained for the loaded CBU-12A/A and CBU-46/A and for the expended CBU-12A/A or CBU-46/A. External geometry was the same for these models, so that the differences in trajectory data for these stores are a result of changes in store mass, inertia, and ejector force. Trajectory data for the loaded CBU-12A/A and CBU-46/A are presented in Figs. 20 and 21, respectively. Data for the expended store are presented in Figs. 22.

Data for the CBU-12A/A and CBU-46/A (Figs. 20 and 21) are very similar for corresponding test configurations. In all cases, the stores show a tendency to nose-down pitch as the Mach number increases. The effect on the trajectories resulting from changing the ejector force for store release from the pylon can be seen by comparing Figs. 21c and d. Only small changes are indicated, especially at the higher Mach number. A comparison of Figs. 21b and e shows the effect of the presence of the CBU-30/A store on the center pylon. The largest effect shown is an increased outboard yaw when the store was present, and the effect is fairly small.

Data for the expended store (Fig. 22) show much larger pitch and yaw motions than for the loaded stores. The expended store exhibits a rather large nose-up pitch motion at the lower Mach numbers when ejected from the TER. A comparison of Figs. 22c and d shows that the change in ejector force increased the store nose-up pitch at the low Mach number and produced little effect at the high Mach number. Presence of the CBU-30/A on the center pylon produced essentially the same effect for the expended store (Figs. 22b and e) as was shown for the loaded store. No store-to-parent contact occurred during trajectories for these stores.

4.3 LAU-3/A DATA

Trajectory data were obtained for both the loaded and expended LAU-3/A for various store load configurations. Data for the loaded LAU-3/A are presented in Fig. 23, and data for the expended LAU-3/A are presented in Fig. 24.

Trajectory data for the loaded LAU-3/A (Fig. 23) show that, when separating from the No. 1 TER position (Figs. 23d, e, and g), the store tends to pitch nose up for Mach numbers somewhat less than 0.569, with nose-down pitch indicated for the higher Mach numbers. For separation from the TER shoulder stations (Figs. 23a, b, c, f, and h), the nose-up pitch tendency persists to slighty greater Mach numbers. In general, the store yawed nose outboard with only small lateral movement when separating from the No. 1 TER position, whereas the store yawed nose toward the TER and moved laterally away from the TER when separating from the TER shoulder stations.

Trajectories for the loaded LAU-3/A from the aircraft pylons (Figs. 23i and j) show that the store tended to pitch nose down at all Mach numbers. The store yaw was, in general, nose outboard with little store lateral movement.

Trajectory data for the expended LAU-3/A (Fig. 24) indicate a nose-down pitch tendency for all trajectories. For separations from the No. 1 TER position (Figs. 24a, f, h, and i), the store tends to yaw nose inboard (except for small outboard yaw for configuration 19R when the store was in the 300 gal tank flow field) with only small lateral translation. During all trajectories from the TER shoulder stations (Figs. 24b, c, d, e, g, and j), the store yawed nose away from the TER, and the store moved laterally away from the TER. These angular motions are opposite to those shown for the loaded LAU-3/A. A significant effect on store axial movement is shown with Mach number variation for all of the expended LAU-3/A data.

Trajectory data for the expended LAU-3/A from the aircraft pylons (Figs. 24k through r) show that the store experiences a large nose-down pitch rate at all Mach numbers. Changes in the ejector force (Figs. 24m, n, o, and p) produced little effect on the separation characteristics. No store-to-parent contact occurred during the trajectories except for one trajectory for the expended store (Fig. 24i) when the aft end of the store apparently contacted the TER.

4.4 CBU-30/A DATA

Trajectory data were obtained only for the expended CBU-30/A separating from the aircraft pylons. These data are presented in Fig. 25. Here again, a rapid nose-down pitch is indicated at the higher Mach number, and the store yawed outboard with very little Mach number effect. The presence of the 300-gal fuel tanks on the inboard and outboard pylons produced only small effects on the trajectories. No store-to-aircraft contact occurred during these trajectories.

4.5 LAU-68A/A DATA

Trajectory data for the loaded and expended LAU-68A/A stores are presented in Figs. 26 and 27, respectively. Separation characteristics for the loaded and expended stores were similar, with the angular motions somewhat greater for the expended store. Also, axial translation for the expended LAU-68A/A varied more with Mach number than for the loaded store. With the exception of the store launches from the TER inboard shoulder station at M_∞ = 0.407, all trajectories showed a nose-down pitch. From the No. 1 TER position and the pylon, the stores yawed outboard with little lateral translation. The stores yawed nose away from the TER with lateral movement away from the TER for all launches from the TER shoulder stations. No store-to-aircraft contact occurred during these trajectories.

APPENDIXES

I. ILLUSTRATIONS
II. TABLES

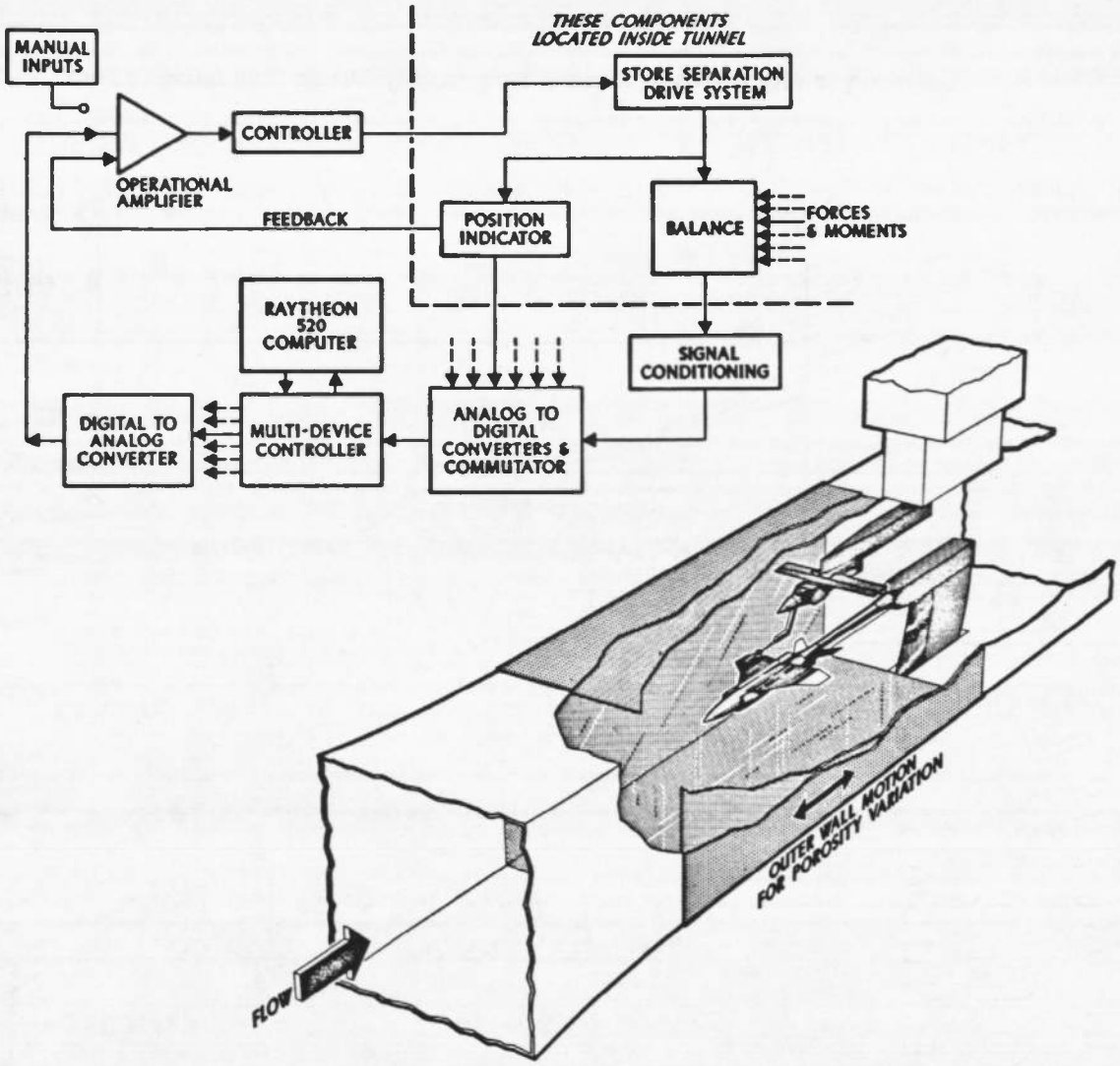

Fig. 1 Isometric Drawing of a Typical Store Separation Installation and a Block Diagram of the Computer Control Loop

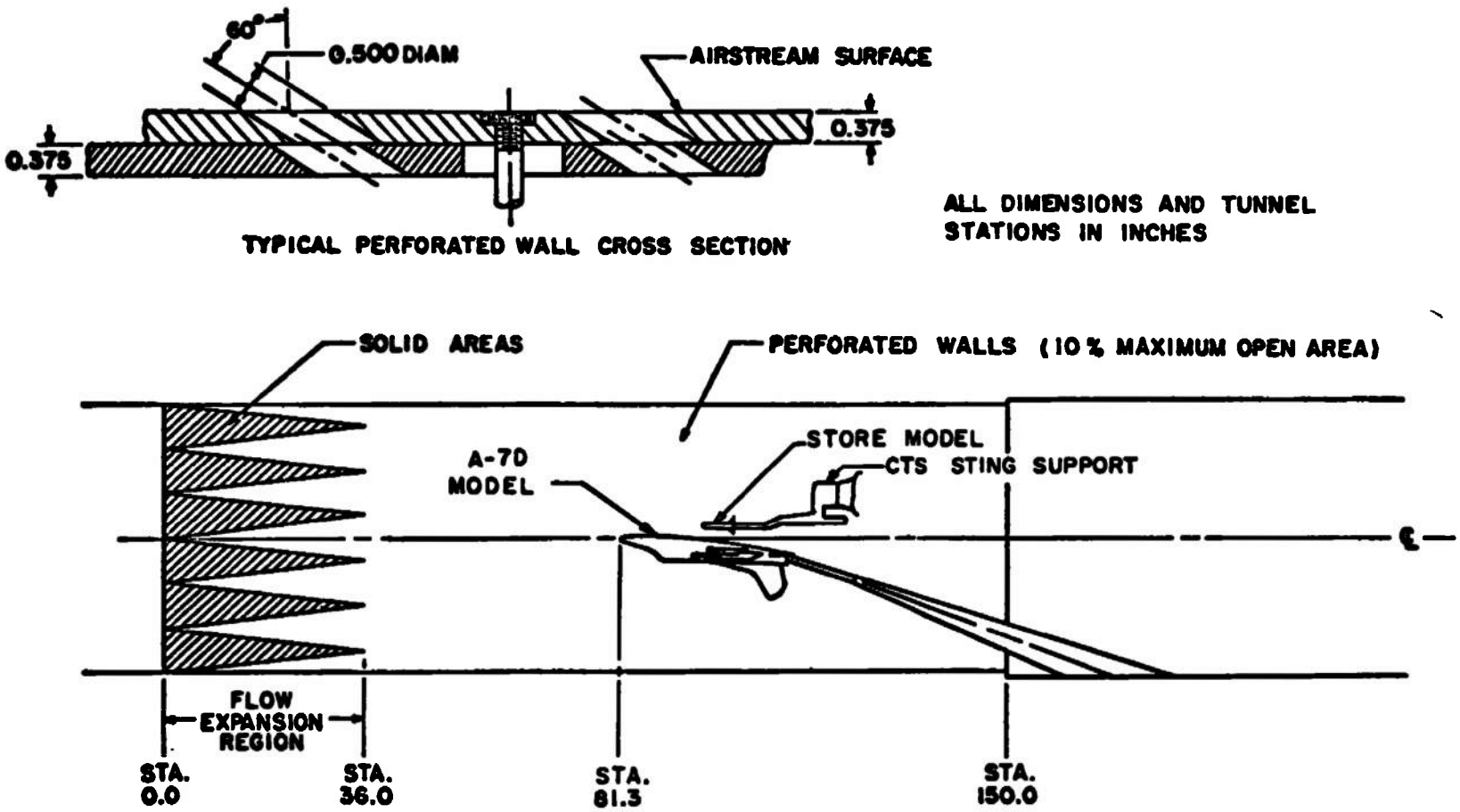

Fig. 2 Schematic of the Tunnel Test Section Showing Model Location

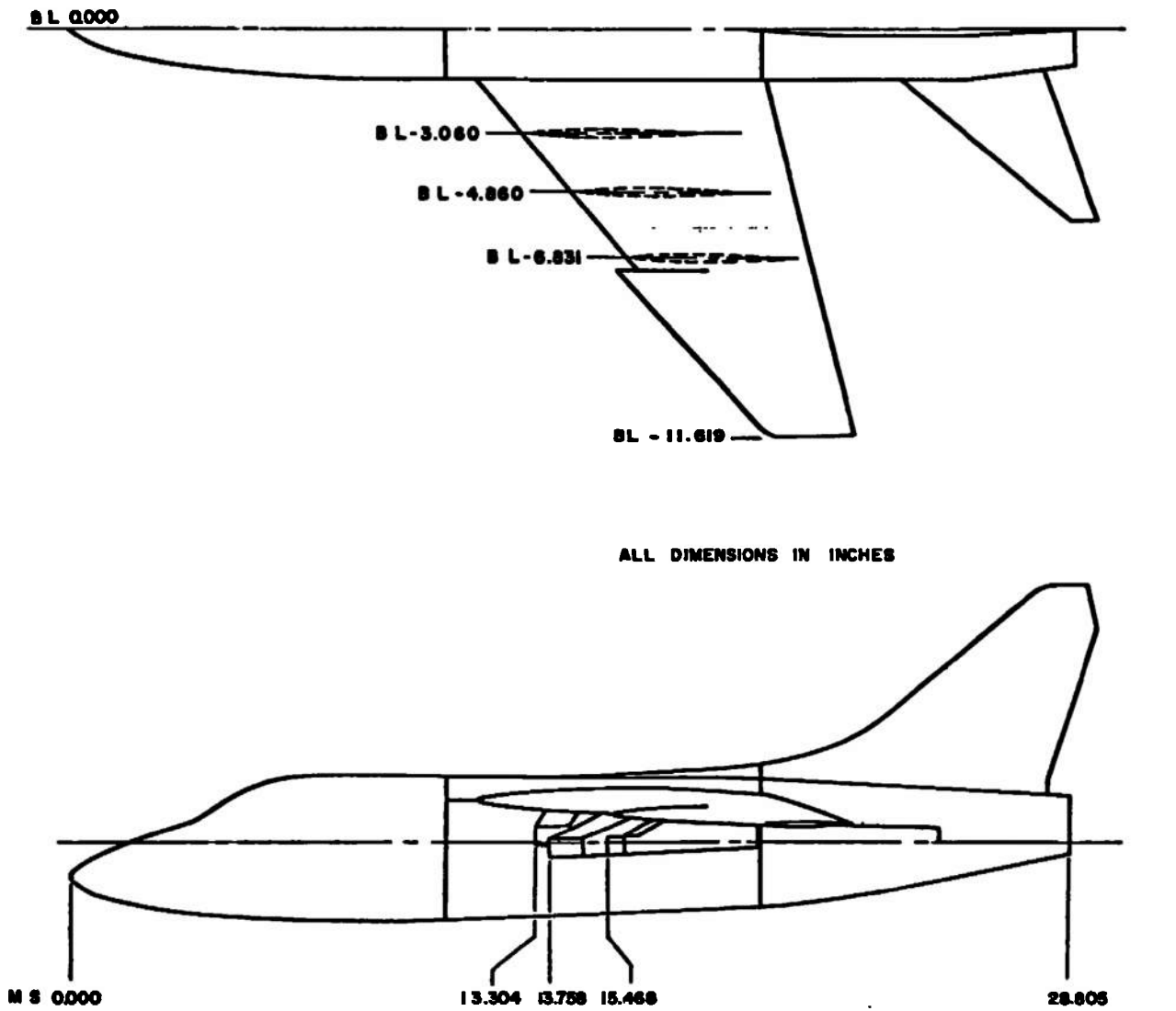

Fig. 3 Sketch of the A-7D Aircraft Model

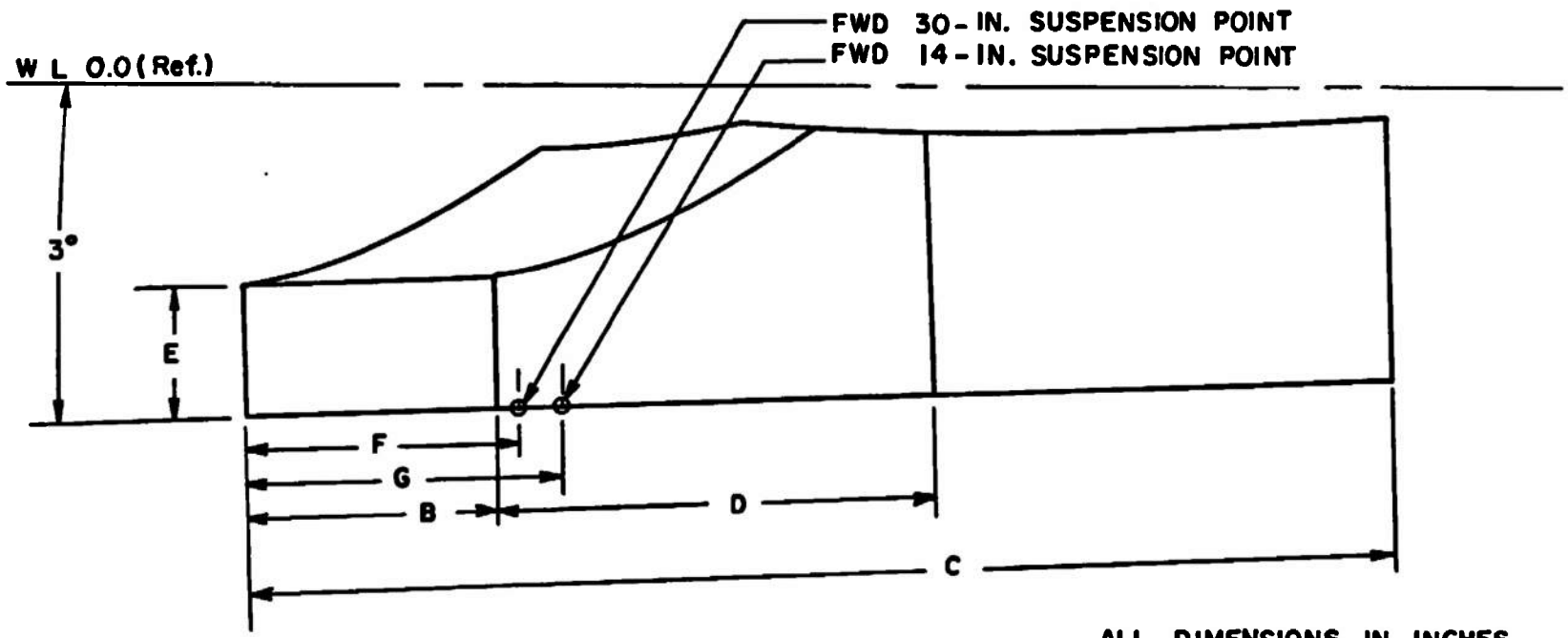

ALL DIMENSIONS IN INCHES

	INBOARD	CENTER	OUTBOARD
B	1.030	1.030	0.515
C	4.580	4.850	4.437
D	1.630	1.905	2.008
E	0.575	0.575	0.513
F	0.950	0.950	0.750
G	1.350	1.350	1.150

Fig. 4 Details and Dimensions of the A-7D Wing Pylon Models

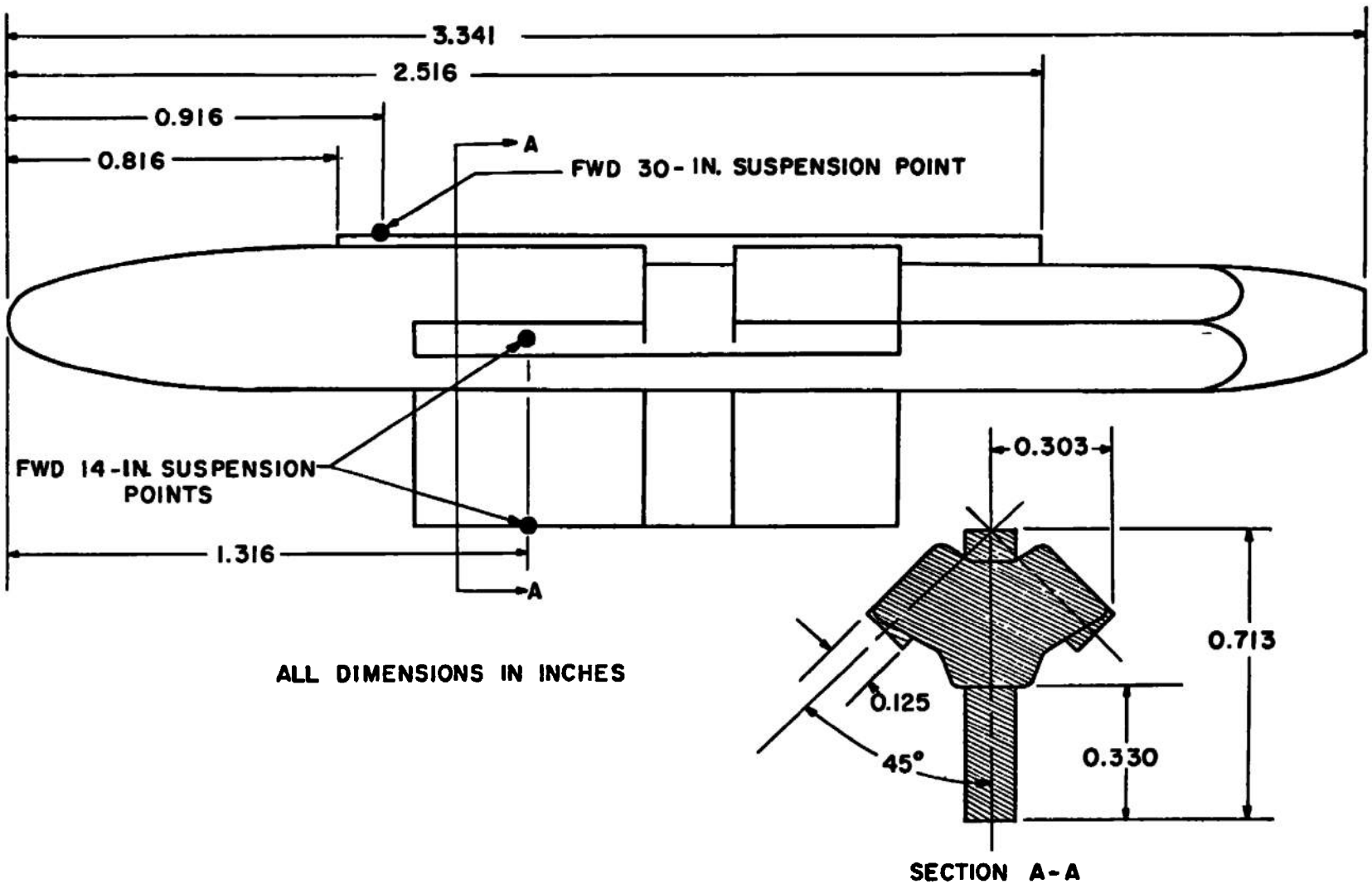

Fig. 5 Details and Dimensions of the TER-9/A Models

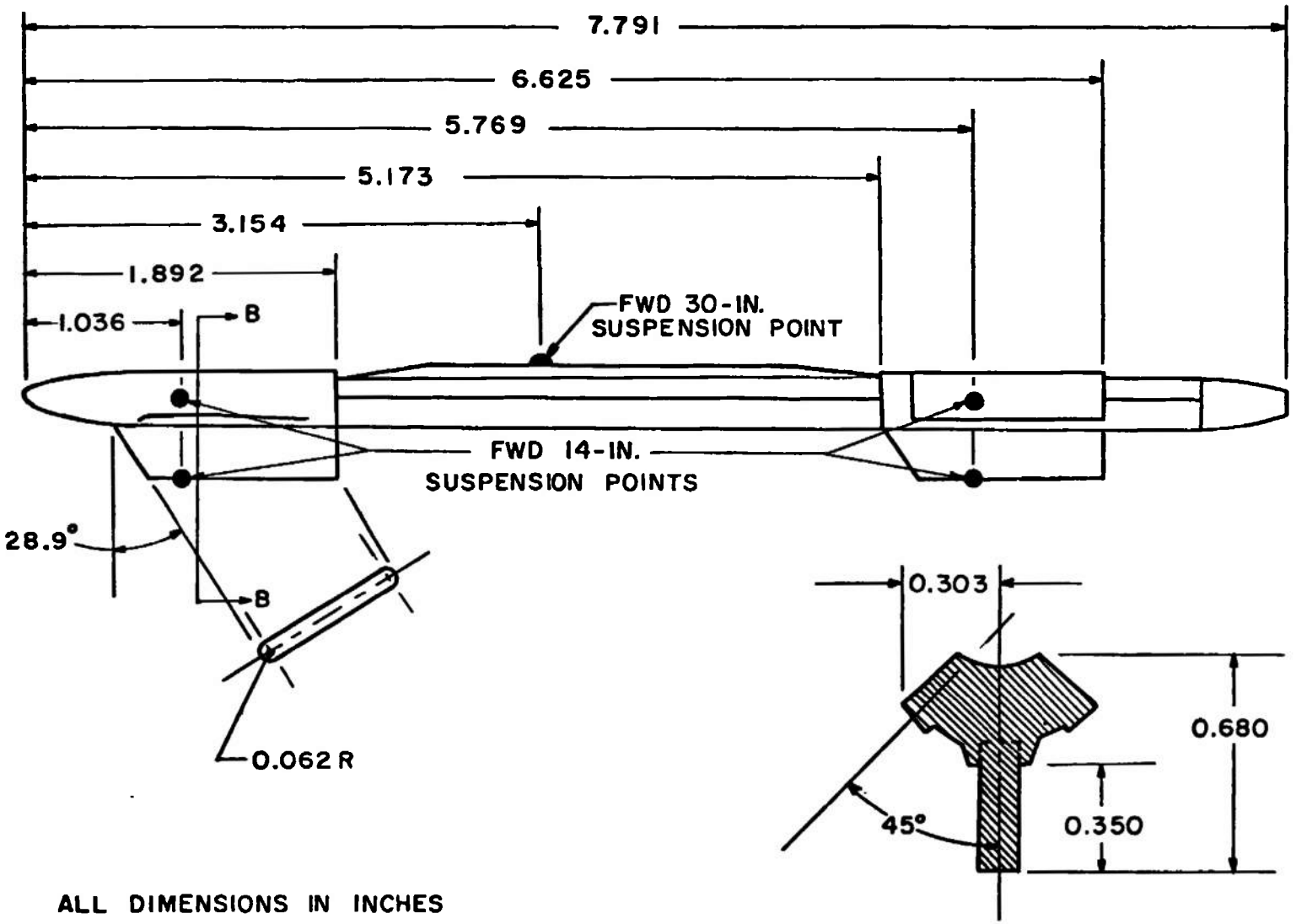

Fig. 6 Details and Dimensions of the MER-10N Model

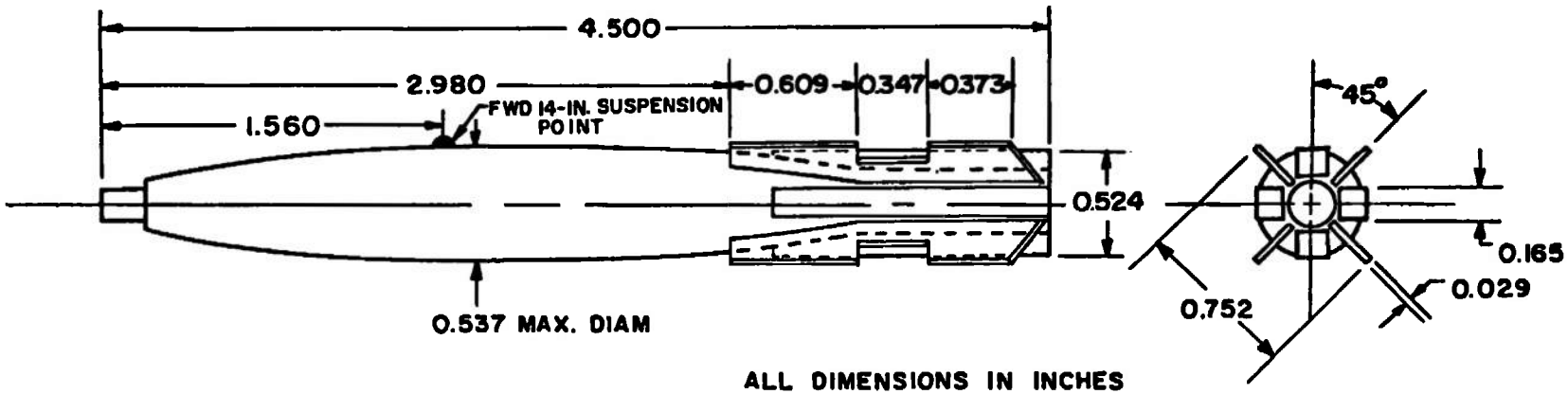

Fig. 7 Details and Dimensions of the Dummy MK-82 Snakeye Models

ORDINATES

MODEL STA "X"	RADIUS "R"	MODEL STA "X"	RADIUS "R"
0.000	0.0000	2.250	0.5531
0.060	0.0000	2.500	0.5777
0.100	0.0511	2.750	0.5989
0.150	0.0751		CONSTANT SLOPE
0.200	0.0981	3.450	0.6625
0.250	0.1203		CONSTANT DIAM
0.300	0.1415	6.636	0.6625
0.350	0.1619		CONSTANT SLOPE
0.400	0.1815	7.713	0.5680
0.450	0.2003	7.763	0.5637
0.500	0.2183	8.013	0.5409
0.550	0.2368	8.263	0.5162
0.600	0.2521	8.513	0.4899
0.650	0.2680	8.763	0.4620
0.700	0.2833	9.013	0.4327
0.750	0.2979	9.113	0.4206
0.800	0.3119		CONSTANT SLOPE
0.850	0.3253	10.900	0.1815
0.900	0.3383	10.950	0.1733
1.000	0.3628	11.000	0.1646
1.250	0.4153	11.100	0.1441
1.500	0.4587	11.200	0.1170
1.750	0.4950	11.300	0.0725
2.000	0.5260	11.350	0.0000

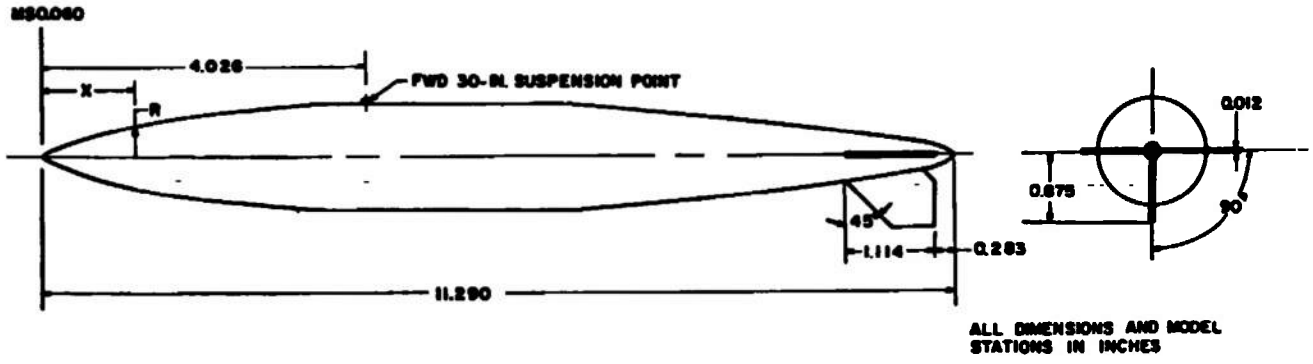

Fig. 8 Details and Dimensions of the Dummy 300-gal Fuel Tank Models

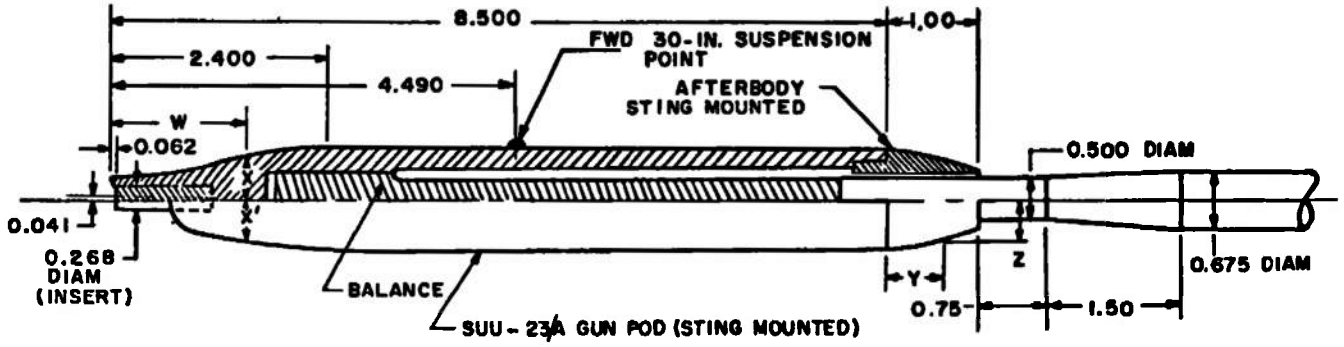

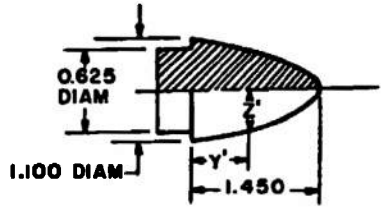

AFTERBODY (DUMMY)

ALL DIMENSIONS IN INCHES

COORDINATES		
W	X	X'
0.000	0.257	-0.241
0.050	0.258	-0.147
0.100	0.259	-0.116
0.175	0.261	-0.096
0.200	0.262	-0.092
0.250	0.264	-0.087
0.300	0.266	-0.083
0.325	0.268	-0.081
0.350	0.270	-0.079
0.400	0.273	-0.072
0.450	0.277	-0.064
0.500	0.281	-0.050
0.550	0.285	-0.025
0.592	0.290	-0.000
0.600	0.292	0.007
0.650	0.298	0.057
0.700	0.305	0.166
0.750	0.312	0.254
0.800	0.322	0.306
0.850	0.334	0.331
0.900	0.345	0.345
0.950	0.357	X = X'
1.000	0.368	
1.100	0.390	
1.200	0.410	
1.300	0.431	
1.400	0.449	
1.500	0.465	
1.600	0.480	
1.700	0.495	
1.800	0.507	
1.900	0.518	
2.000	0.528	
2.100	0.536	
2.200	0.543	
2.300	0.548	
2.400	0.550	

AFTERBODY COORDINATES	
Y & Y'	Z & Z'
0	0.650
0.050	0.648
0.100	0.640
0.150	0.635
0.200	0.630
0.250	0.622
0.300	0.615
0.350	0.607
0.400	0.497
0.450	0.489
0.500	0.478
0.550	0.468
0.600	0.453
0.650	0.439
0.700	0.428
0.750	0.410
0.800	0.394
0.850	0.375
0.900	0.356
0.950	0.537
1.000	0.318

CONTINUATION OF COORDINATES FOR AFTERBODY (DUMMY)	
Y'	Z'
1.050	0.293
1.100	0.269
1.150	0.244
1.200	0.217
1.250	0.189
1.300	0.158
1.350	0.124
1.400	0.086
1.450	0.000

Fig. 9 Details and Dimensions of the SUU-23/A Models

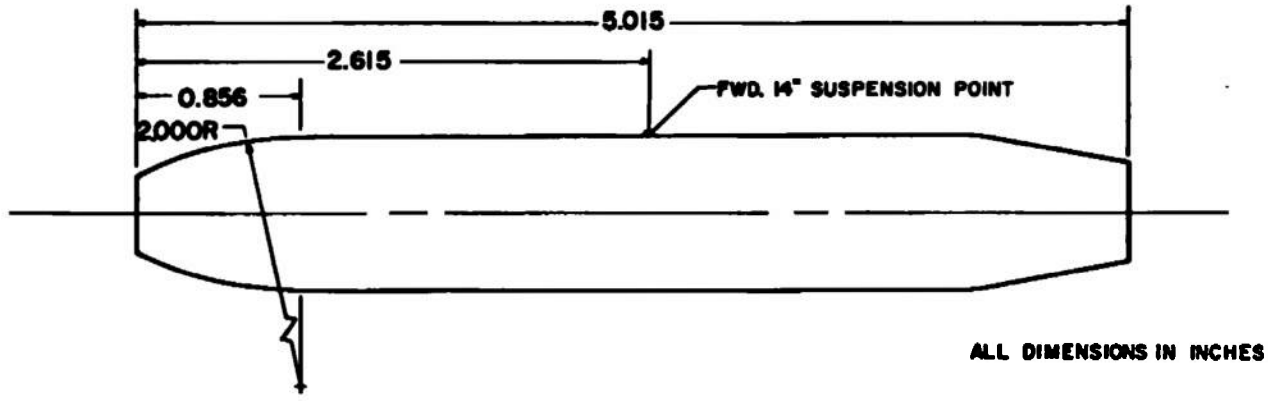

a. Sting-Mounted Model

Fig. 10 Details and Dimensions of the CBU-12A/A and CBU-46/A Models

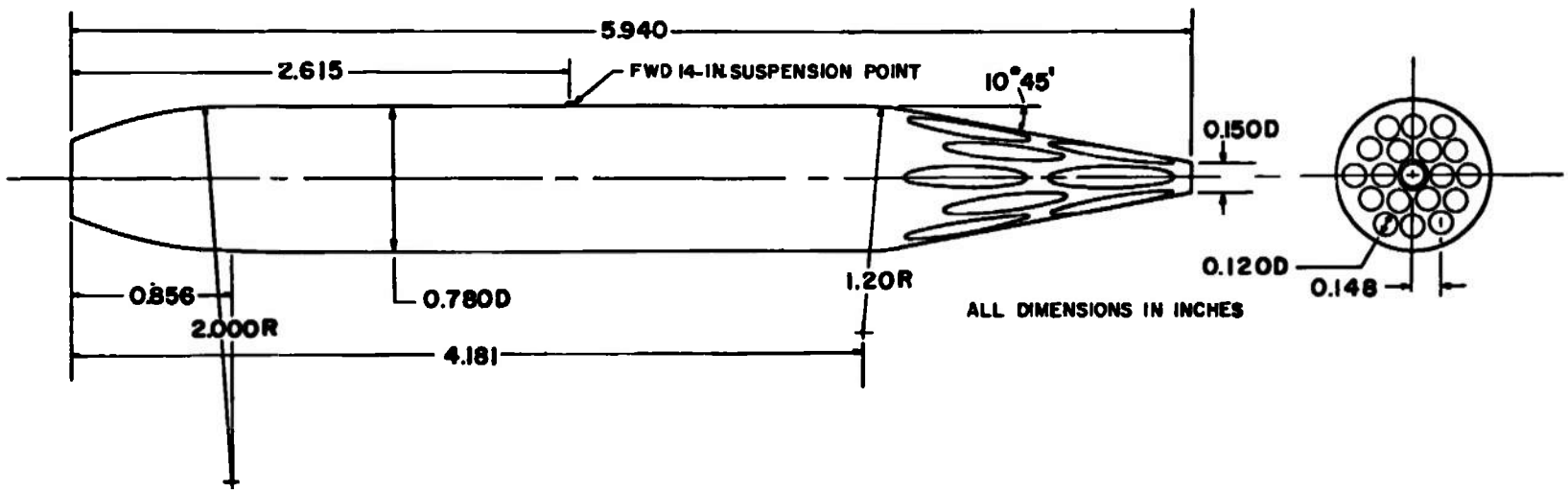

b. Dummy Model
Fig. 10 Concluded

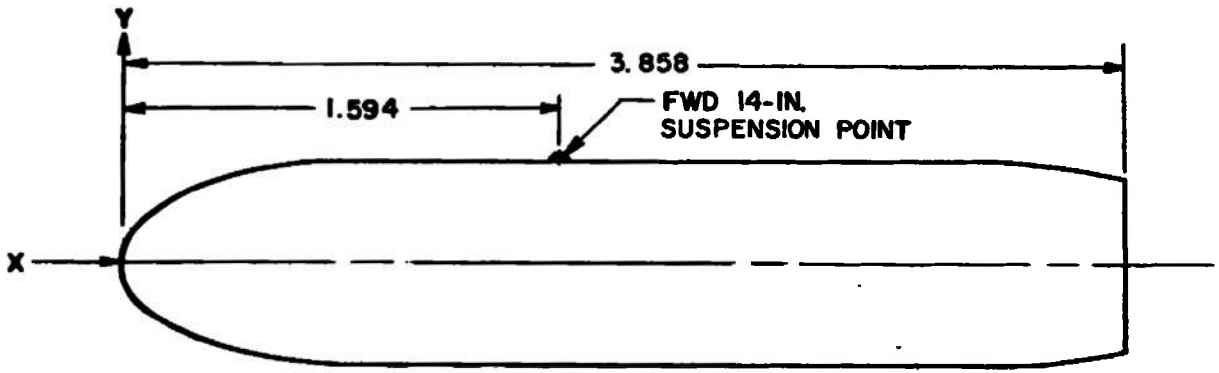

X	Y
0.000	0.000
0.100	0.182
0.200	0.249
0.300	0.296
0.400	0.333
0.500	0.359
0.600	0.376
0.700	0.386
0.800	0.391
0.900	0.393
3.450	0.393
3.550	0.391
3.650	0.385
3.750	0.373
3.858	0.358

ALL DIMENSIONS IN INCHES

a. Loaded LAU-3/A

Fig. 11 Details and Dimensions of the LAU-3/A Models

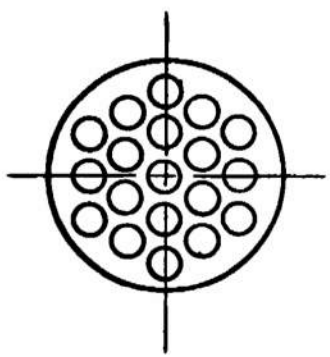

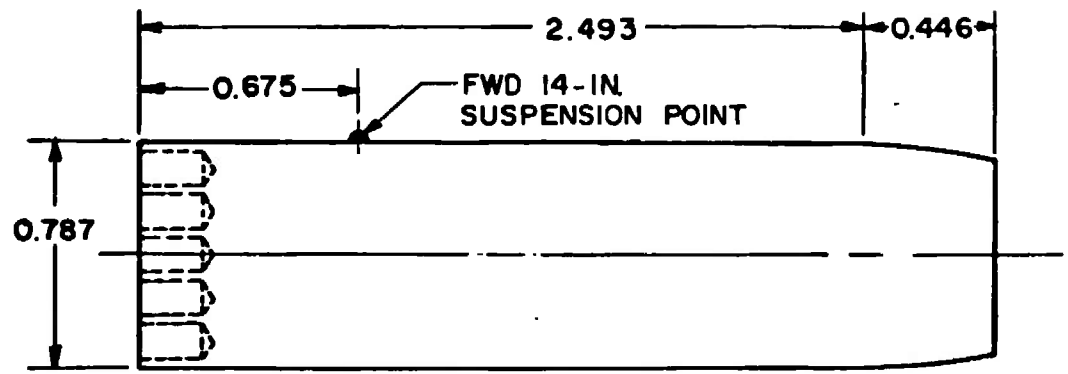

ALL DIMENSIONS IN INCHES

b. Expanded LAU-3/A

Fig. 11 Concluded

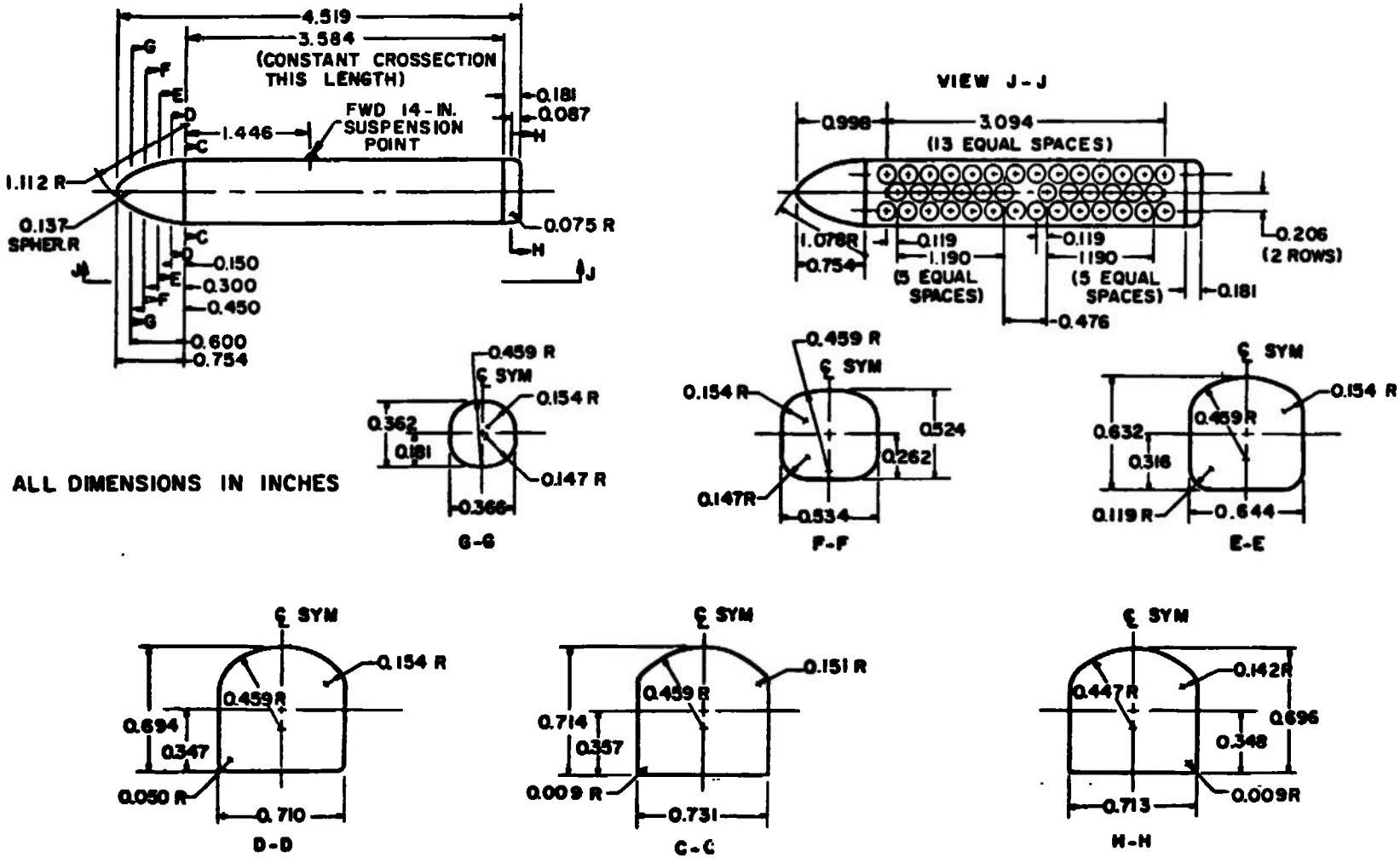

Fig. 12 Details and Dimensions of the CBU-30/A Models

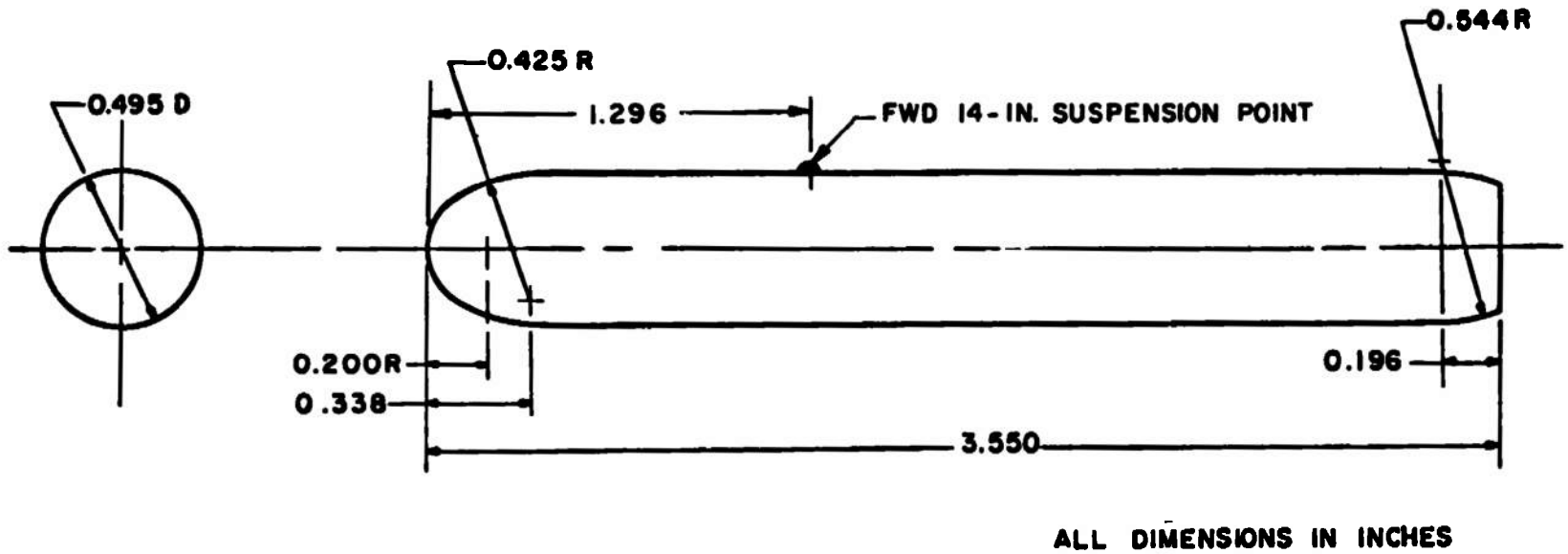

a. Loaded LAU-68A/A

Fig. 13 Details and Dimensions of the LAU-68A/A Models

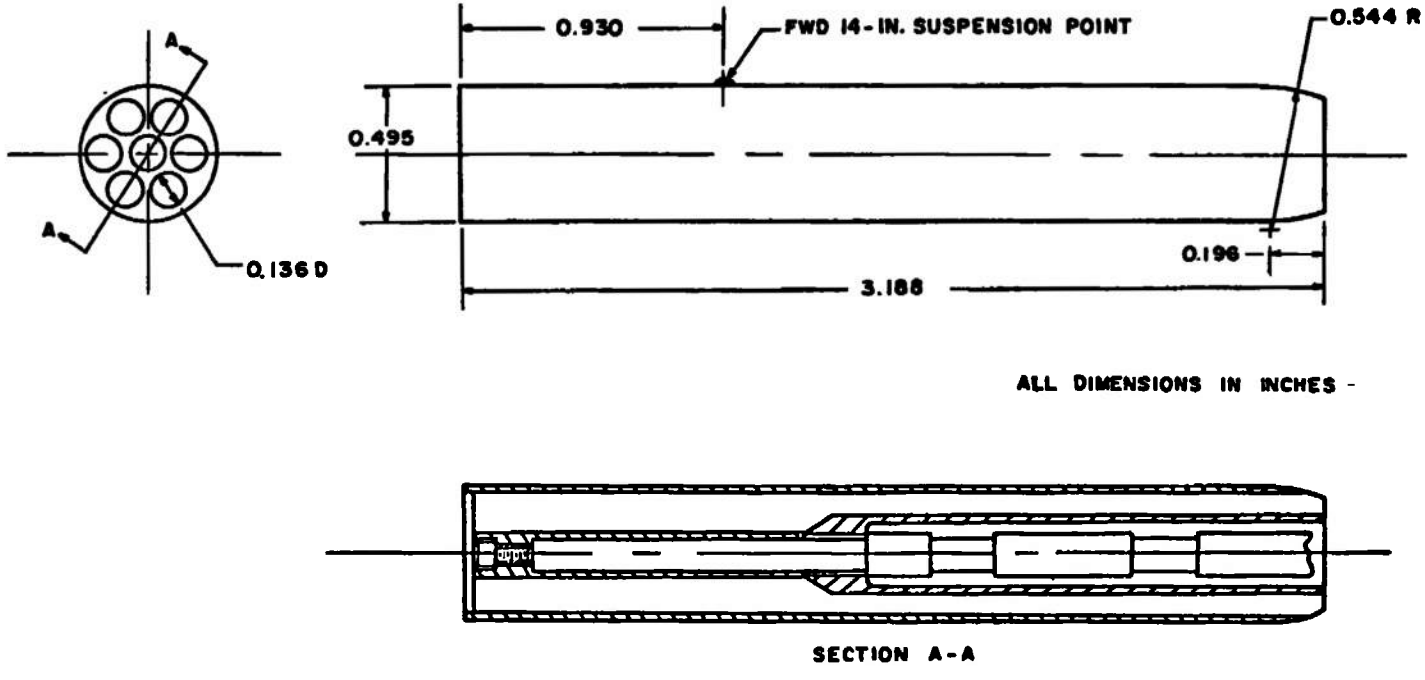

b. Expended LAU-68A/A Sting-Mounted Model
Fig. 13 Continued

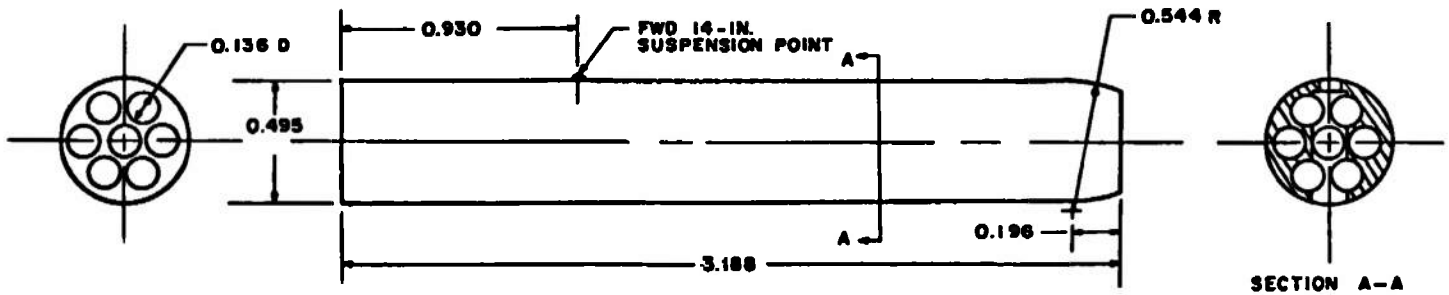

ALL DIMENSIONS IN INCHES

c. Expended LAU-68A/A Dummy Model
Fig. 13 Concluded

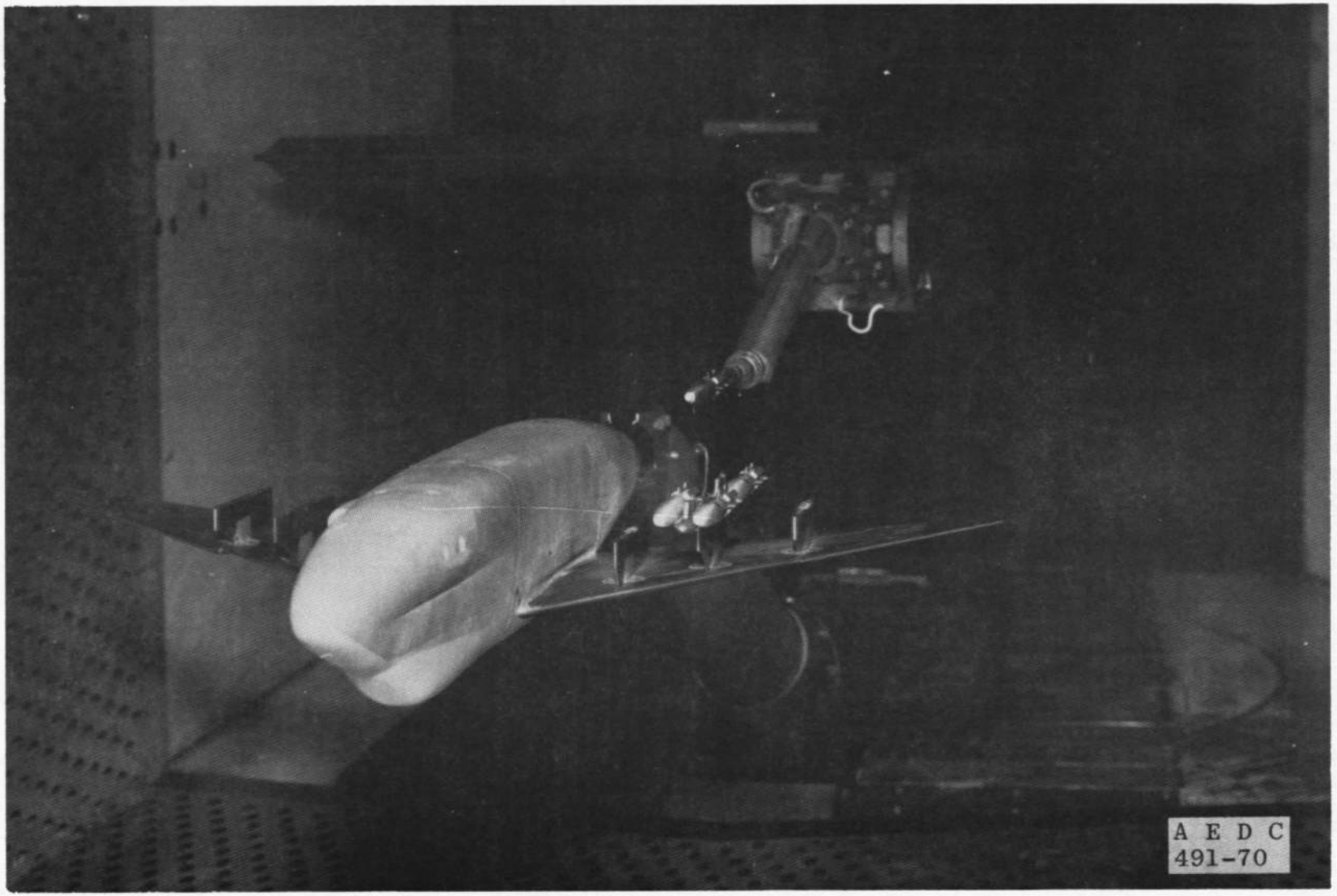

Fig. 14 Photograph of a Typical A-7D CTS Test Installation in the Tunnel

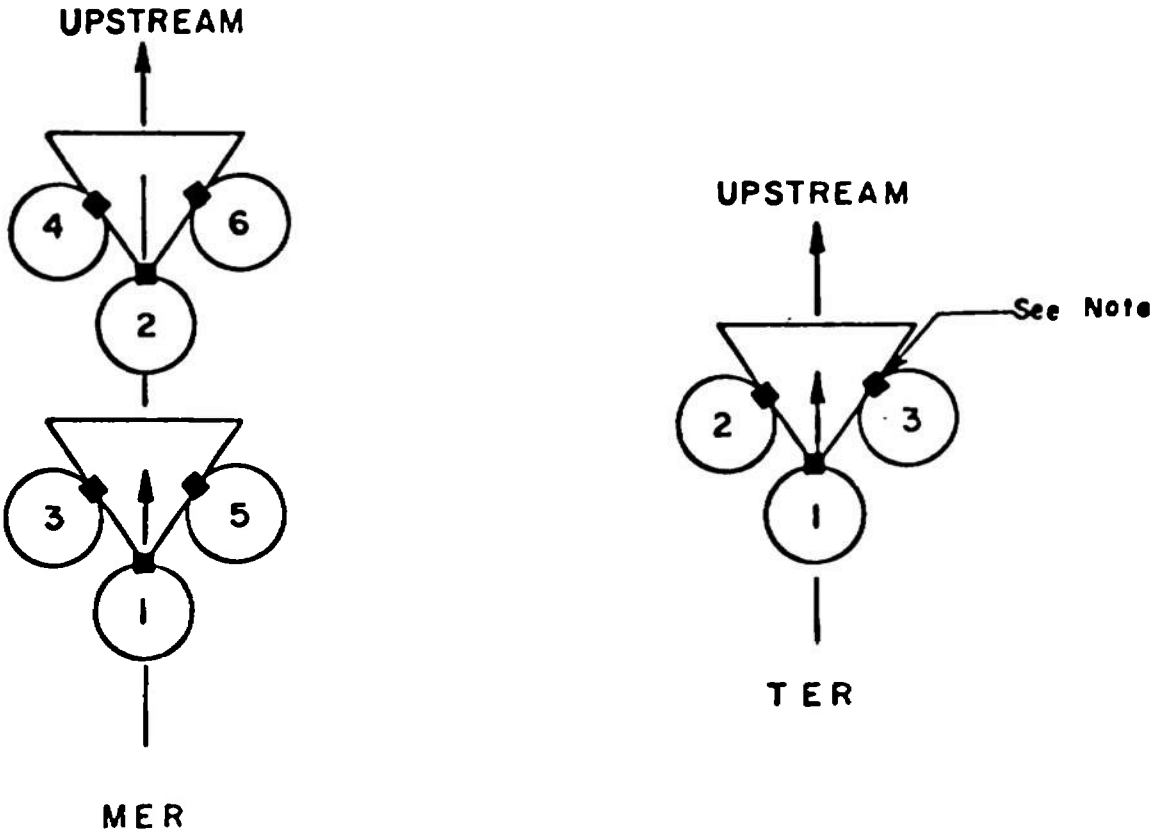

NOTE: The square indicates the orientation of the suspension lugs

TYPE RACK	STATION	ROLL ORIENTATION, deg
MER	1	0
	2	0
	3	45
	4	45
	5	-45
	6	-45
TER	1	0
	2	45
	3	-45

Fig. 15 Identification of TER and MER Store Stations and Orientations

SYMBOL	CONF	M_∞	α
▯	1L	0.325	12.9
○	1L	0.651	3.9
△	1L	0.732	3.4
◁	1L	0.814	3.0

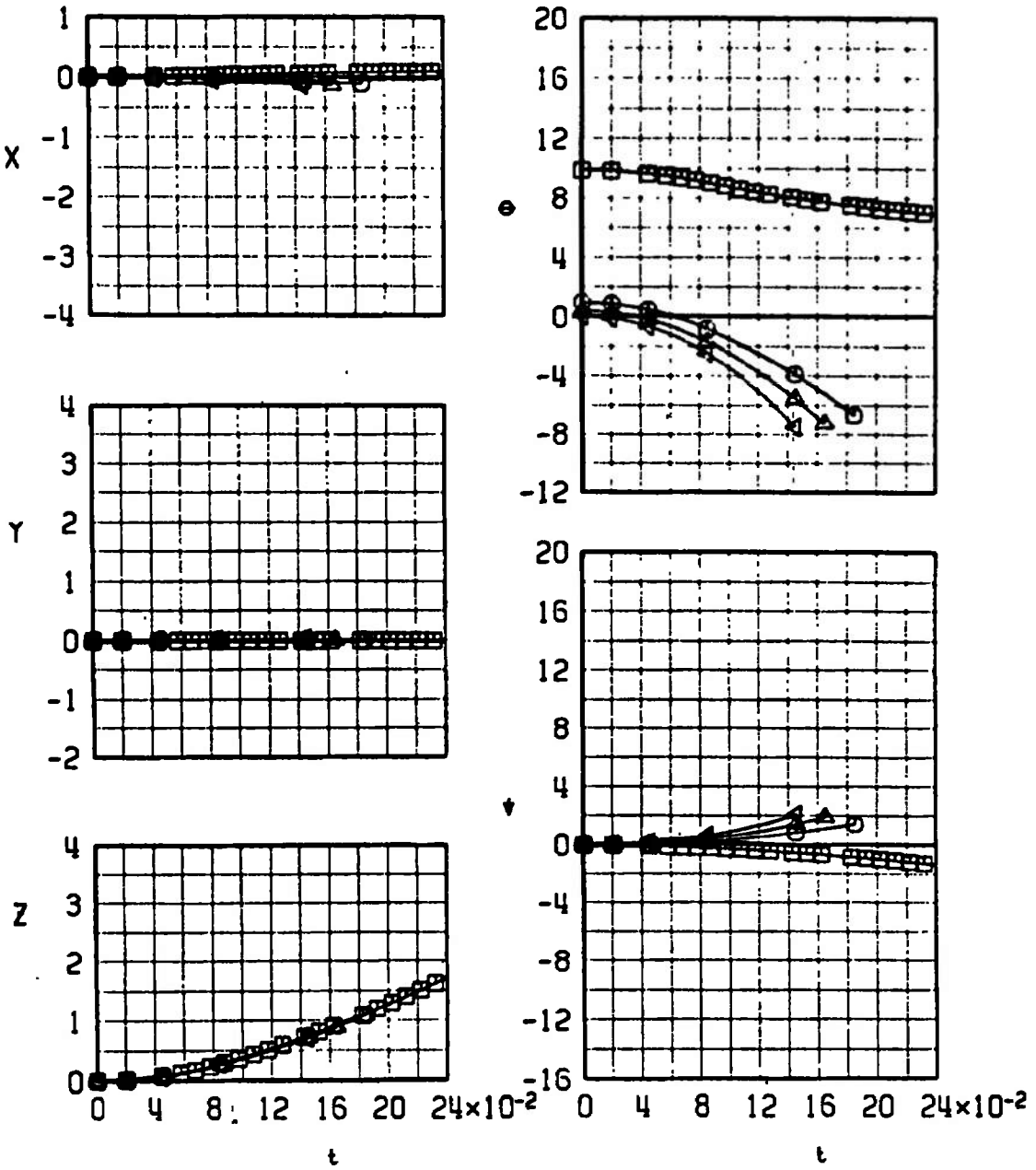

a. Configuration 1L

Fig. 16 Trajectory Data for the Loaded SUU-23/A Gun Pod, Ejector 3

SYMBOL	CONF	M_∞	α
□	1R	0.325	12.9
○	1R	0.569	4.9
△	1R	0.814	3.0

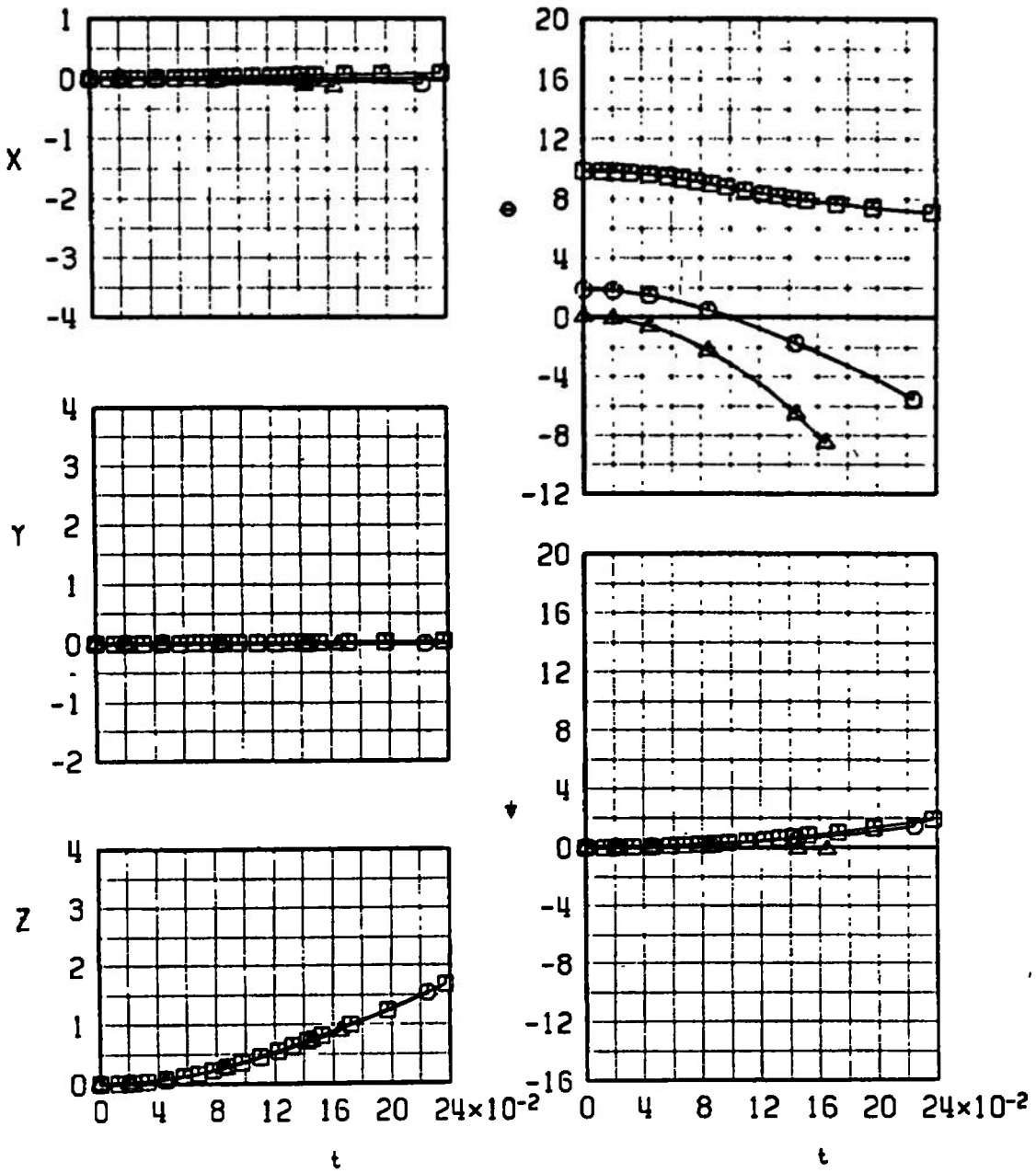

b. Configuration 1R
Fig. 16 Concluded

SYMBOL	CONF	M_∞	α
□	1L	0.325	12.9
○	1L	0.651	3.9
△	1L	0.732	3.4

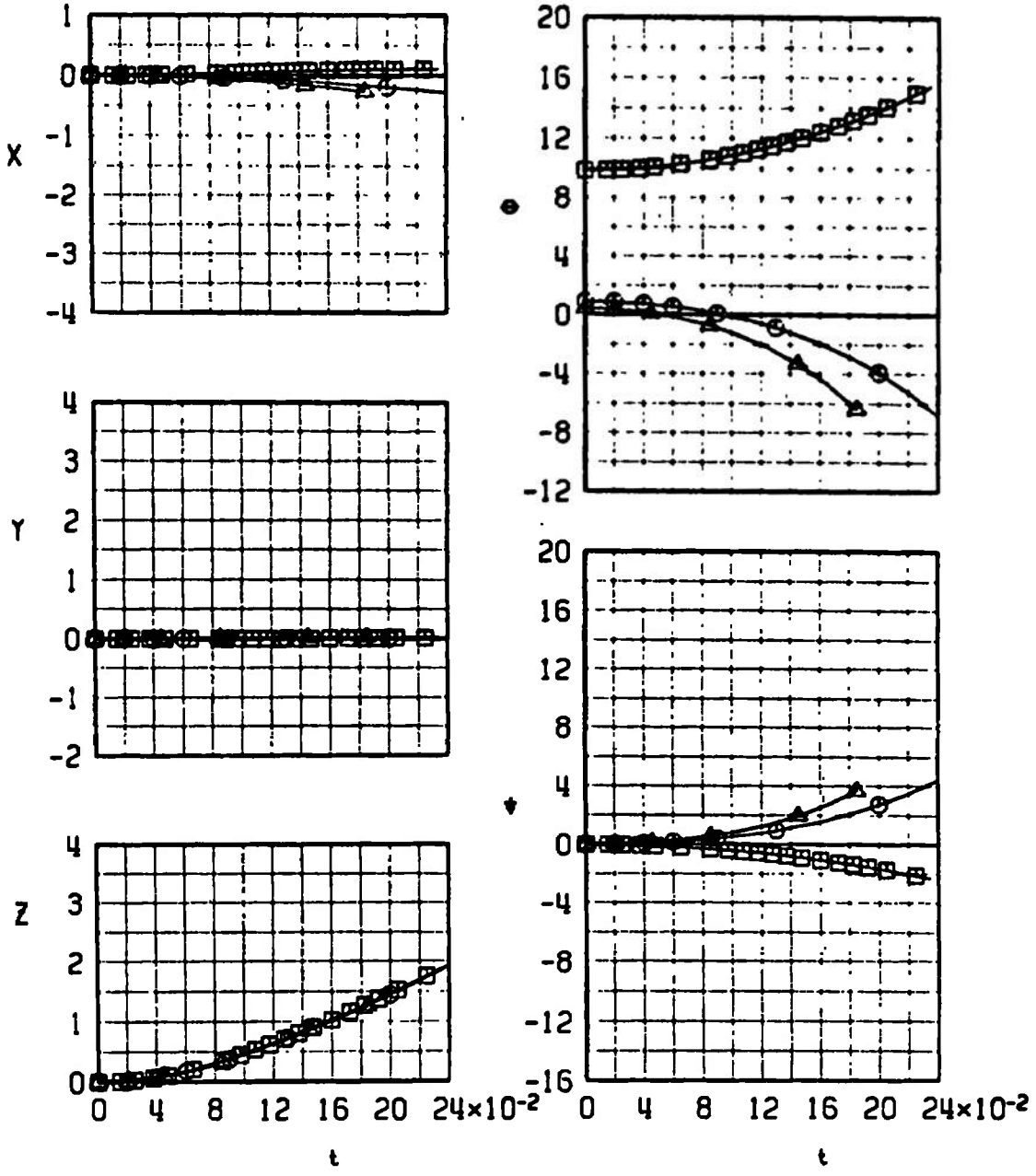

a. Configuration 1L

Fig. 17 Trajectory Data for the Expended SUU-23/A Gun Pod, Ejector 1

SYMBOL	CONF	M_∞	α
□	1R	0.325	12.9
○	1R	0.569	4.9
△	1R	0.814	3.0

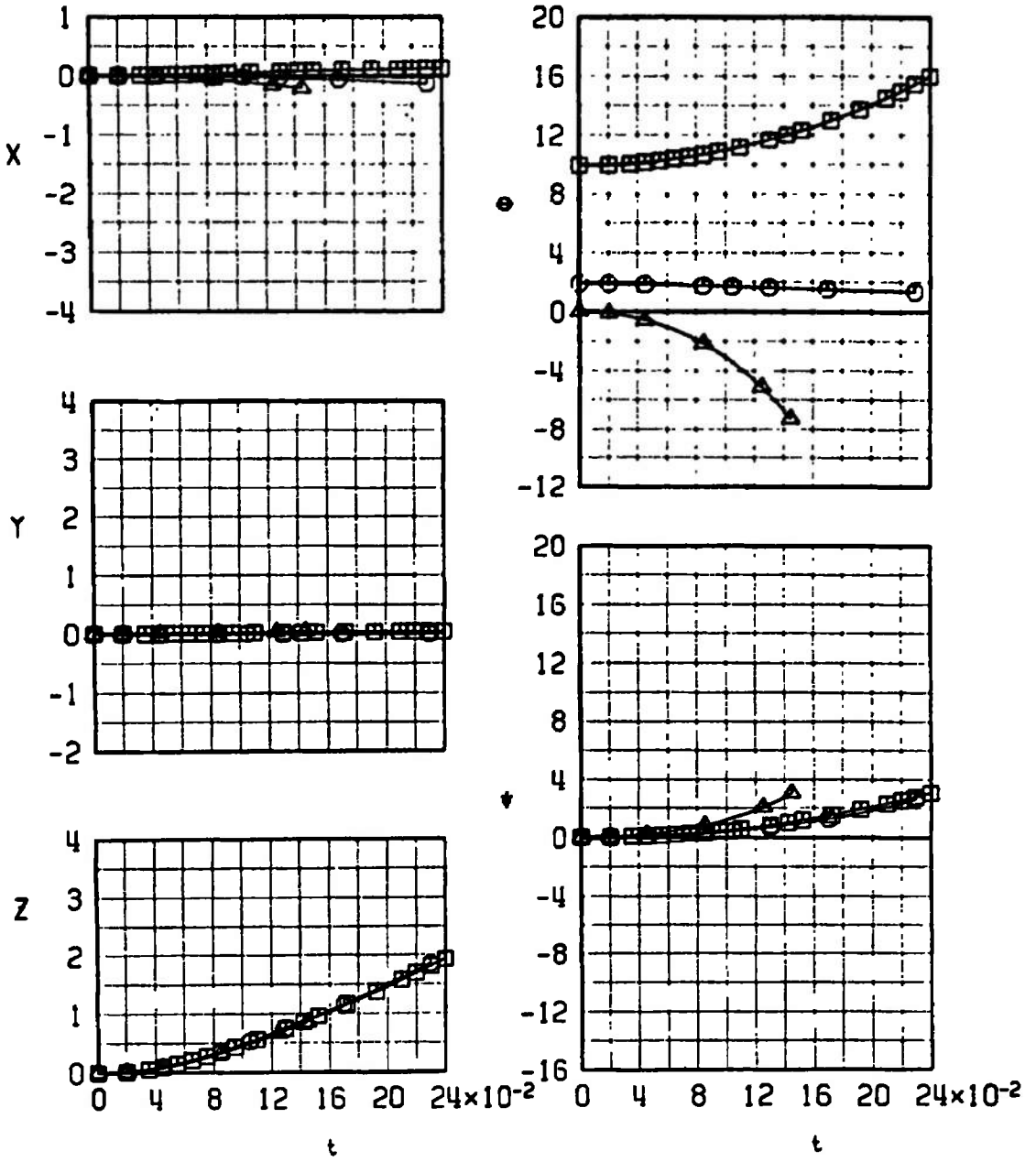

b. Configuration 1R
Fig. 17 Concluded

SYMBOL	CONF	M_∞	α	EJECTOR
□	1L	0.325	12.9	3
○	1L	0.325	12.9	4

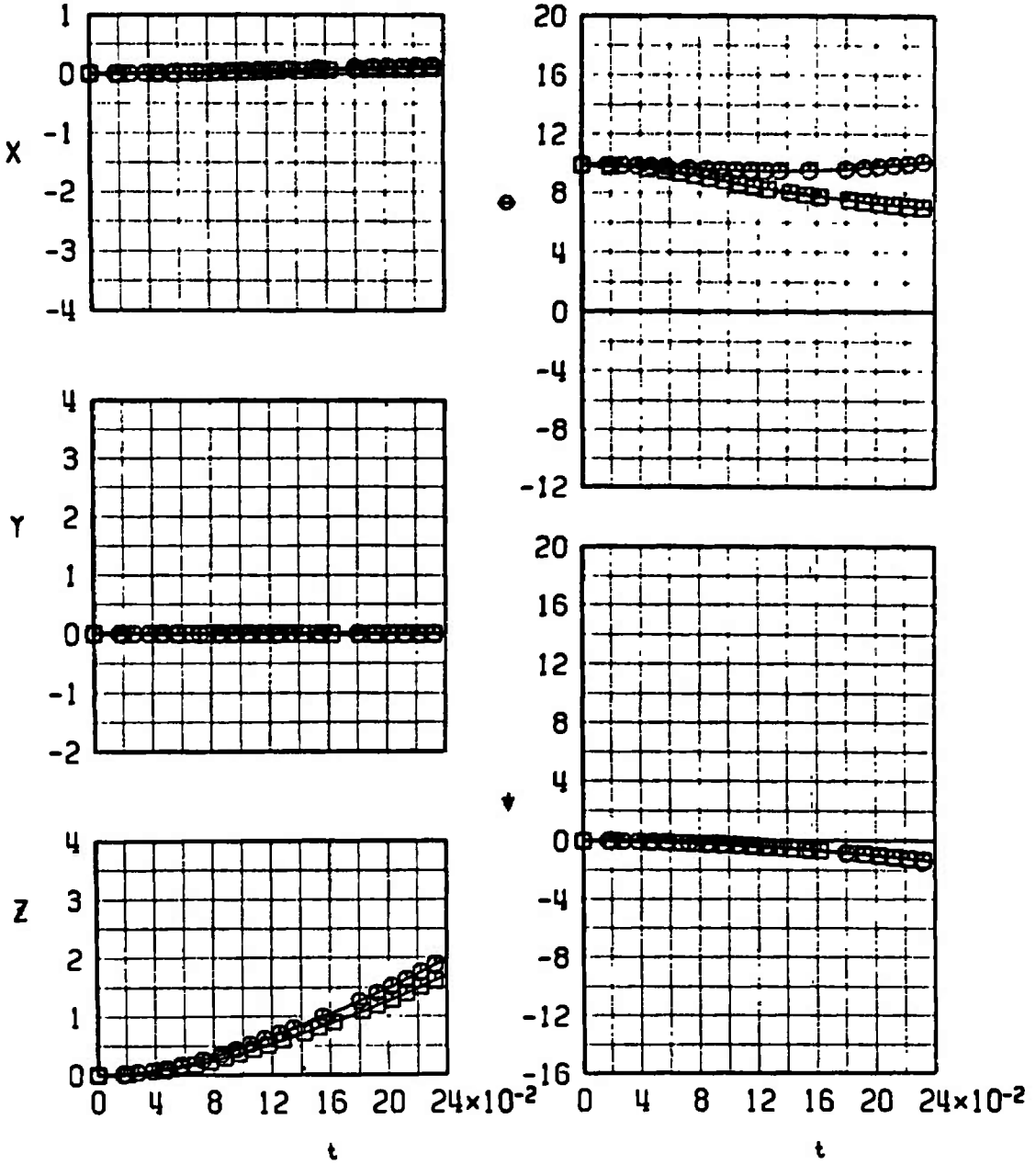

a. $M_\infty = 0.325$

Fig. 18 Trajectory Data for the Loaded SUU-23/A Gun Pod Showing the Effect of Ejector Force, Test Configuration 1L

SYMBOL	CONF	M_∞	α	EJECTOR
□	1L	0.814	3.0	3
○	1L	0.814	3.0	4

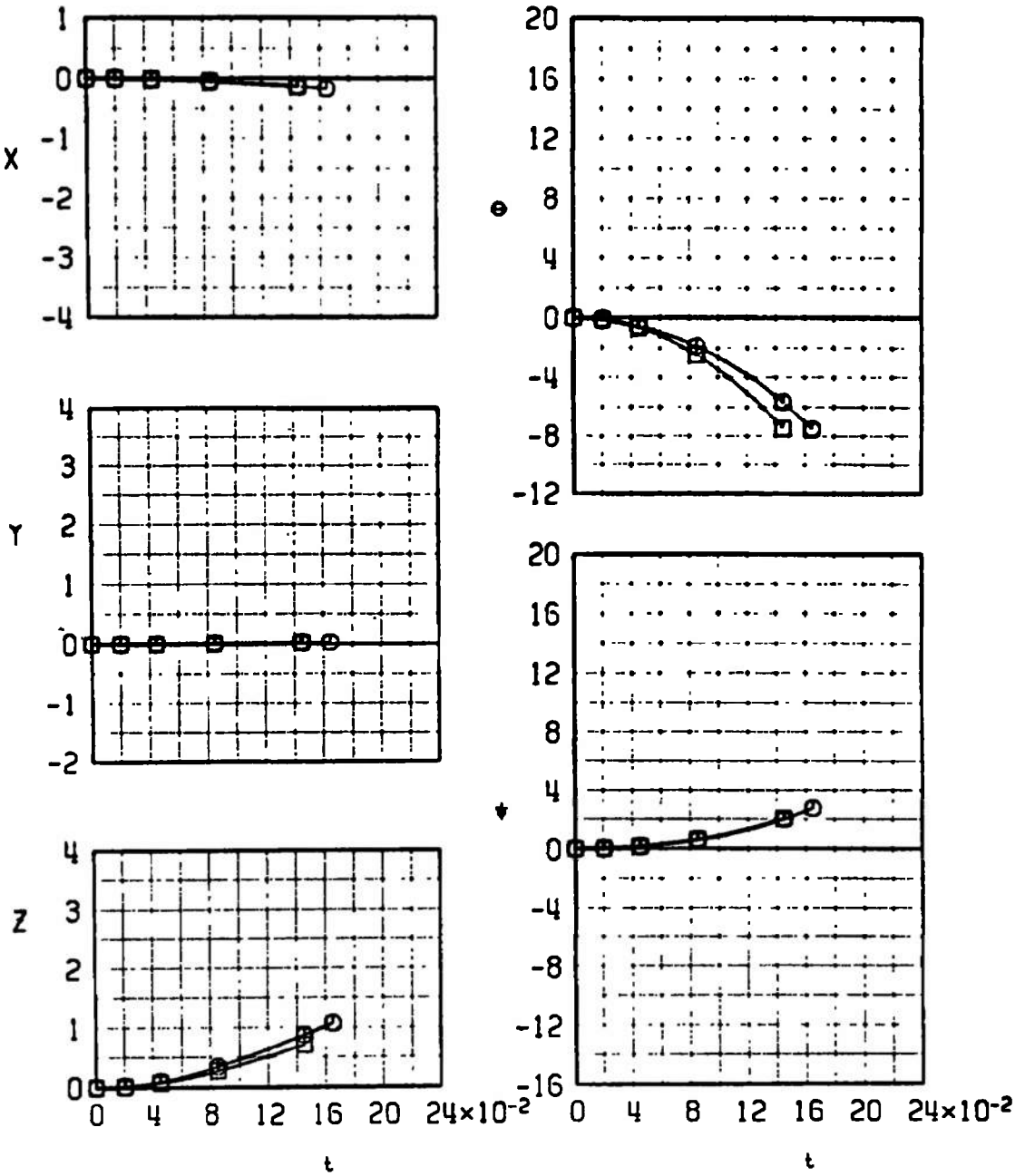

b. $M_\infty = 0.814$
Fig. 18 Concluded

SYMBOL	CONF	M_∞	α	EJECTOR
□	1R	0.569	4.9	2
○	1R	0.569	4.9	1

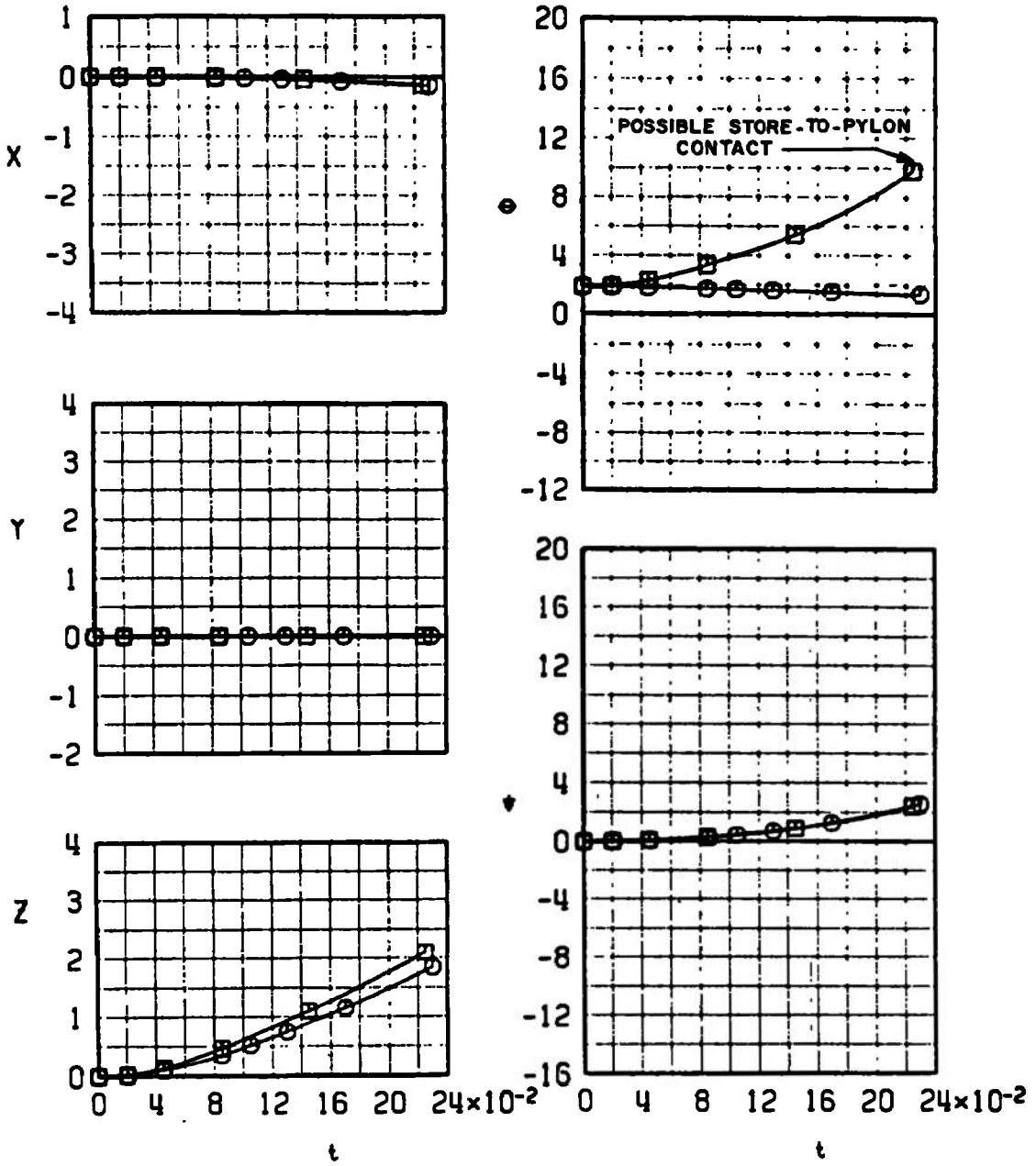

a. $M_\infty = 0.569$

Fig. 19 Trajectory Data for the Expended SUU-23/A Gun Pod Showing the Effect of Ejector Force, Test Configuration 1R

SYMBOL	CONF	M_∞	α	EJECTOR
□	1R	0.814	3.0	2
○	1R	0.814	3.0	1

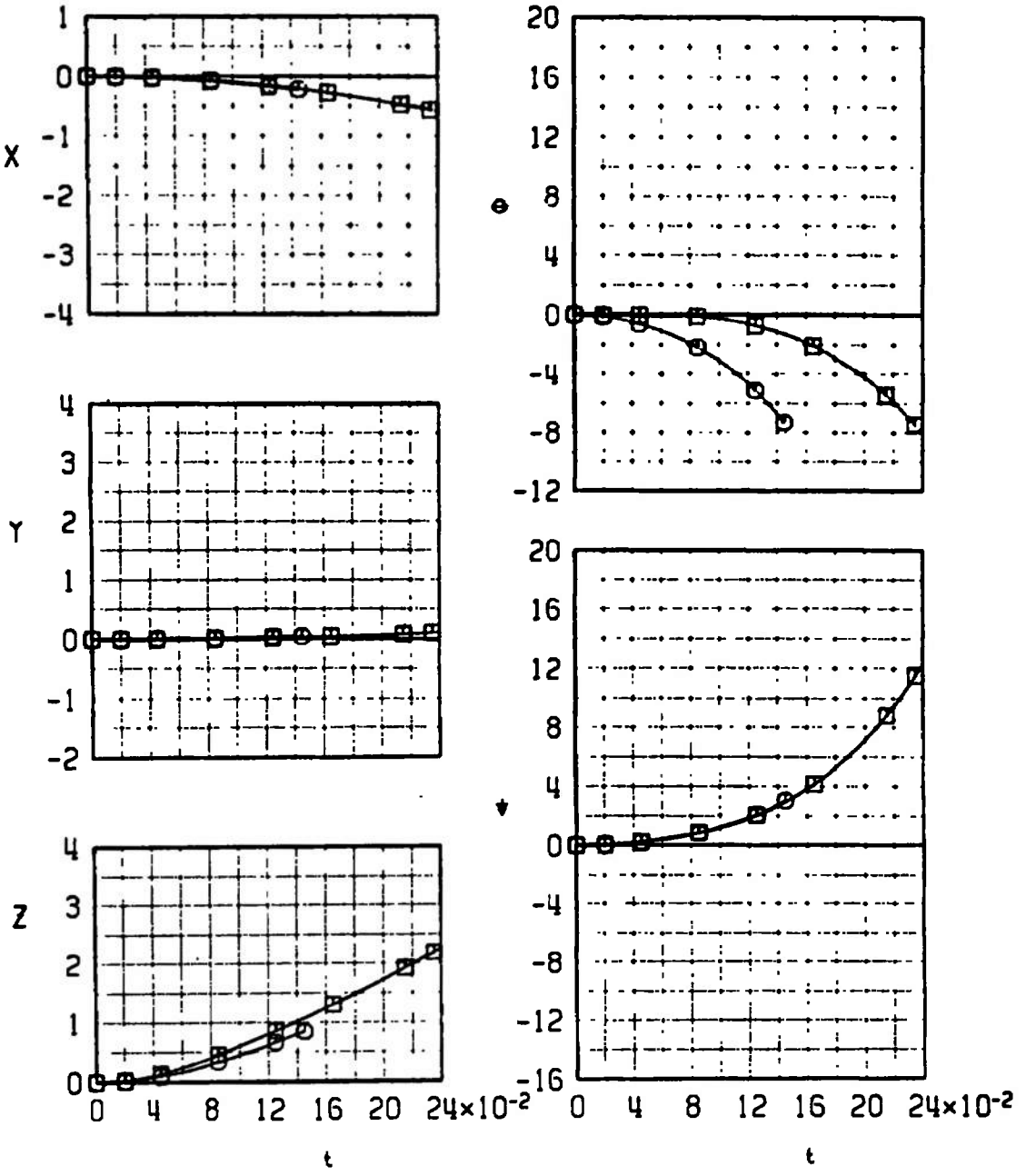

b. $M_\infty = 0.814$

Fig. 19 Concluded

SYMBOL	CONF	M_∞	α
□	2L	0.407	8.6
○	2L	0.569	4.9
△	2L	0.732	3.4

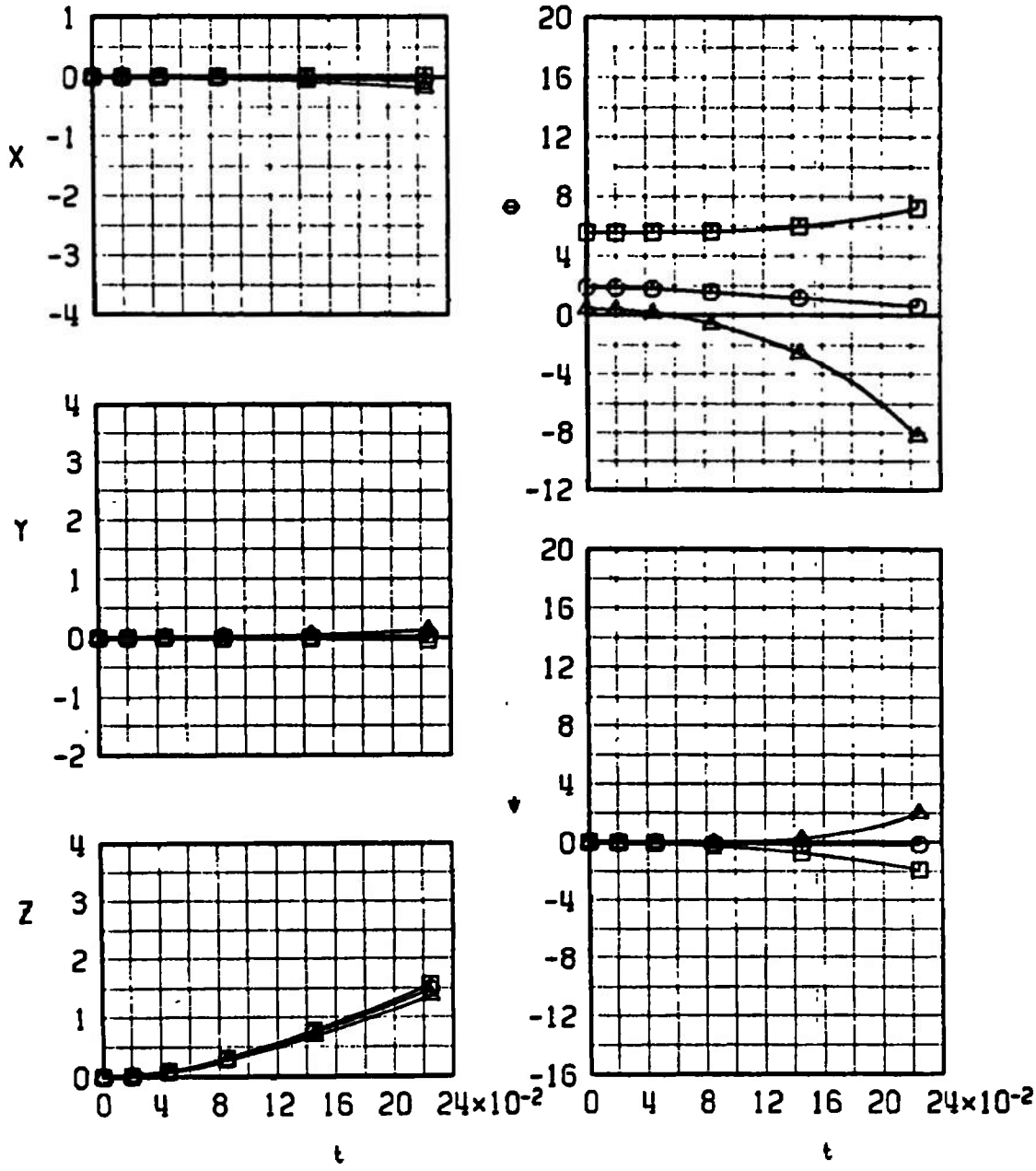

a. Configuration 2L, Ejector 6

Fig. 20 Trajectory Data for the Loaded CBU-12A/A Store

SYMBOL	CONF	M_∞	α
⊡	2R	0.407	8.6
⊙	2R	0.569	4.9
△	2R	0.732	3.4

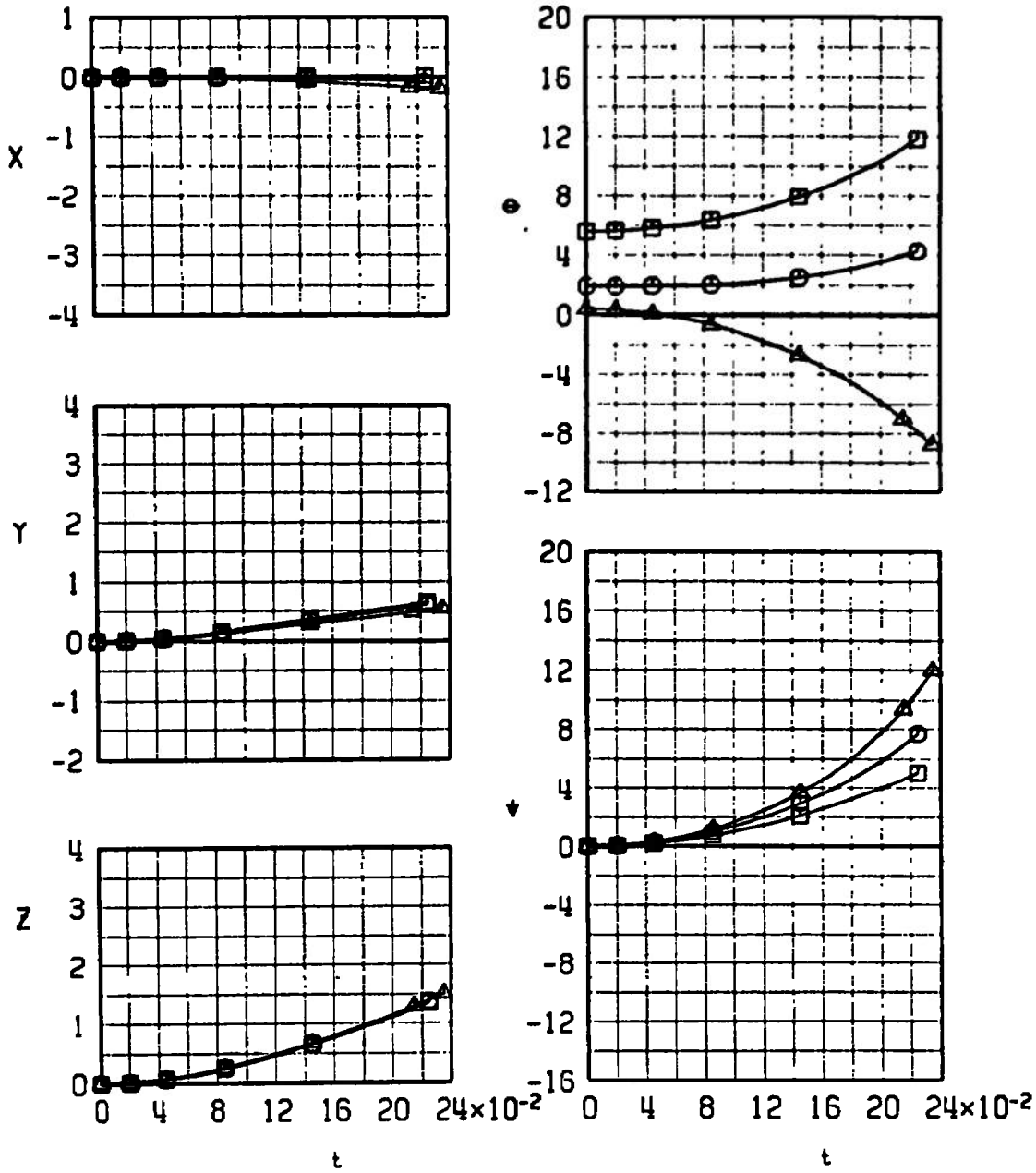

b. Configuration 2R, Ejector 6
Fig. 20 Continued

SYMBOL	CONF	M_∞	α
□	3L	0.325	12.9
○	3L	0.447	7.3
△	3L	0.692	3.6
◁	3L	0.814	3.0

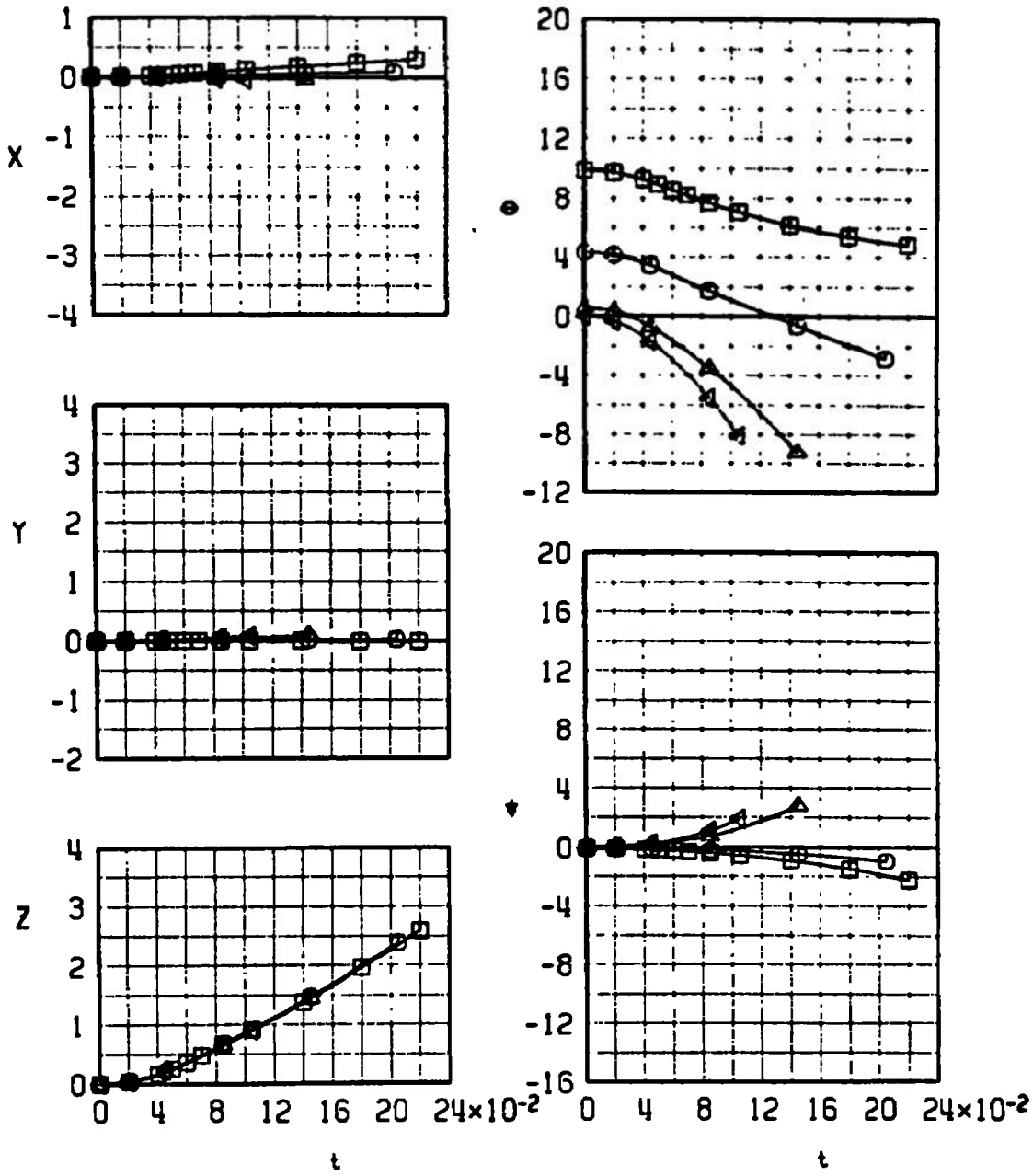

c. Configuration 3L, Ejector 9
Fig. 20 Concluded

SYMBOL	CONF	M_∞	α
□	2L	0.407	8.6
○	2L	0.569	4.9
△	2L	0.732	3.4

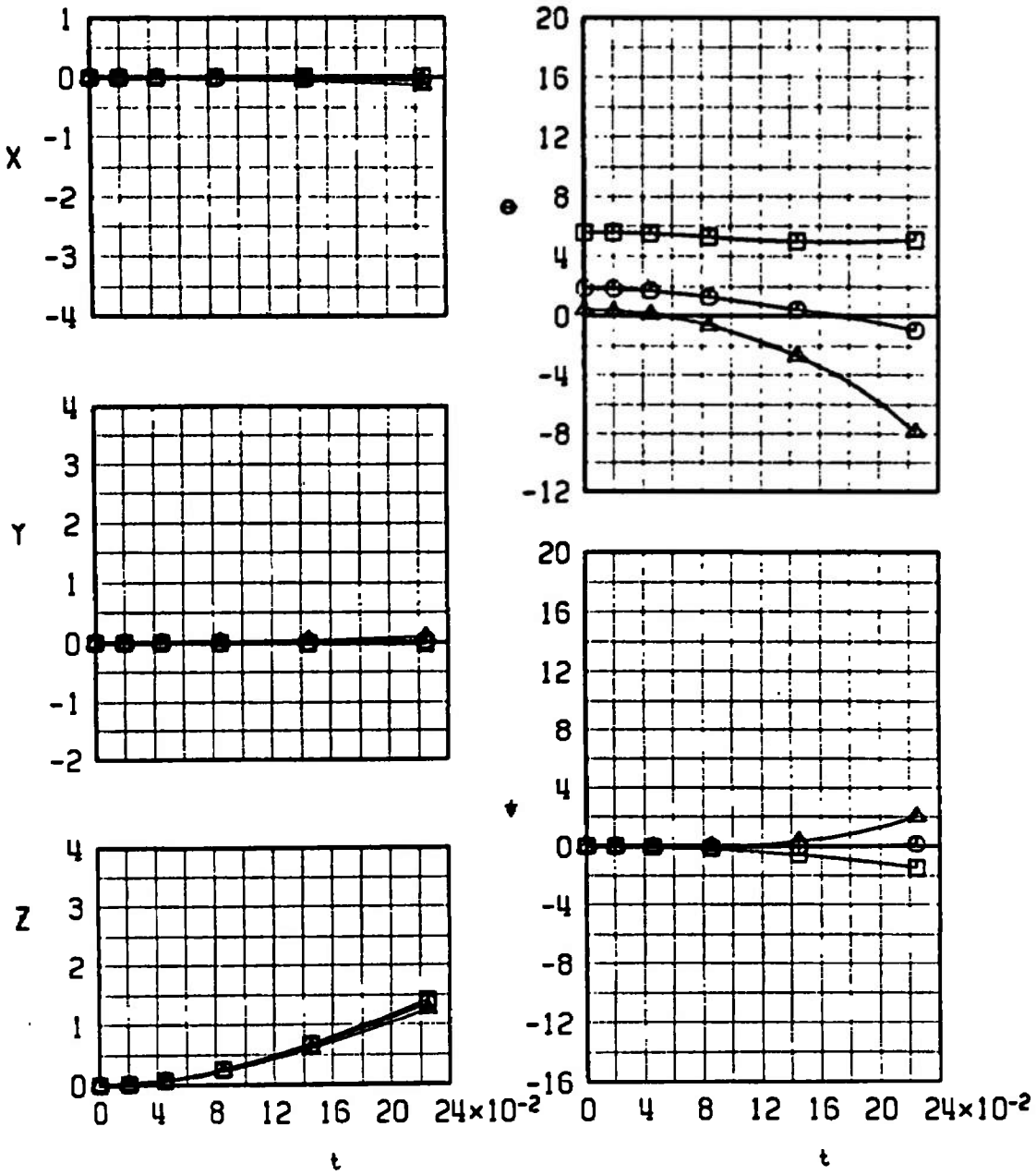

a. Configuration 2L, Ejector 7

Fig. 21 Trajectory Data for the Loaded CBU-46A/A Store

SYMBOL	CONF	M_∞	α
□	2R	0.407	8.6
○	2R	0.569	4.9
△	2R	0.732	3.4

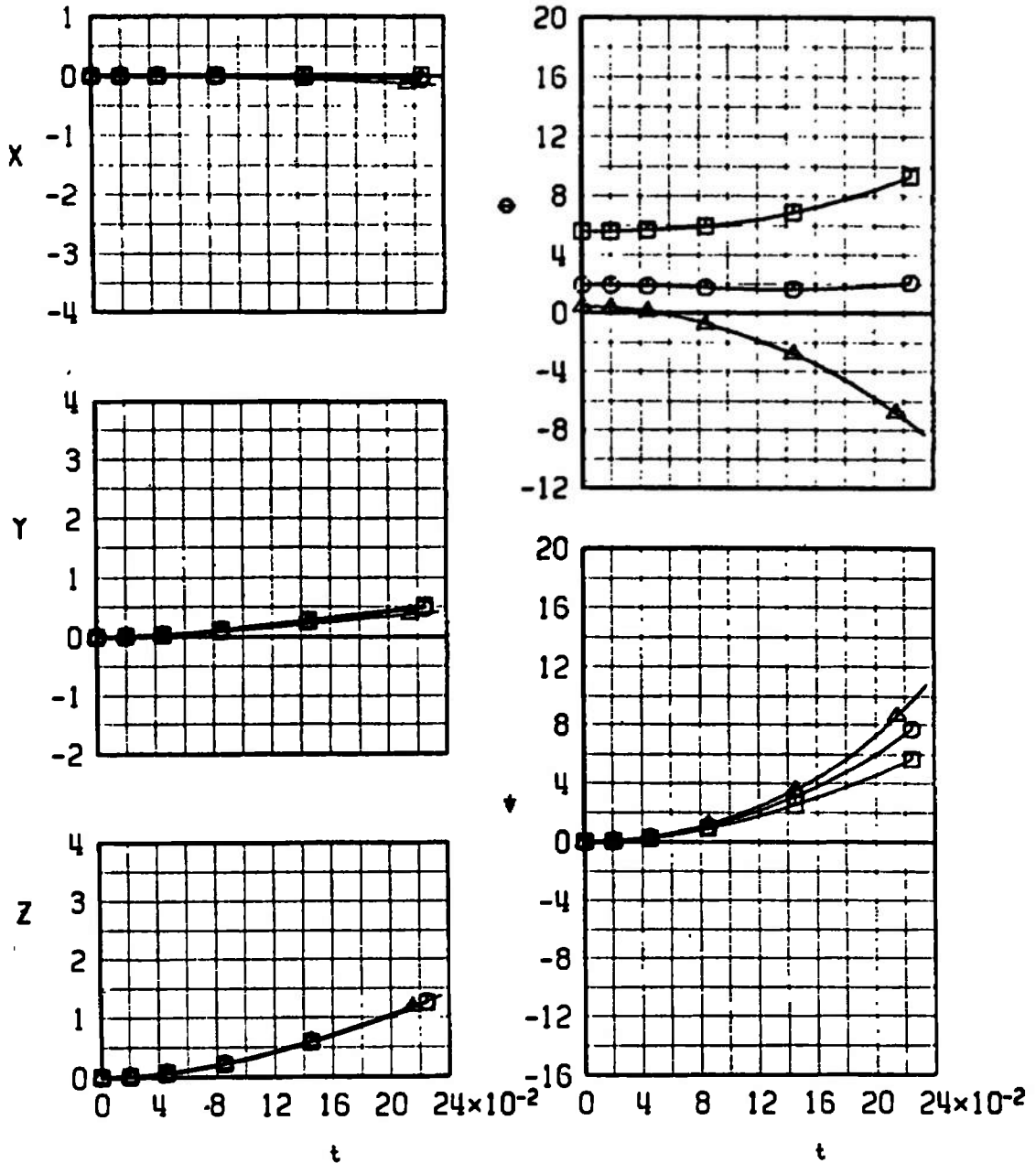

b. Configuration 2R, Ejector 7
Fig. 21 Continued

SYMBOL	CONF	M_∞	α
□	3L	0.325	12.9
○	3L	0.447	7.3
△	3L	0.692	3.6
◁	3L	0.814	3.0

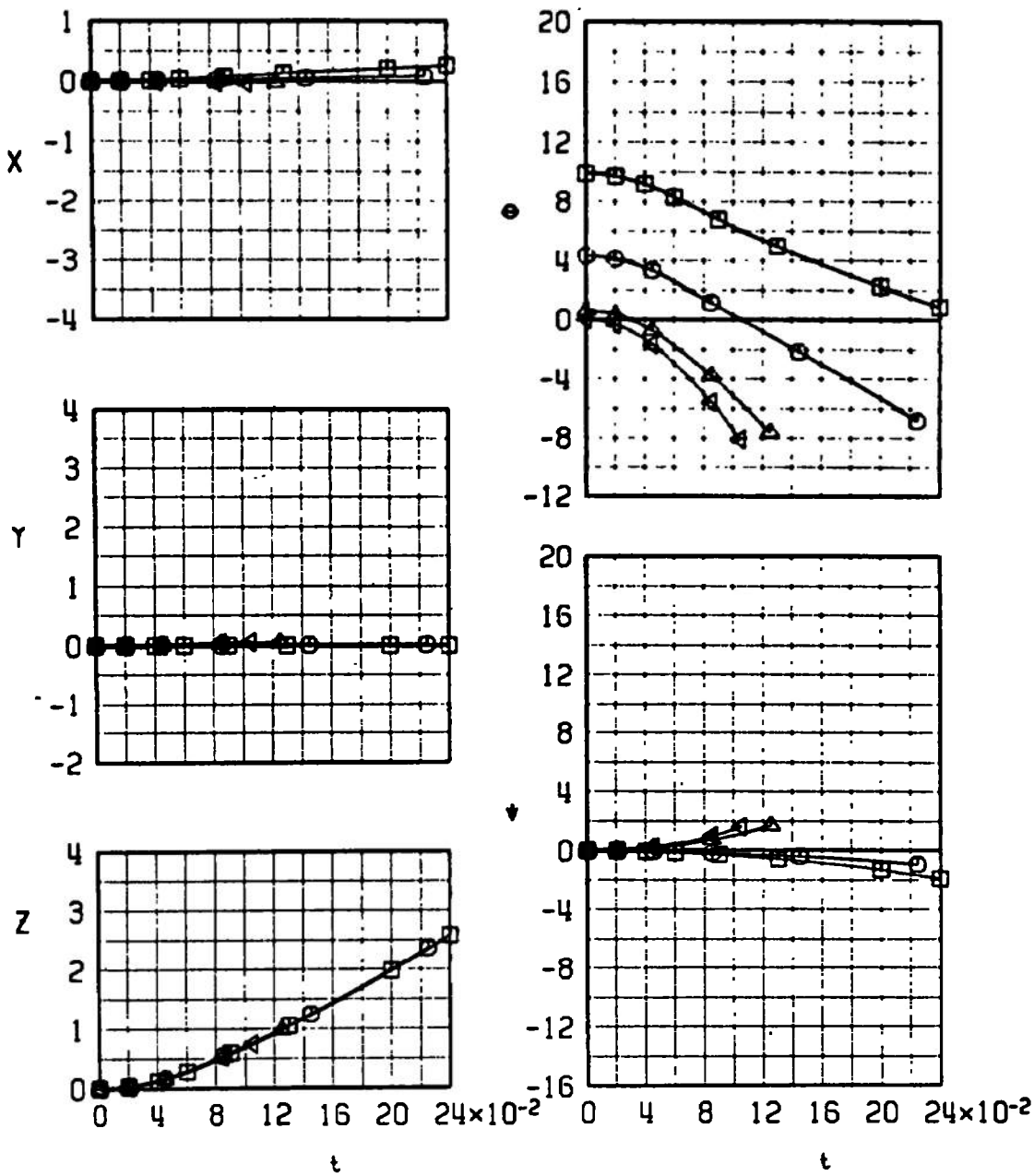

c. Configuration 3L, Ejector 10
Fig. 21 Continued

SYMBOL	CONF	M_∞	α
⊡	3L	0.325	12.9
⊙	3L	0.814	3.0

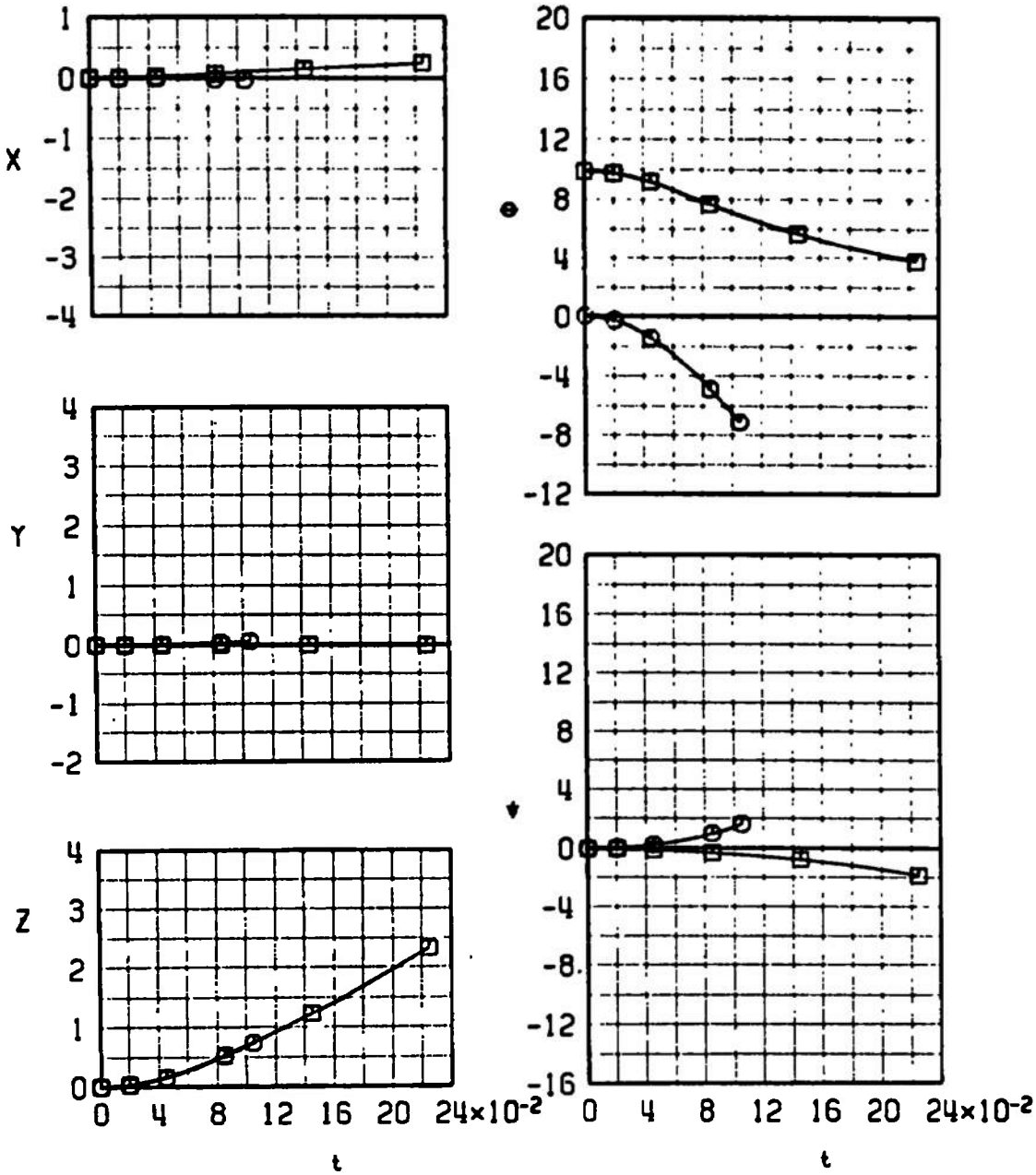

d. Configuration 3L, Ejector 13
Fig. 21 Continued

SYMBOL	CONF	M_∞	α
□	3R	0.407	8.6
○	3R	0.732	3.4

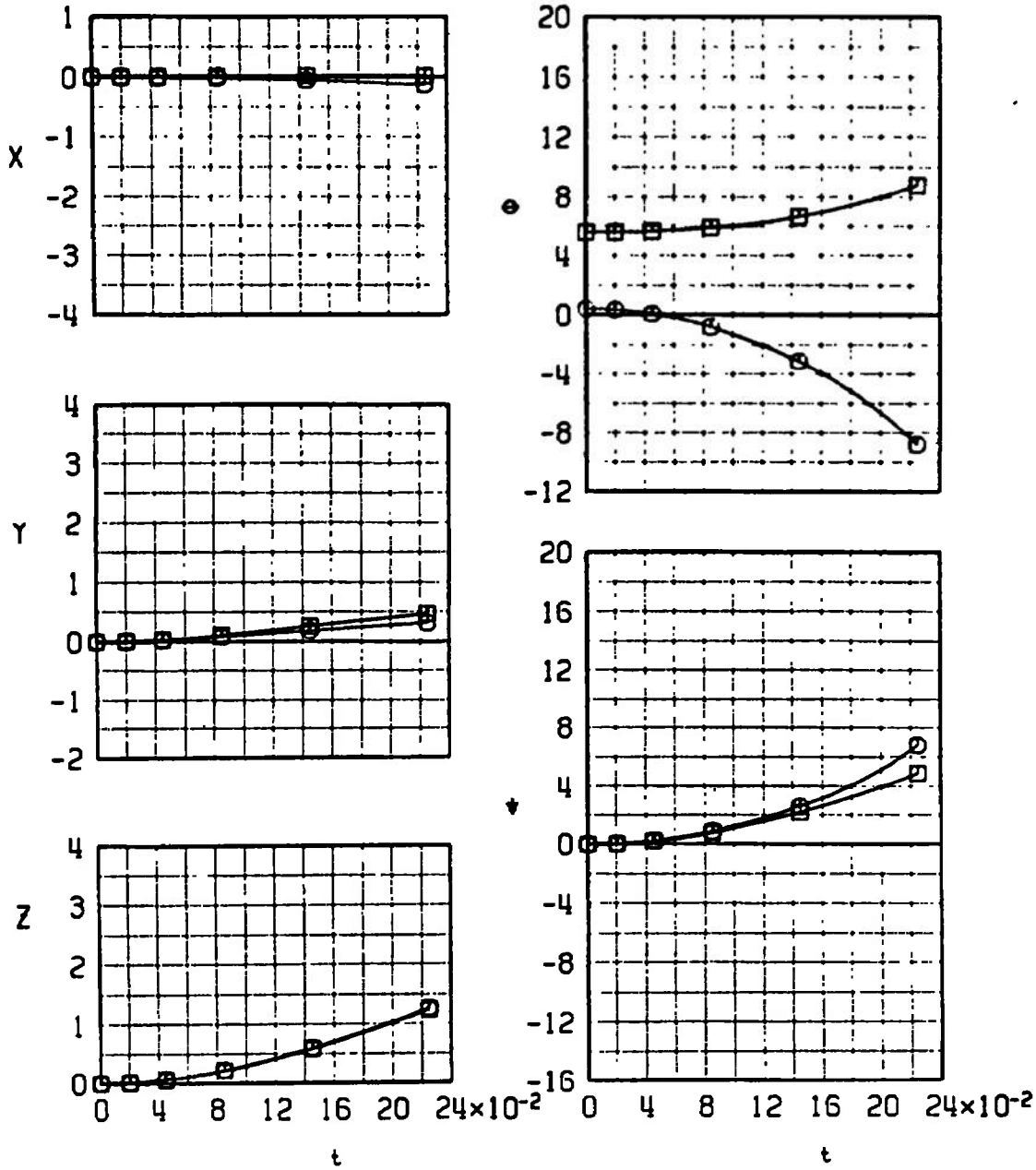

e. Configuration 3R, Ejector 7
Fig. 21 Concluded

SYMBOL	CONF	M_∞	α
□	2L	0.407	8.6
○	2L	0.569	4.9
△	2L	0.732	3.4

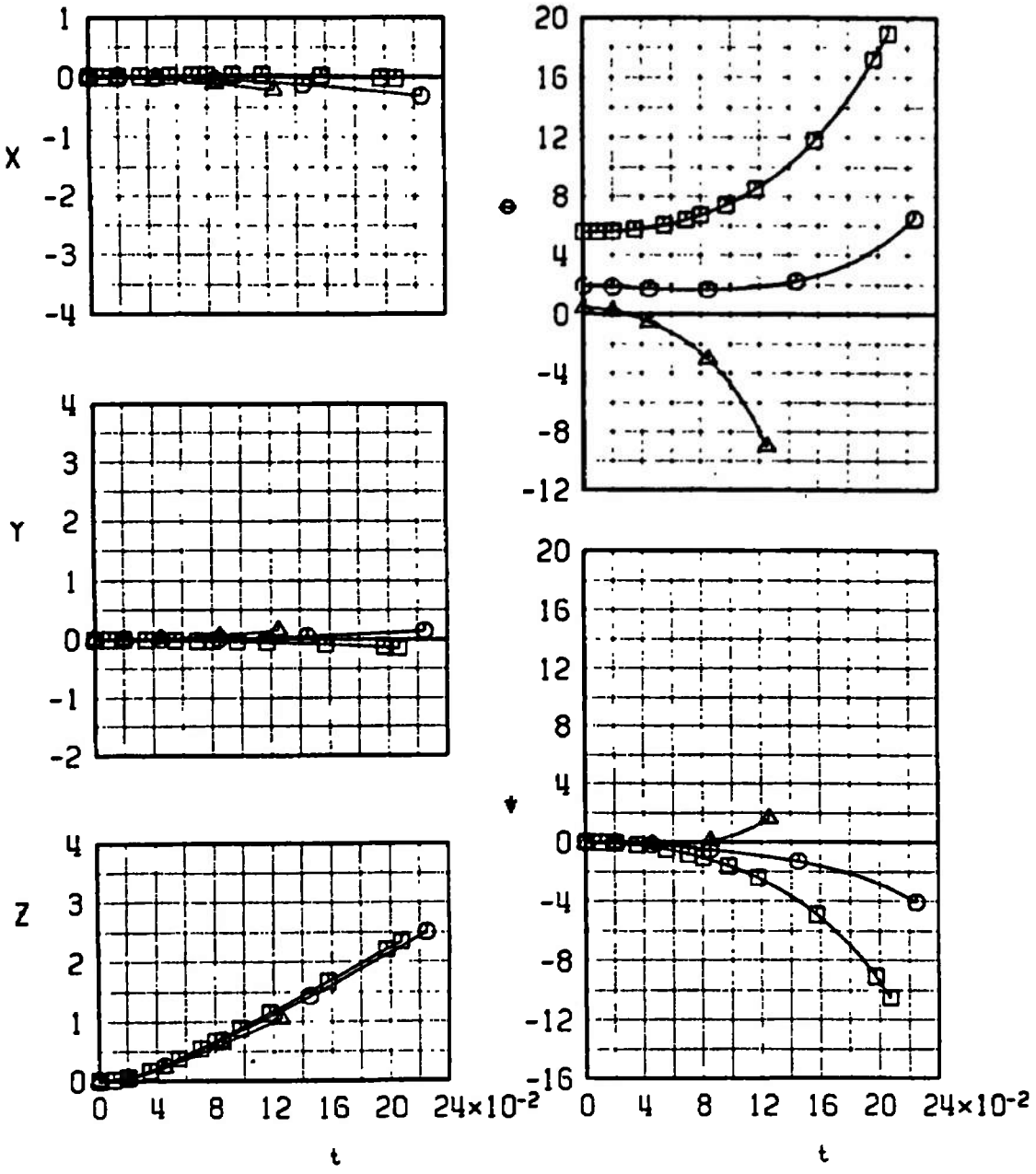

a. Configuration 2L, Ejector 5

Fig. 22 Trajectory Data for the Expended CBU-12A/A or CBU-46/A Store

SYMBOL	CONF	M_∞	α
□	2R	0.407	8.6
○	2R	0.569	4.9
△	2R	0.732	3.4

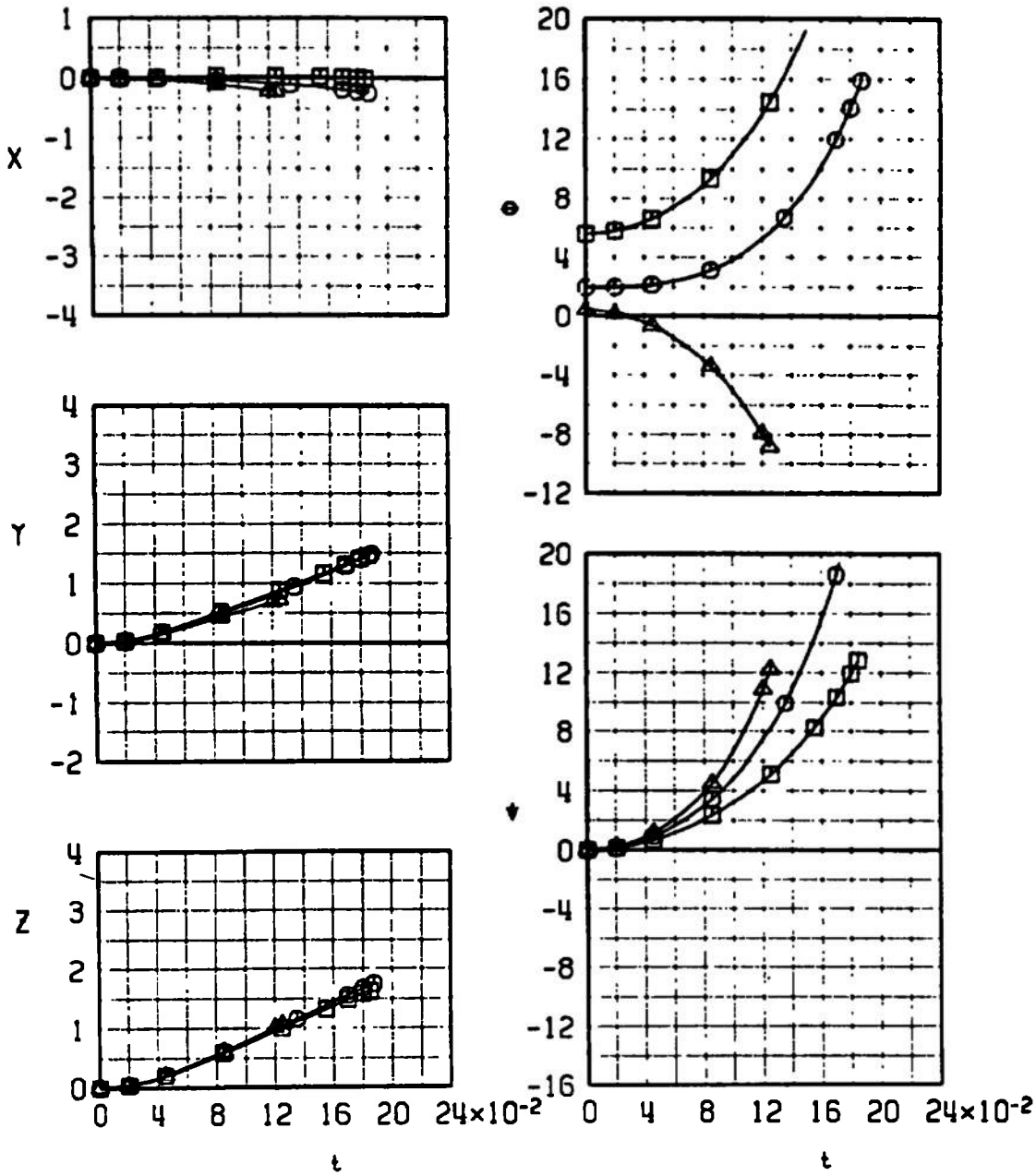

b. Configuration 2R, Ejector 5
Fig. 22 Continued

SYMBOL	CONF	M_∞	α
□	3L	0.325	12.9
○	3L	0.447	7.3
△	3L	0.692	3.6
◁	3L	0.814	3.0

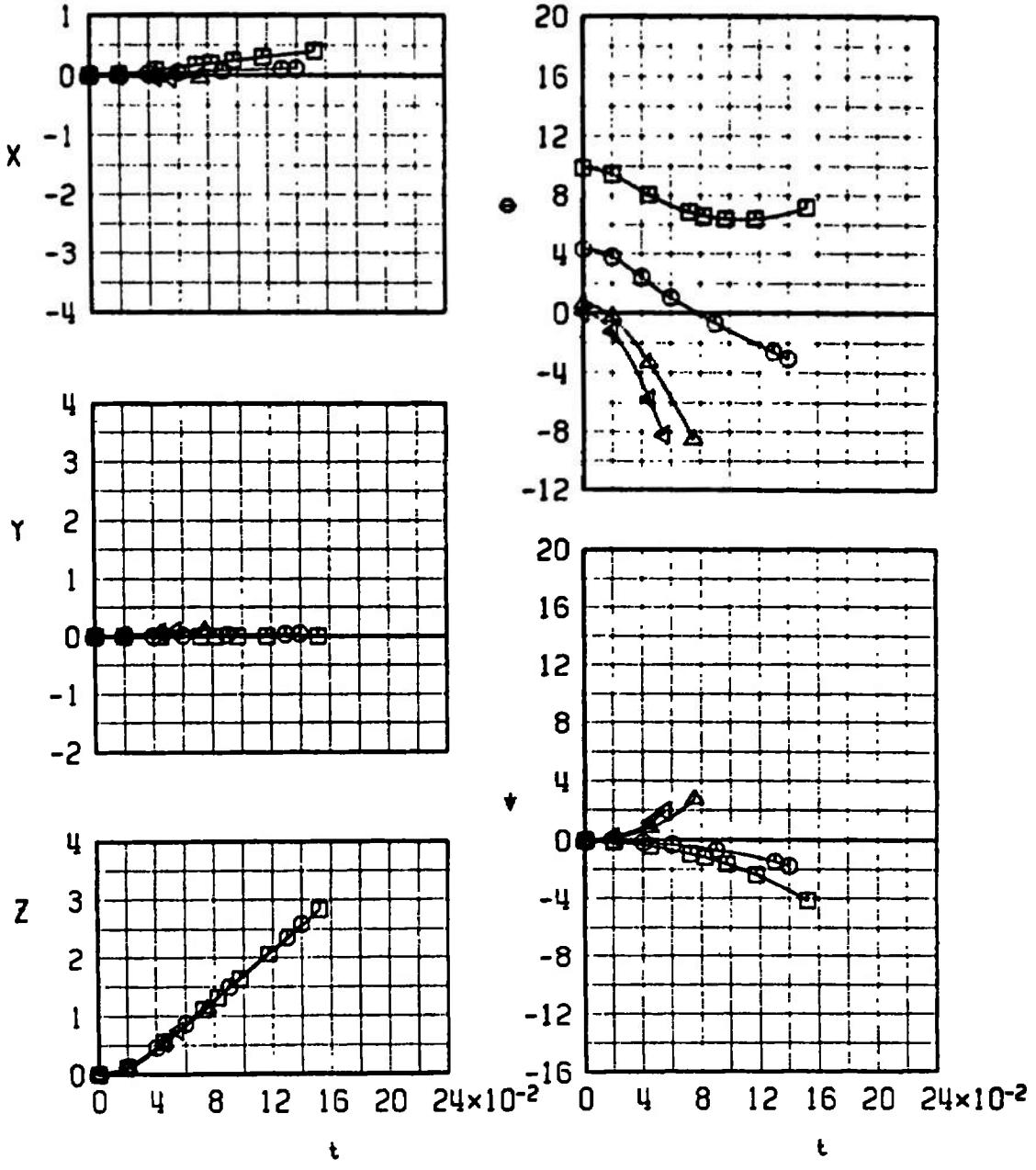

c. Configuration 3L, Ejector 8
Fig. 22 Continued

SYMBOL	CONF	M_∞	α
□	3L	0.325	12.9
○	3L	0.814	3.0

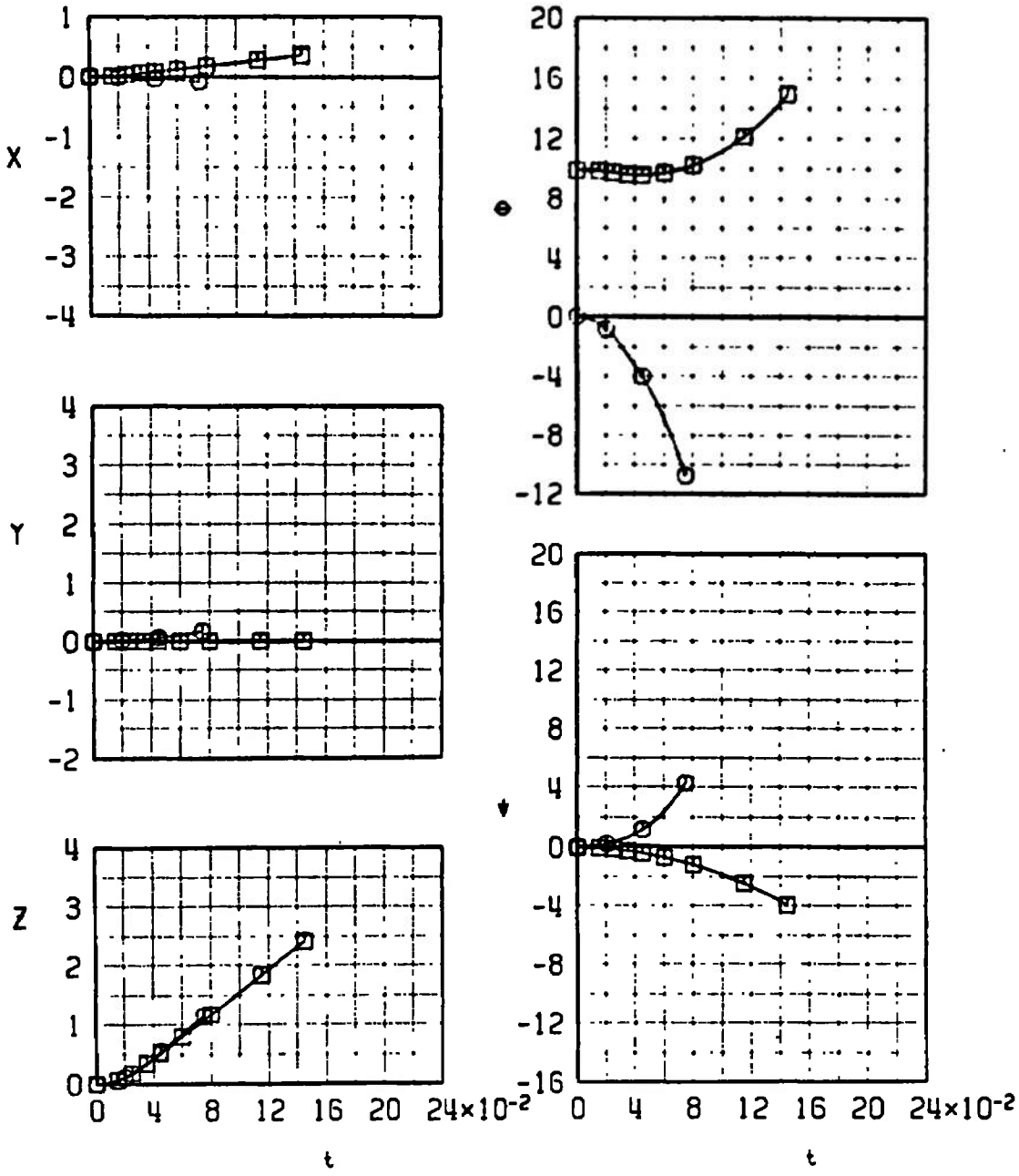

d. Configuration 3L, Ejector 11
Fig. 22 Continued

SYMBOL	CONF	M_∞	α
□	3R	0.407	8.6
○	3R	0.732	3.4

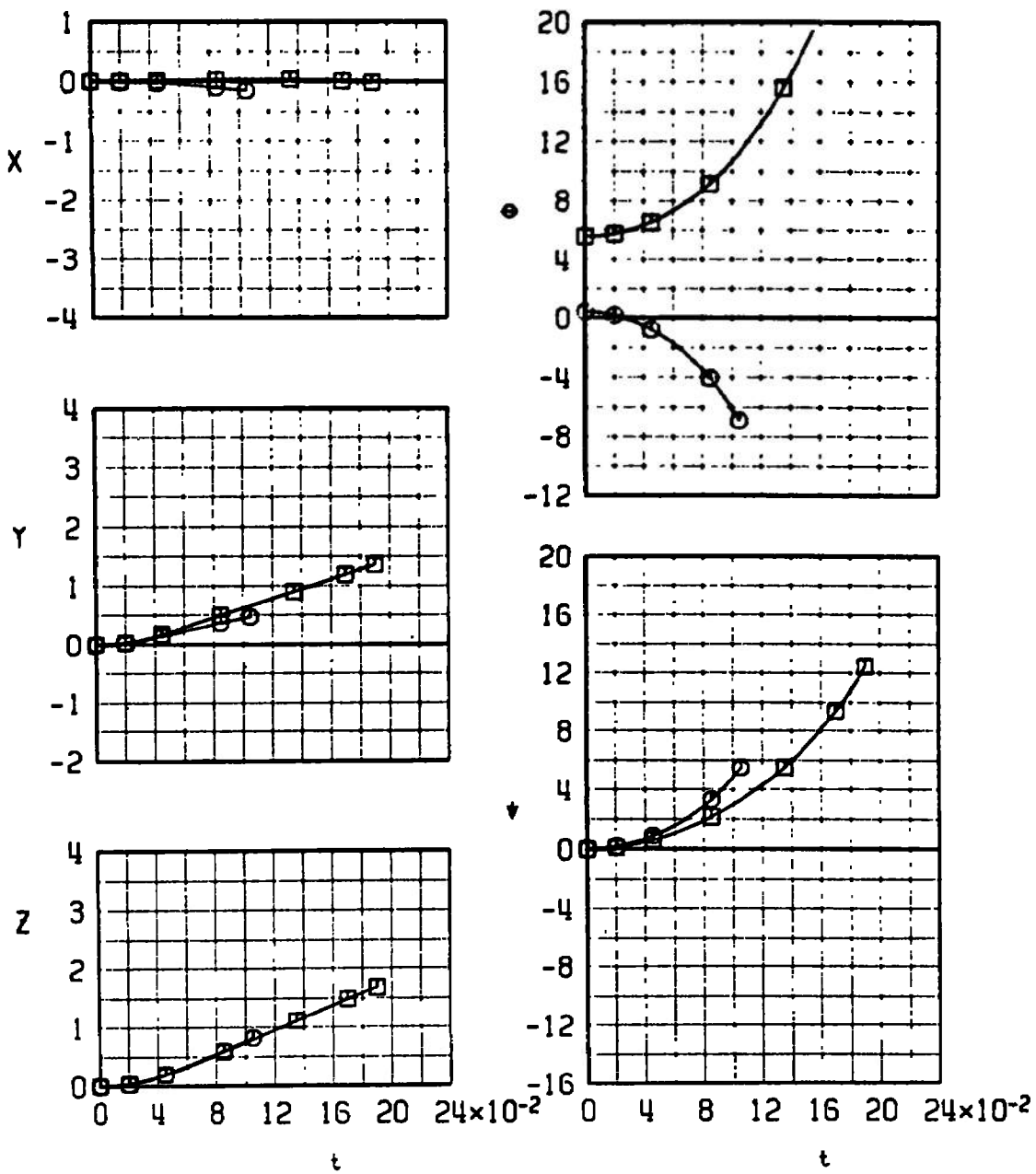

e. Configuration 3R, Ejector 5
Fig. 22 Concluded

SYMBOL	CONF	M_∞	α
□	14L	0.407	8.6
○	14L	0.569	4.9
△	14L	0.732	3.4

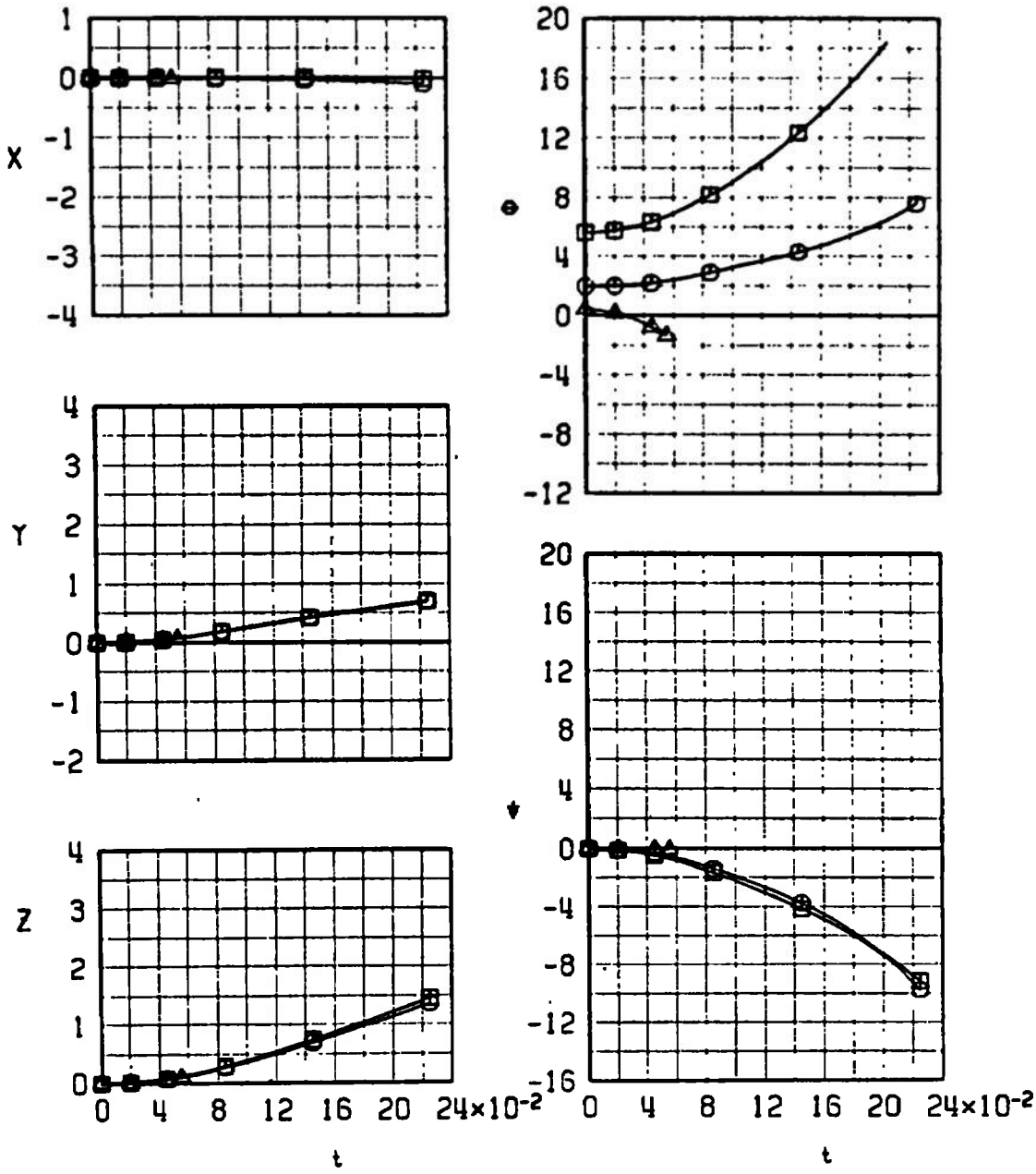

a. Configuration 14L, Ejector 15

Fig. 23 Trajectory Data for the Loaded LAU-3/A Store

SYMBOL	CONF	M_∞	α
□	15R	0.407	8.6
○	15R	0.569	4.9
△	15R	0.732	3.4

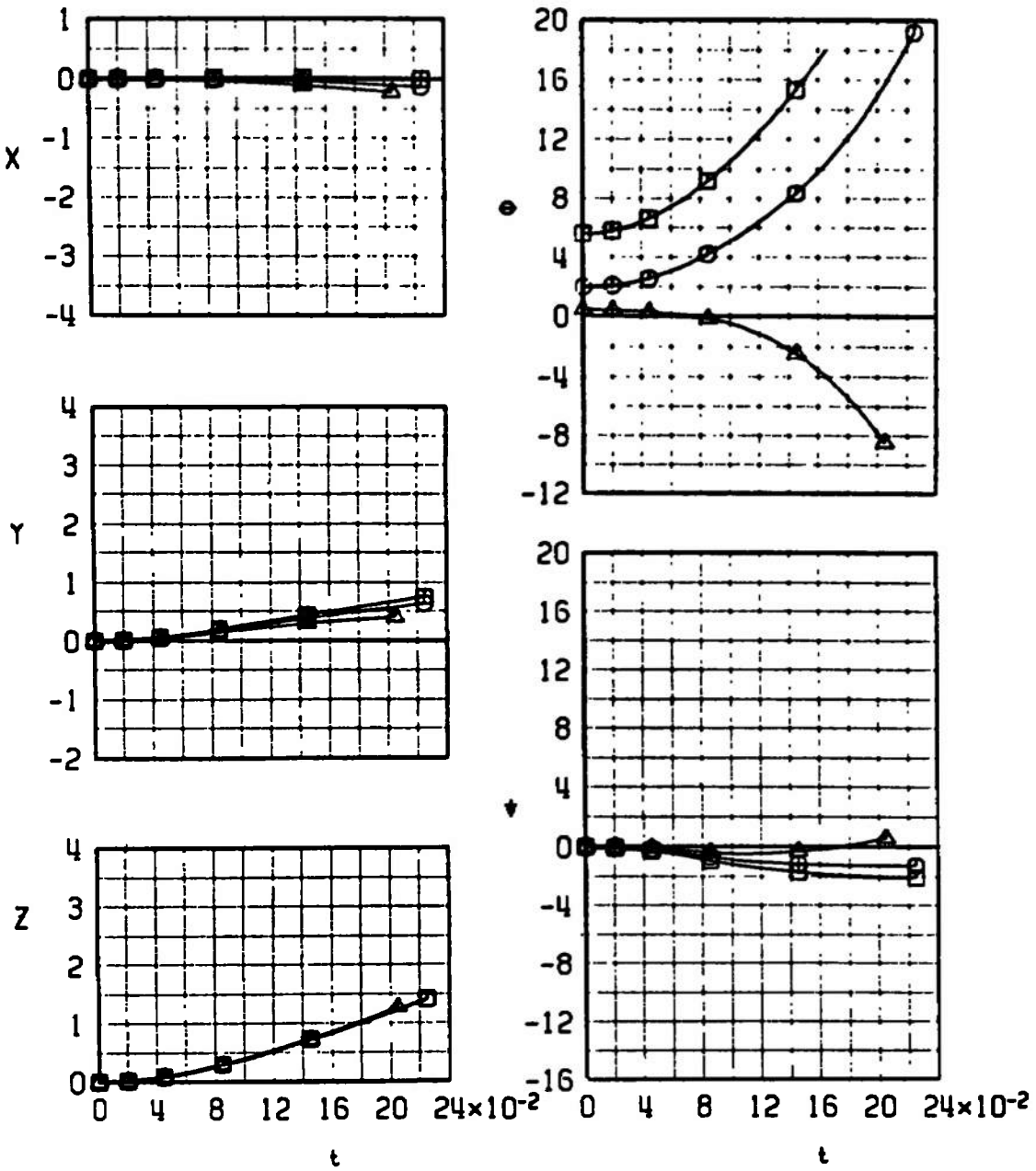

b. Configuration 15R, Ejector 15
Fig. 23 Continued

SYMBOL	CONF	M_∞	α
□	16L	0.407	8.6
○	16L	0.569	4.9
△	16L	0.732	3.4

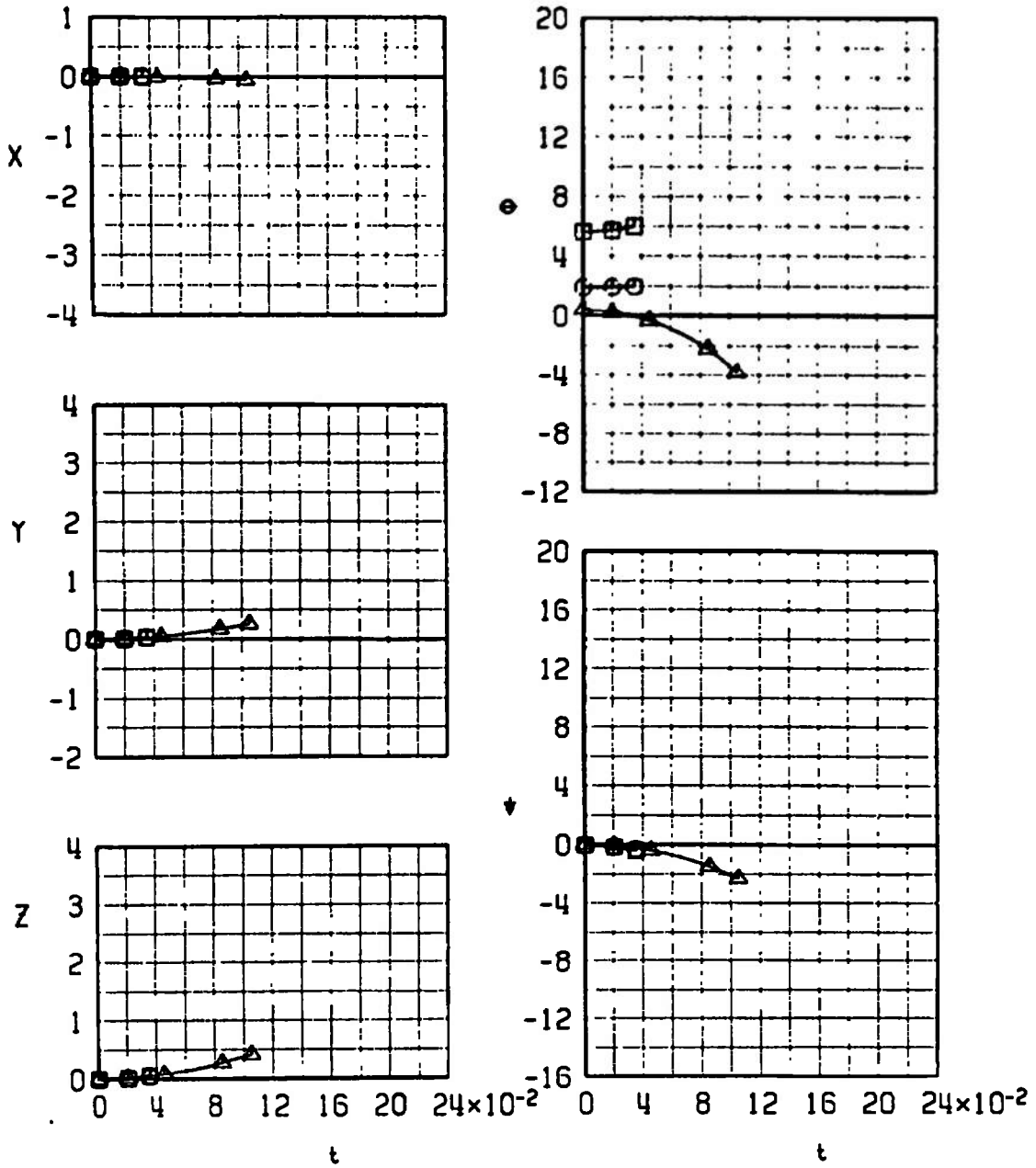

c. Configuration 16L, Ejector 15
Fig. 23 Continued

SYMBOL	CONF	M_∞	α
⊡	16R	0.407	8.6
⊙	16R	0.569	4.9
△	16R	0.732	3.4

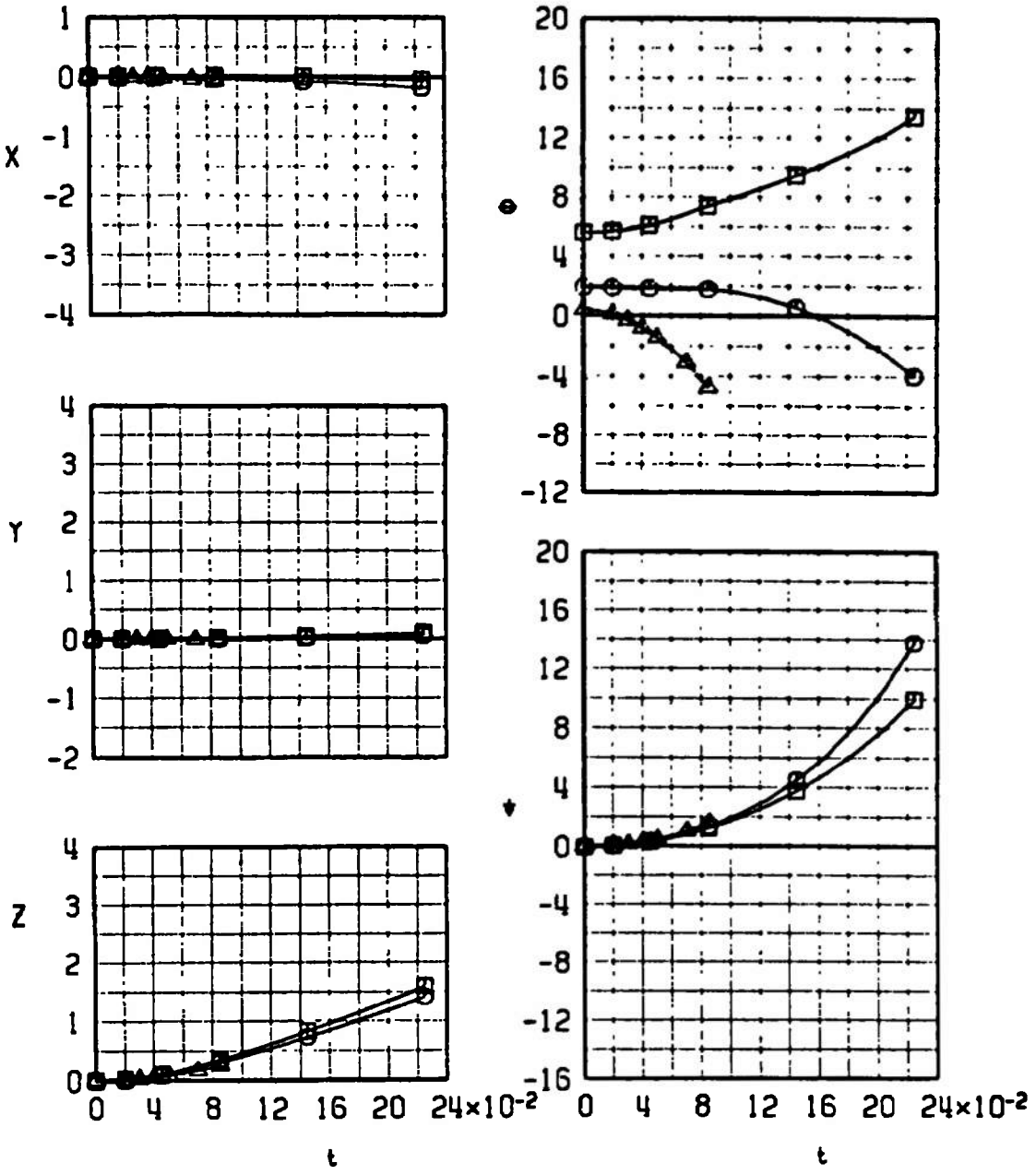

d. Configuration 16R, Ejector 15
Fig. 23 Continued

SYMBOL	CONF	M_∞	α
⊡	20L	0.407	8.6
⊙	20L	0.569	4.9

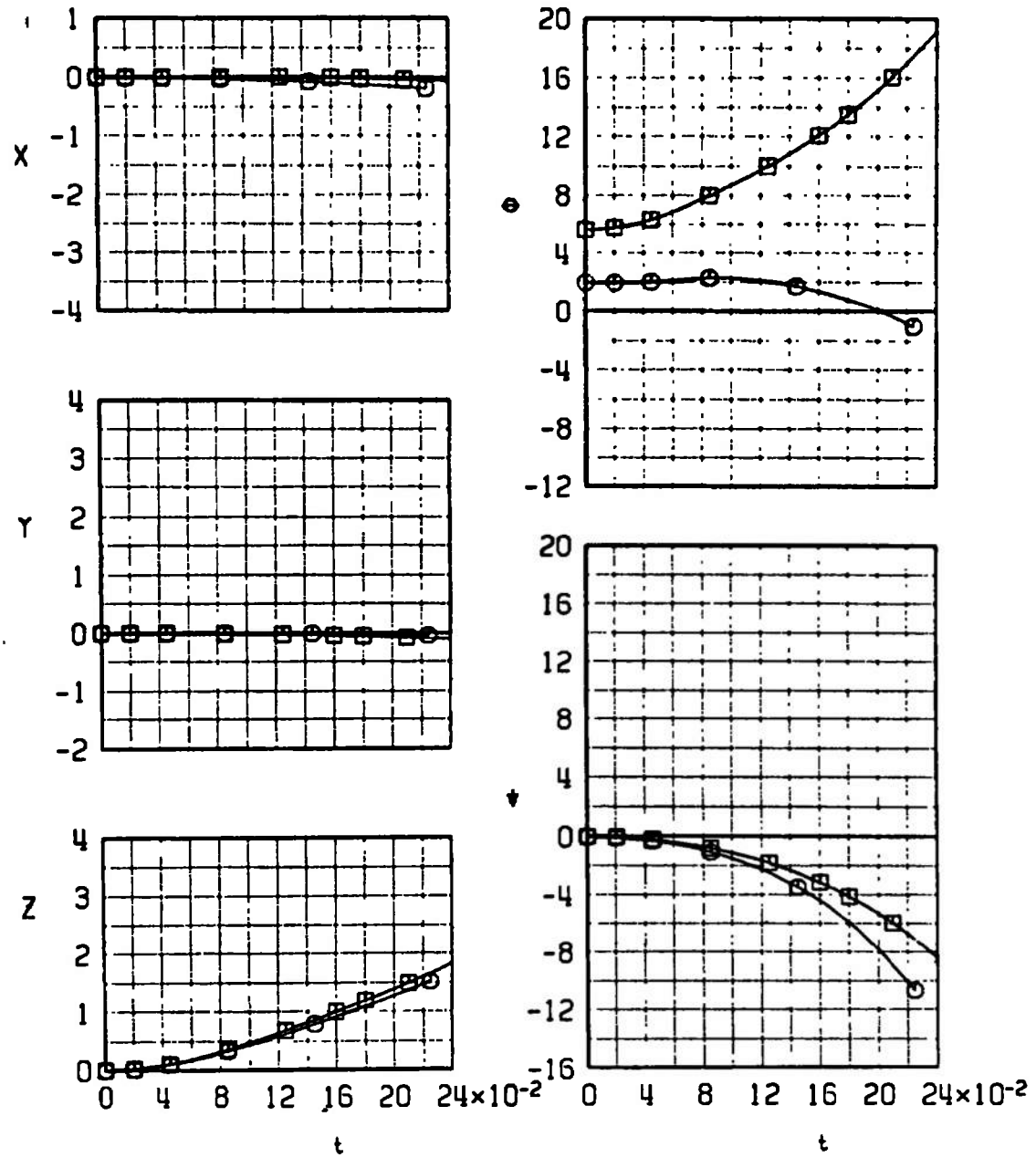

e. Configuration 20L, Ejector 15
Fig. 23 Continued

SYMBOL	CONF	M_∞	α
⊡	20R	0.407	8.6
⊙	20R	0.569	4.9

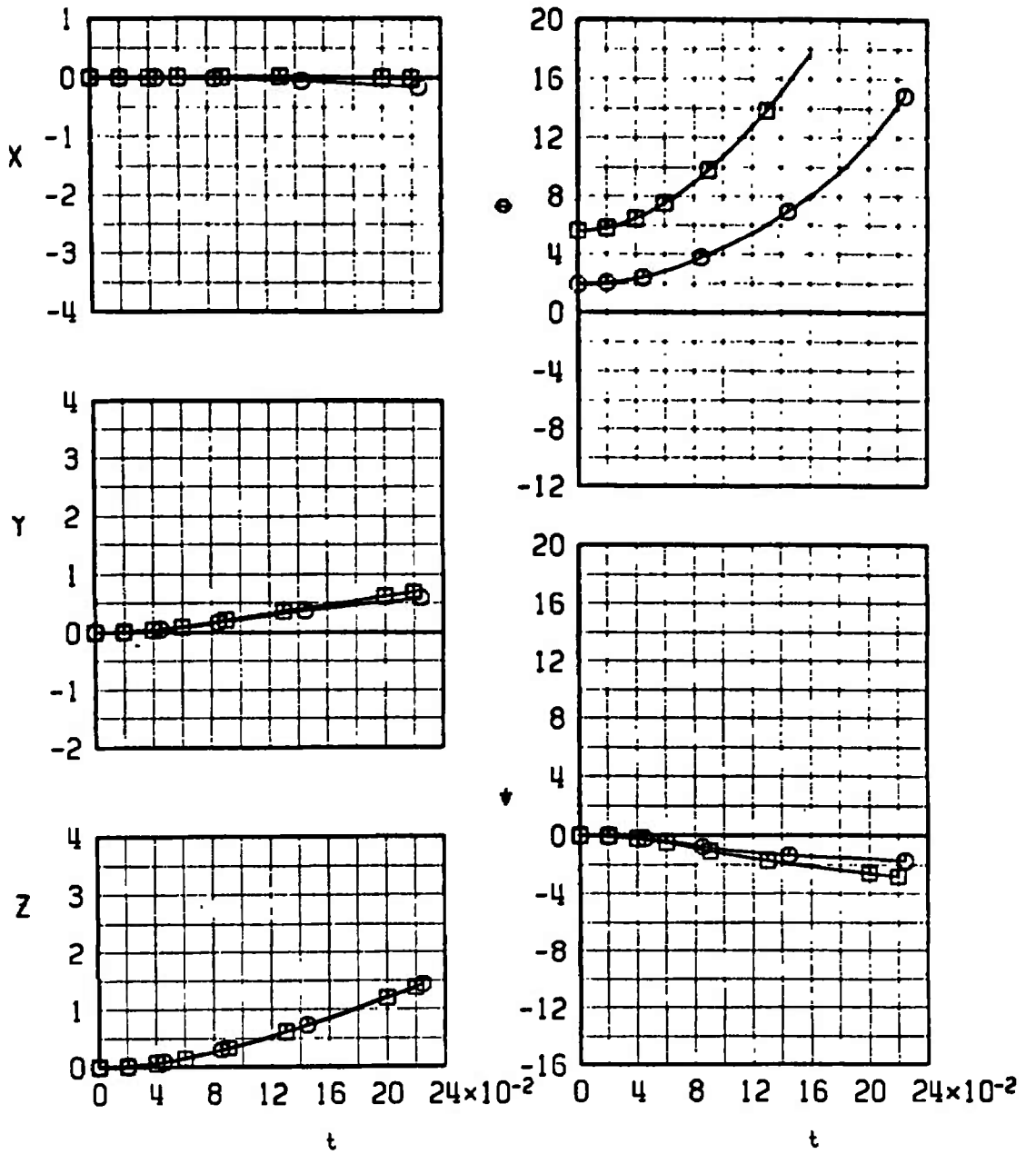

f. Configuration 20R, Ejector 15
Fig. 23 Continued

SYMBOL	CONF	M_∞	α
□	13L	0.407	8.6
○	13L	0.569	4.9
△	13L	0.732	3.4

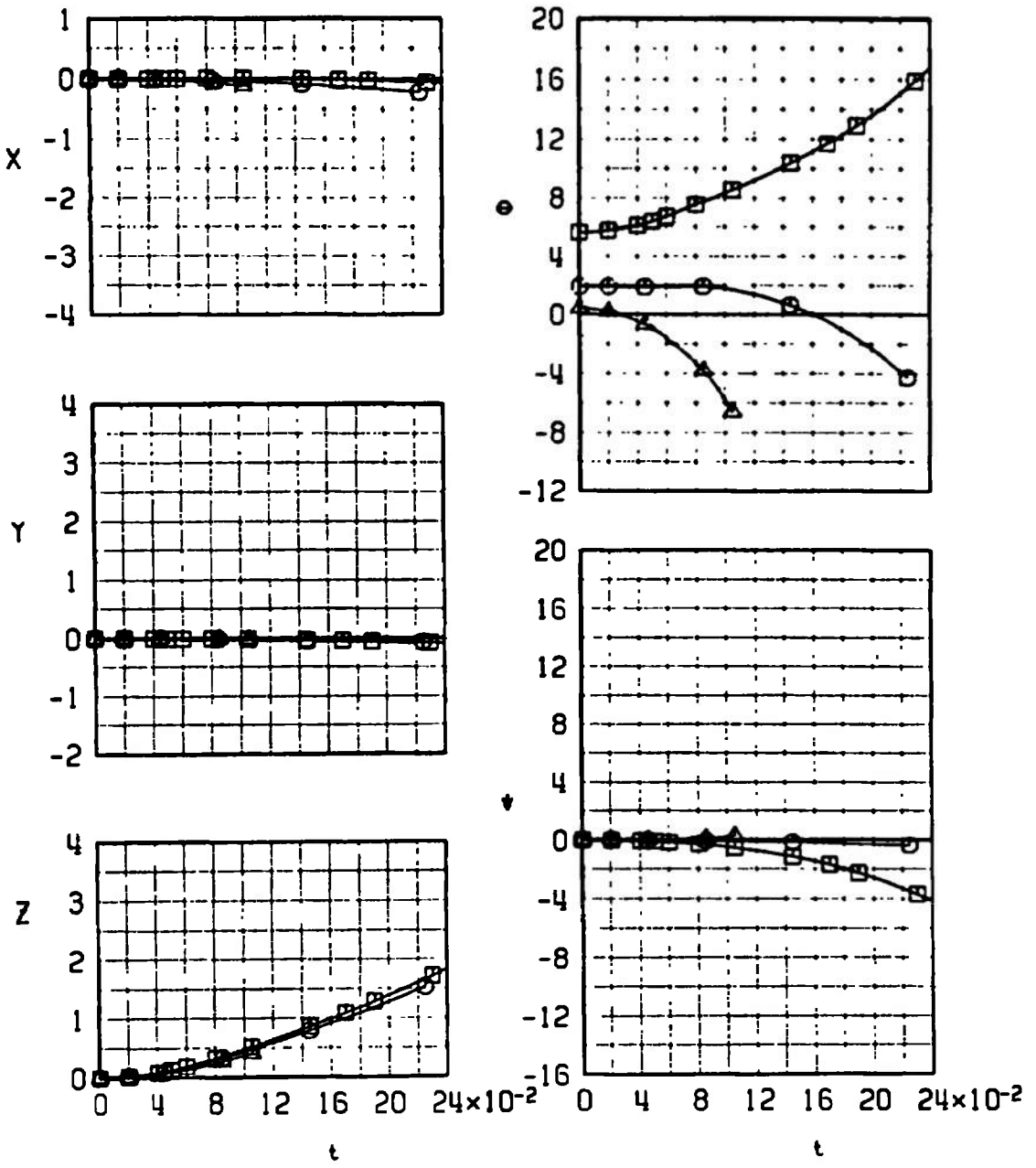

g. Configuration 13L, Ejector 15
Fig. 23 Continued

SYMBOL	CONF	M_∞	α
⊡	13R	0.407	8.6
⊙	13R	0.569	4.9
△	13R	0.732	3.4

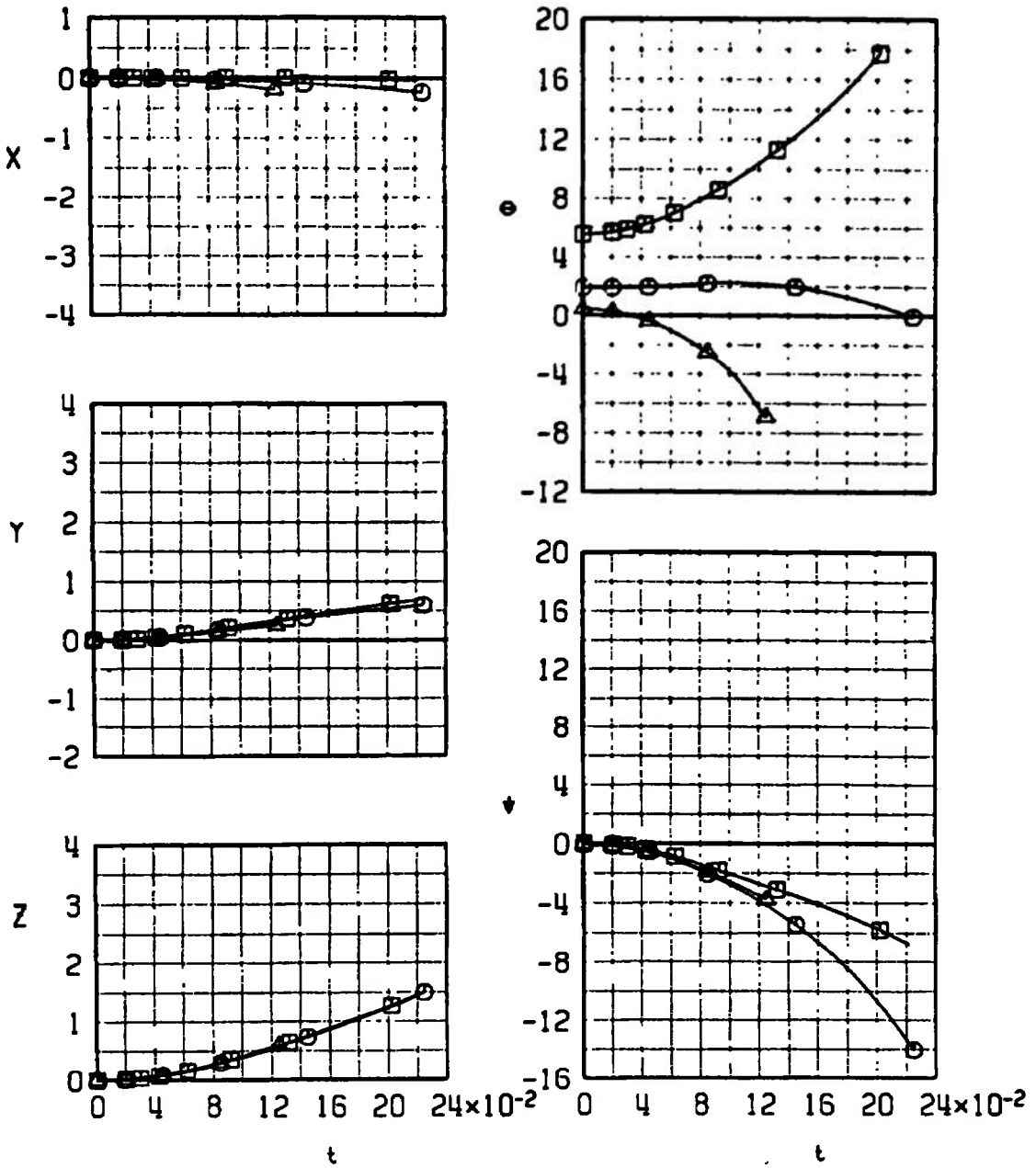

h. Configuration 13R, Ejector 15
Fig. 23 Continued

SYMBOL	CONF	M_∞	α
□	12L	0.407	8.6
○	12L	0.651	3.9
△	12L	0.773	3.2

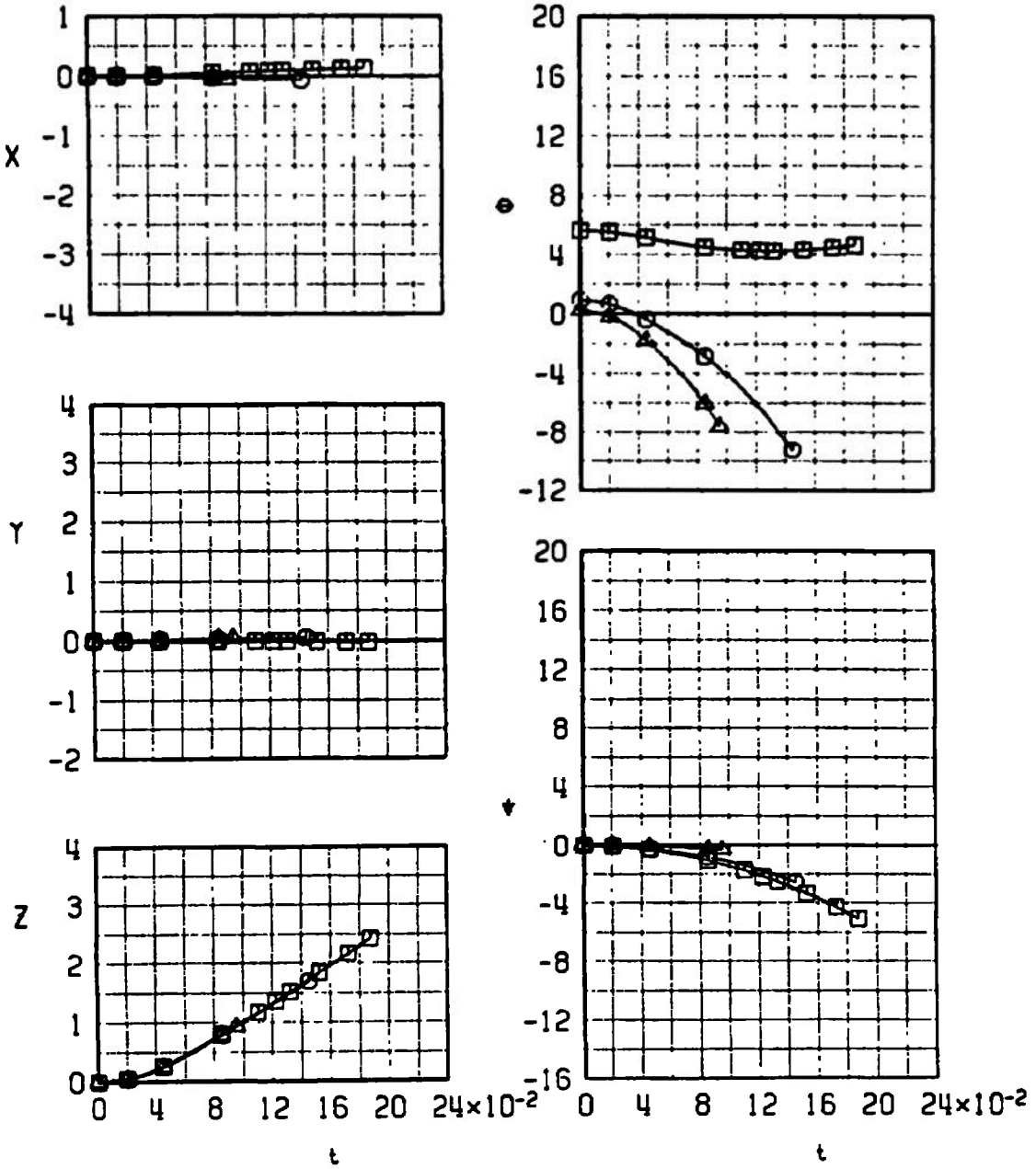

i. Configuration 12L, Ejector 17
Fig. 23 Continued

SYMBOL	CONF	M_∞	α
□	12R	0.407	8.6
○	12R	0.651	3.9
△	12R	0.773	3.2

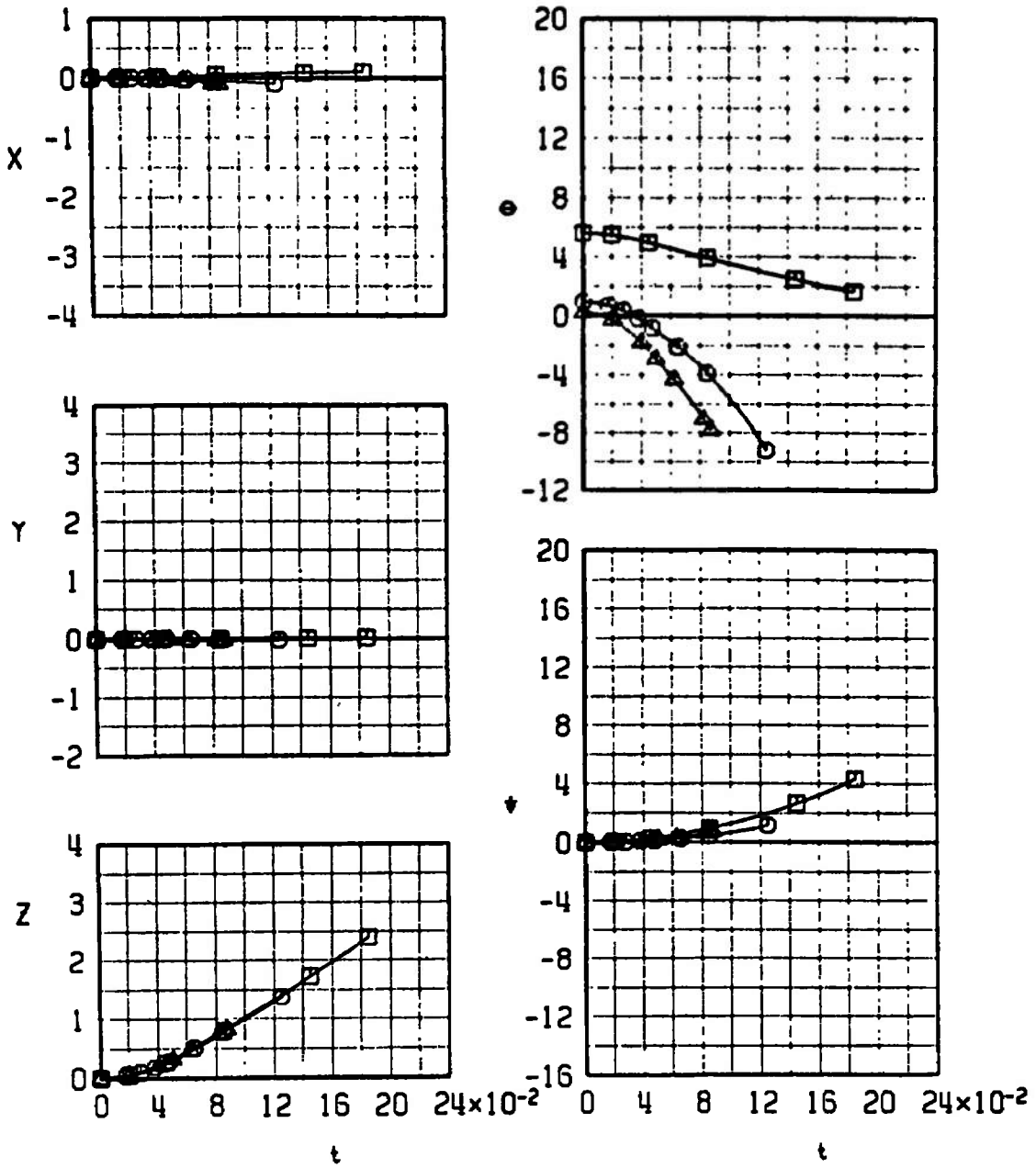

j. Configuration 12R, Ejector 17
Fig. 23 Concluded

SYMBOL	CONF	M_∞	α
⊡	4L	0.407	8.6
⊙	4L	0.569	4.9
△	4L	0.732	3.4

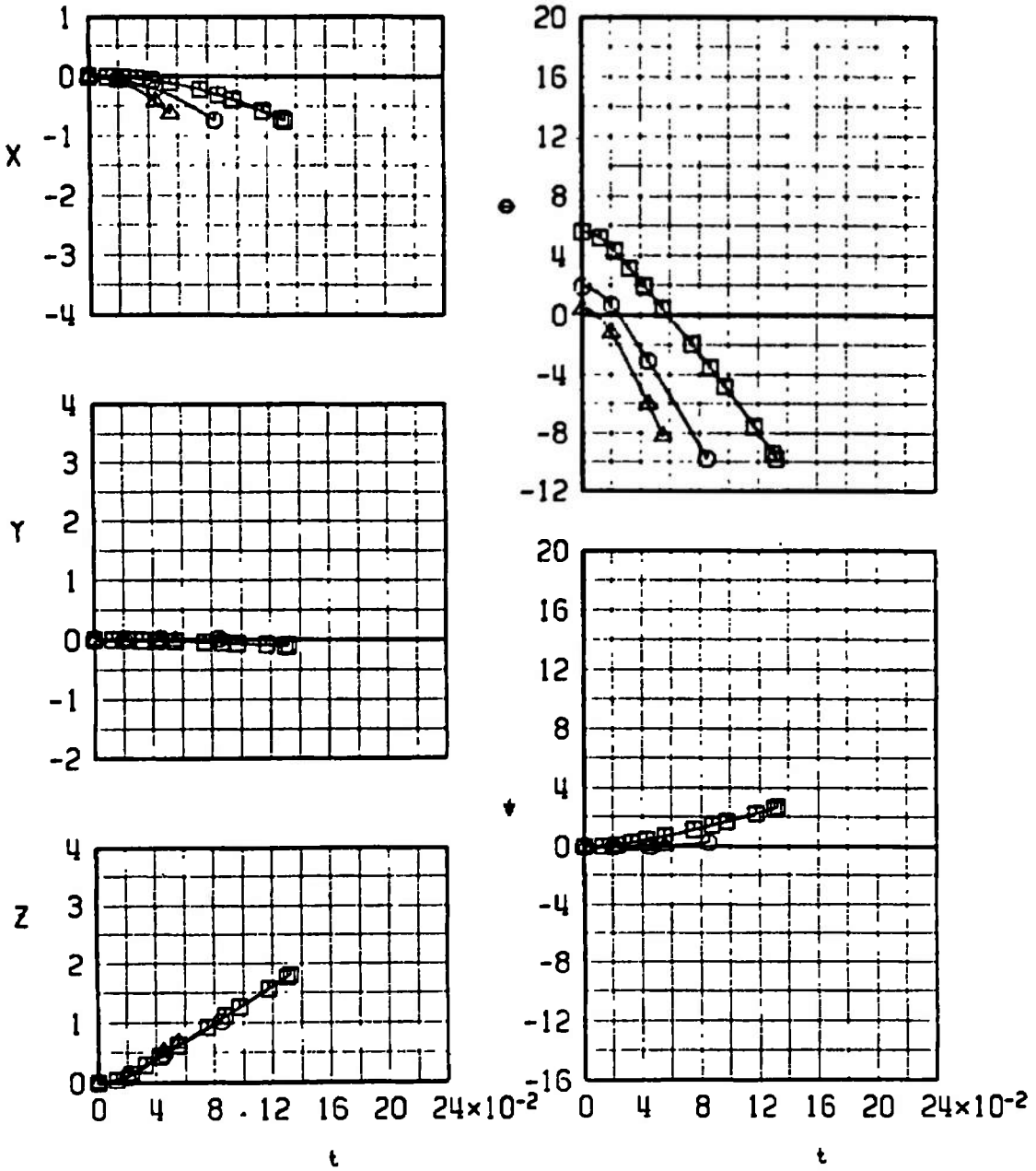

a. Configuration 4L, Ejector 14

Fig. 24 Trajectory Data for the Expended LAU-3/A Store

SYMBOL	CONF	M_∞	α
□	4R	0.407	8.6
○	4R	0.569	4.9
△	4R	0.732	3.4

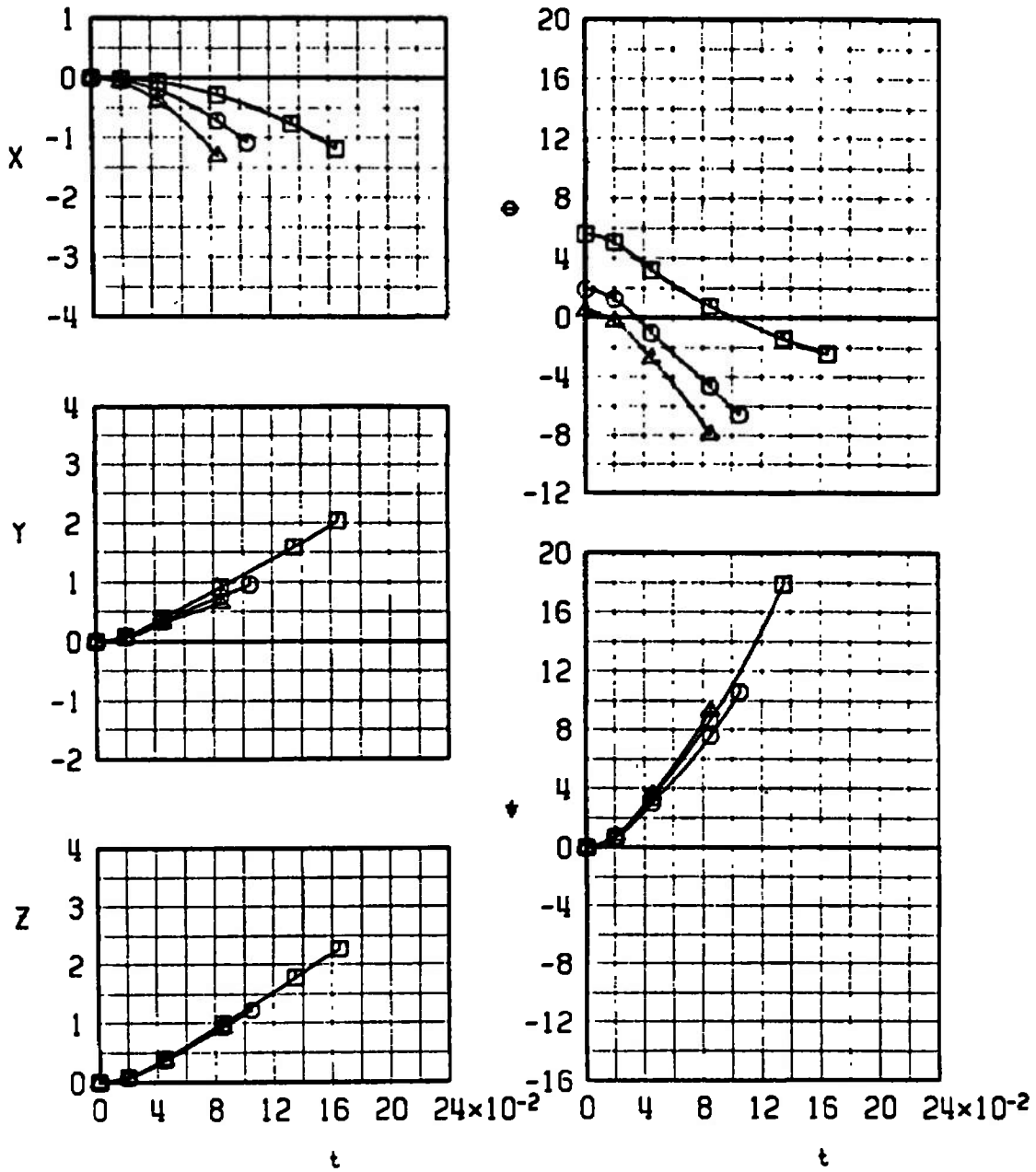

b. Configuration 4R, Ejector 14
Fig. 24 Continued

SYMBOL	CONF	M_∞	α
□	5L	0.407	8.6
○	5L	0.569	4.9
△	5L	0.732	3.4

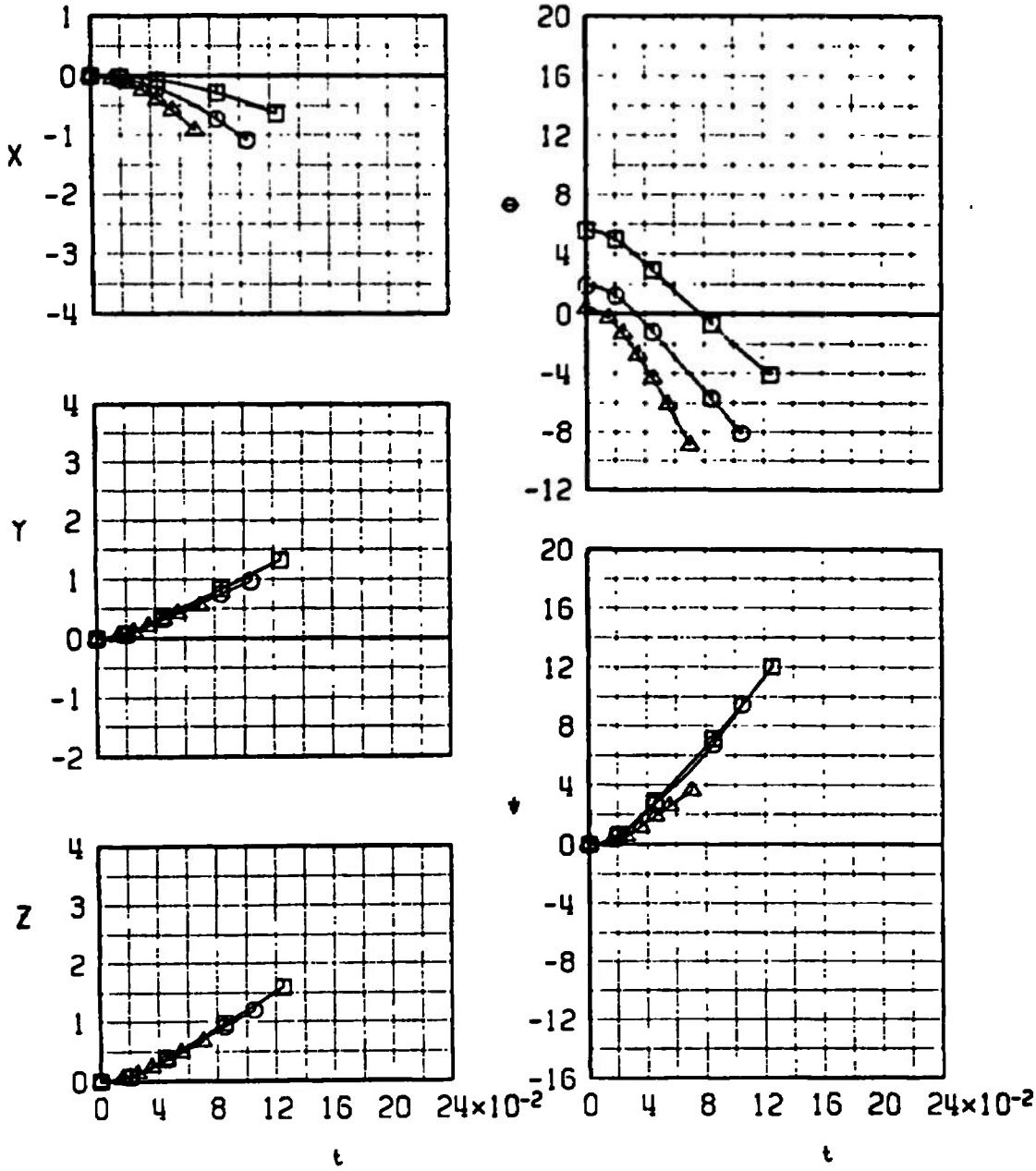

c. Configuration 5L, Ejector 14
Fig. 24 Continued

SYMBOL	CONF	M_∞	α
□	5R	0.407	8.6
○	5R	0.569	4.9

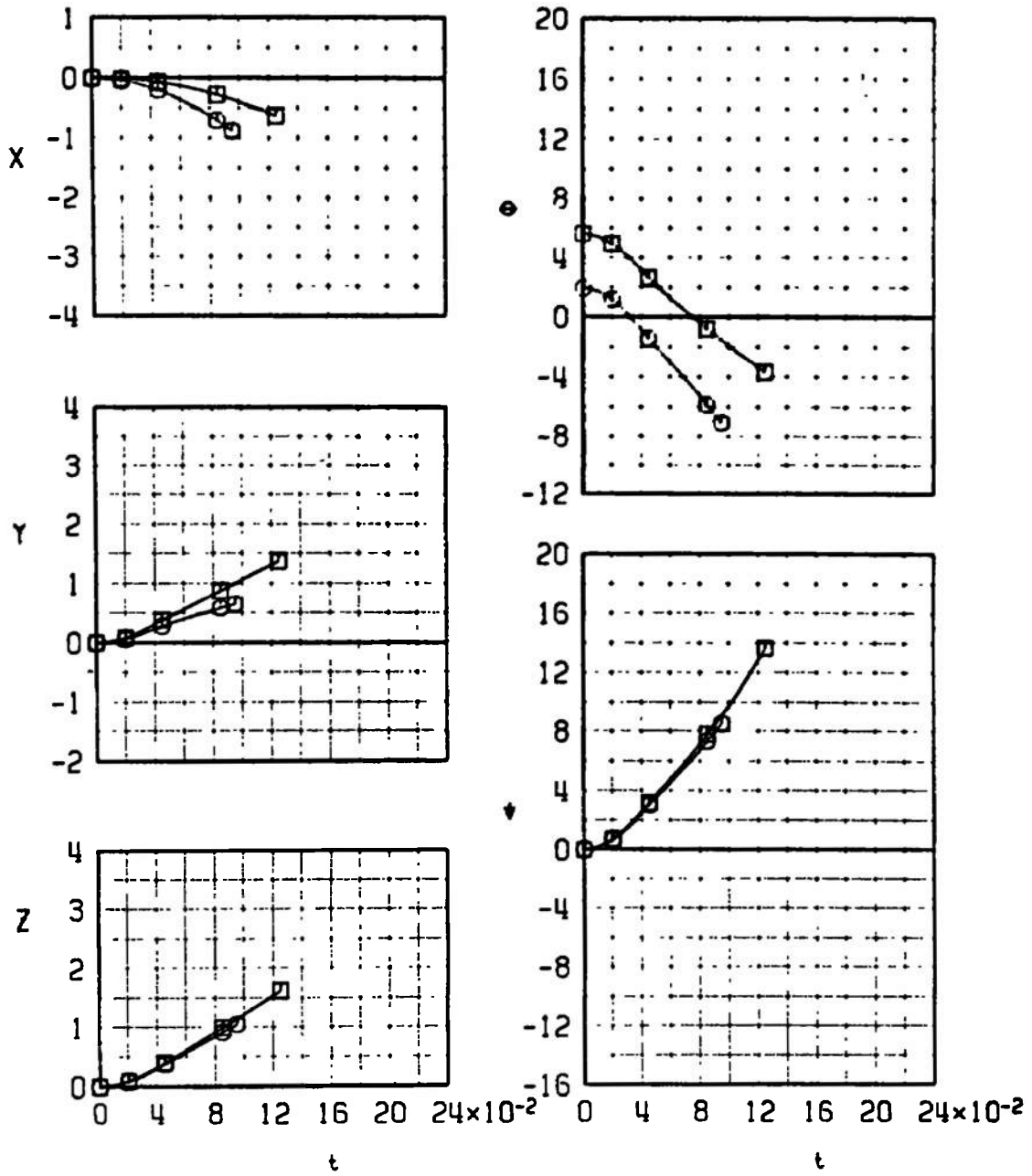

d. Configuration 5R, Ejector 14
Fig. 24 Continued

SYMBOL	CONF	M_∞	α
□	18L	0.407	8.6
○	18L	0.569	4.9
△	18L	0.732	3.4

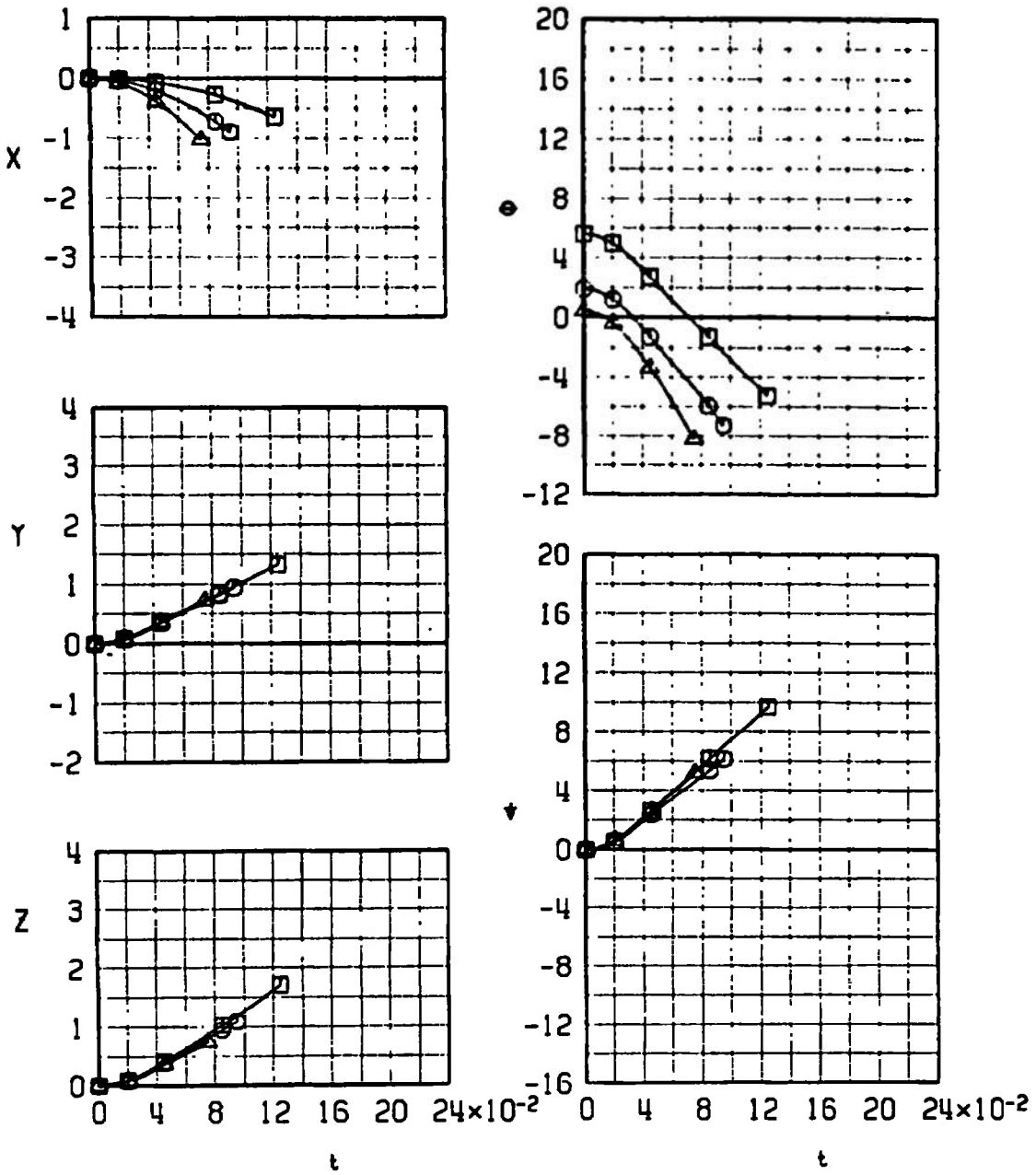

e. Configuration 18L, Ejector 14
Fig. 24 Continued

SYMBOL	CONF	M_∞	α
□	18R	0.407	8.6
○	18R	0.569	4.9
△	18R	0.732	3.4

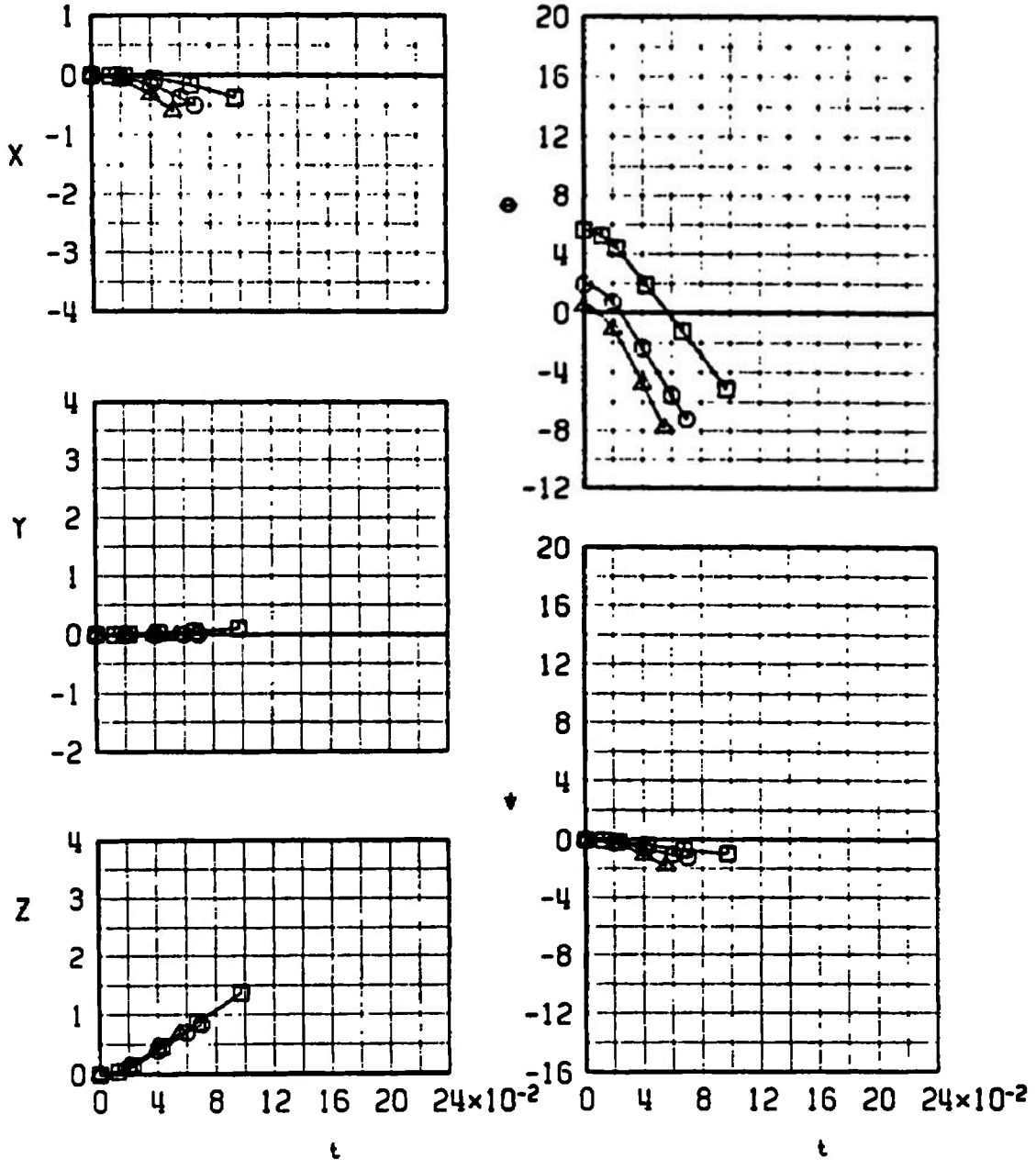

f. Configuration 18R, Ejector 14
Fig. 24 Continued

SYMBOL	CONF	M_∞	α
□	19L	0.407	8.6
○	19L	0.569	4.9

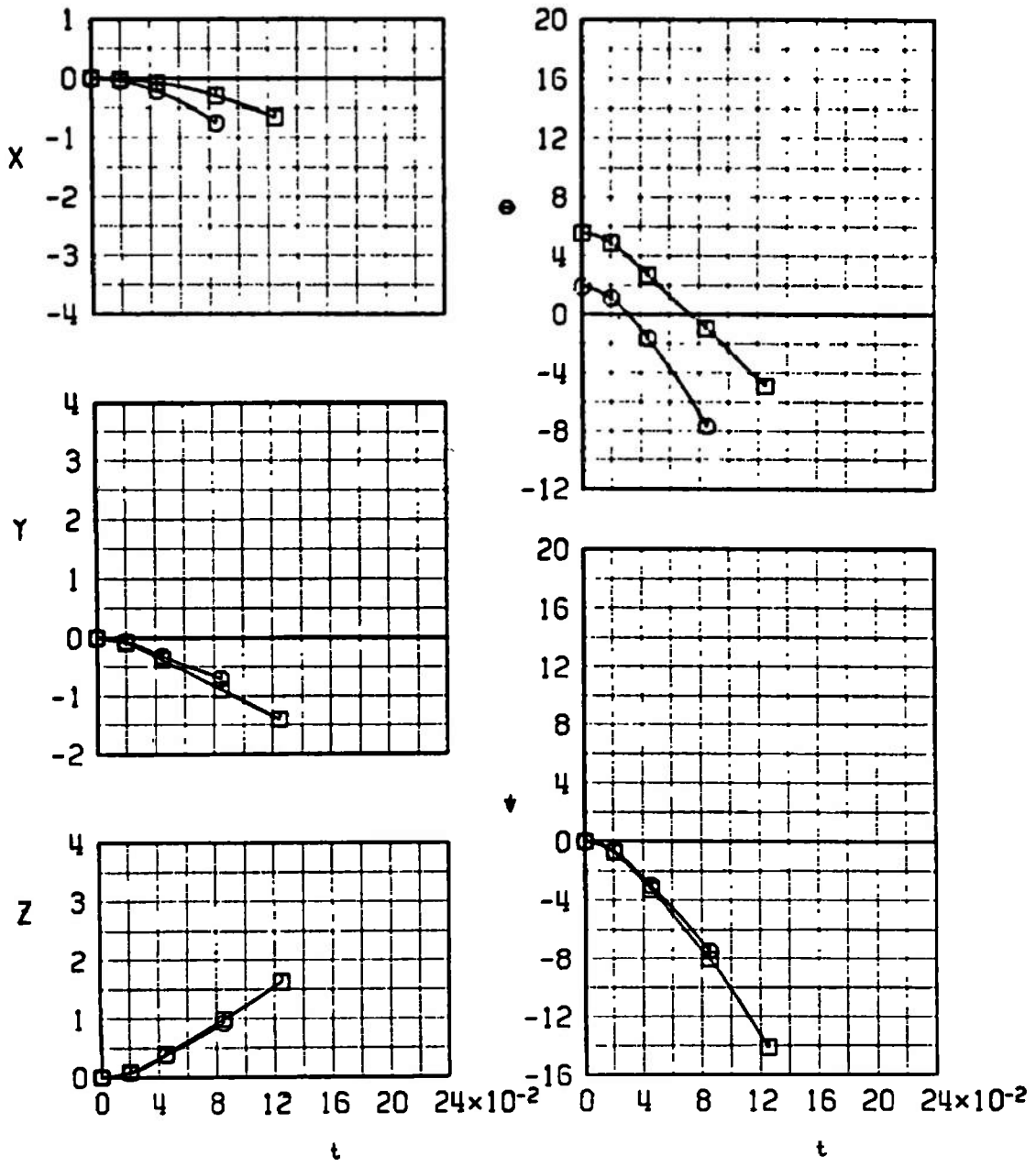

g. Configuration 19L, Ejector 14
Fig. 24 Continued

SYMBOL	CONF	M_∞	α
□	19R	0.407	8.6
○	19R	0.569	4.9

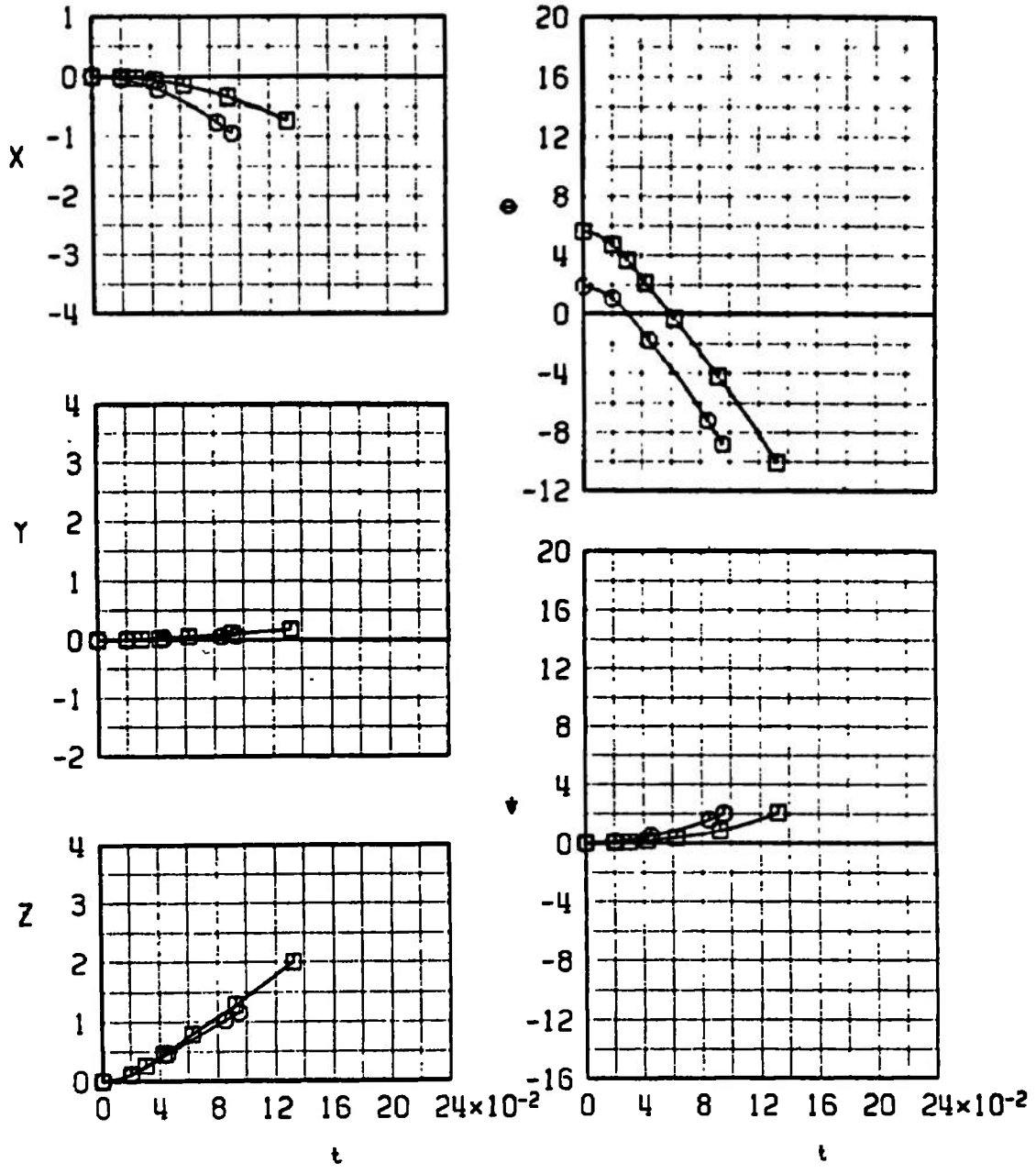

h. Configuration 19R, Ejector 14
Fig. 24 Continued

SYMBOL	CONF	M_∞	α
□	6L	0.407	8.6
○	6L	0.569	4.9
△	6L	0.732	3.4

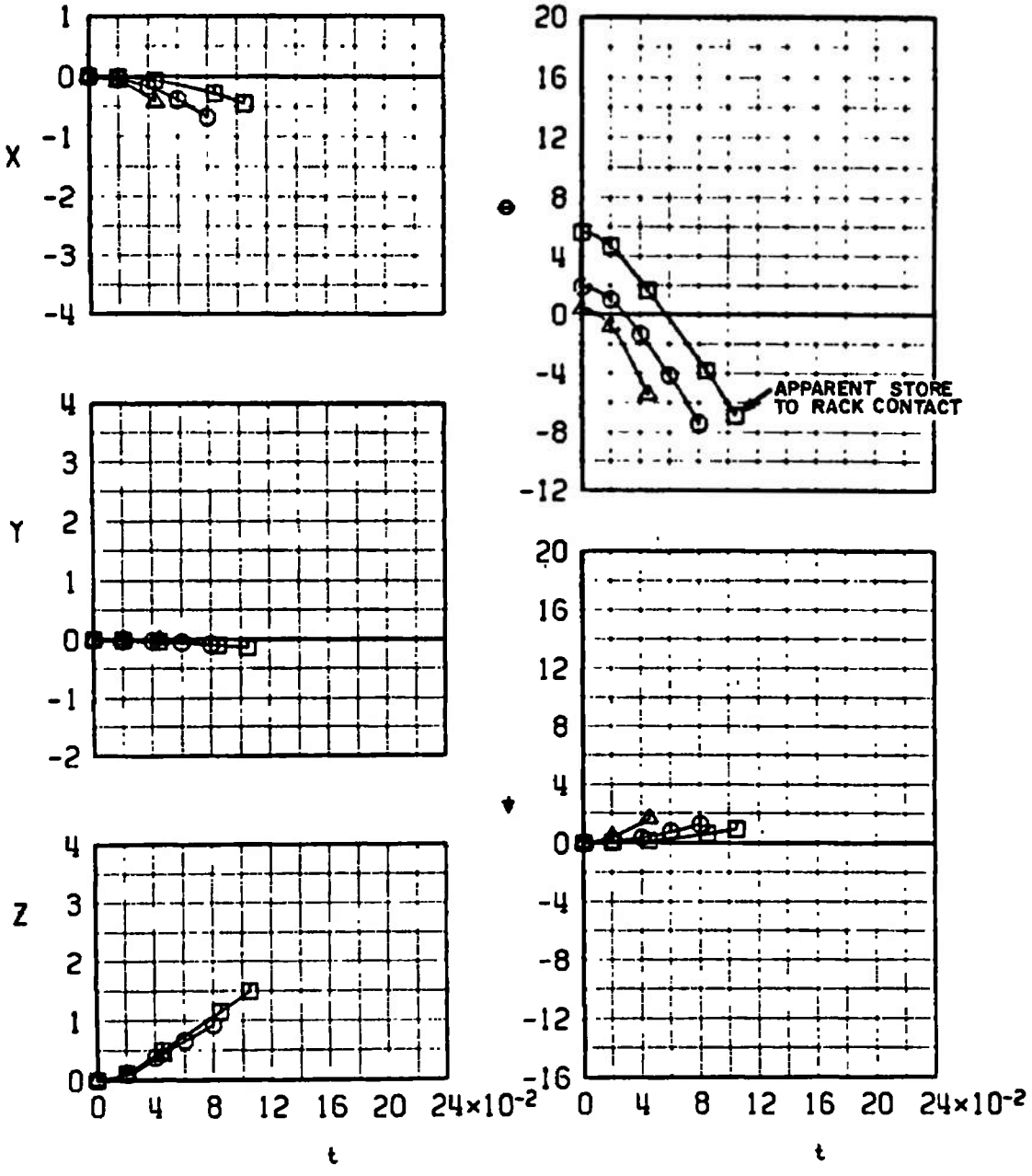

i. Configuration 6L, Ejector 14
Fig. 24 Continued

SYMBOL	CONF	M_∞	α
□	6R	0.407	8.6
○	6R	0.569	4.9
△	6R	0.732	3.4

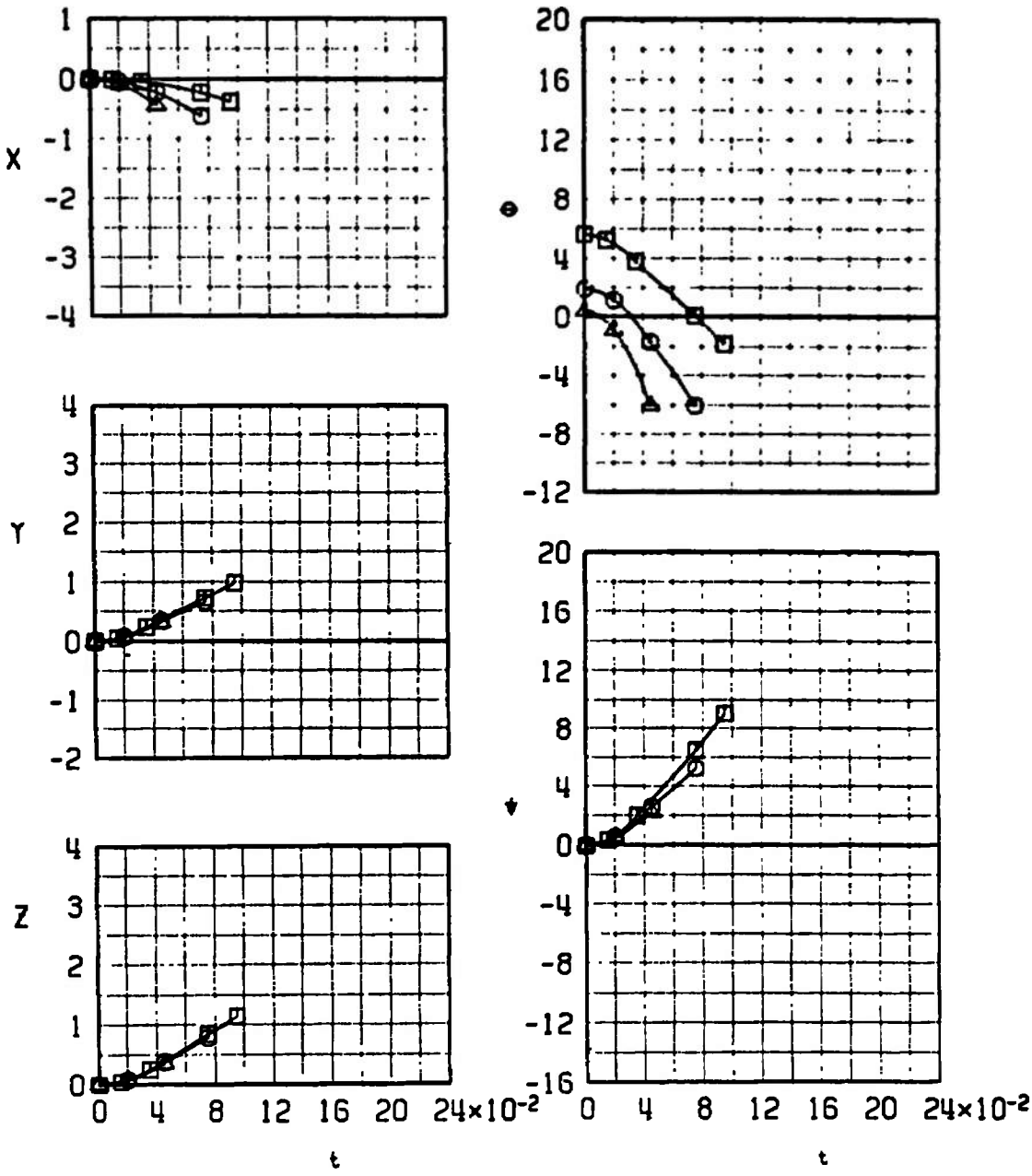

j. Configuration 6R, Ejector 14
Fig. 24 Continued

SYMBOL	CONF	M_∞	α
□	8L	0.407	8.6
○	8L	0.651	3.9
△	8L	0.773	3.2

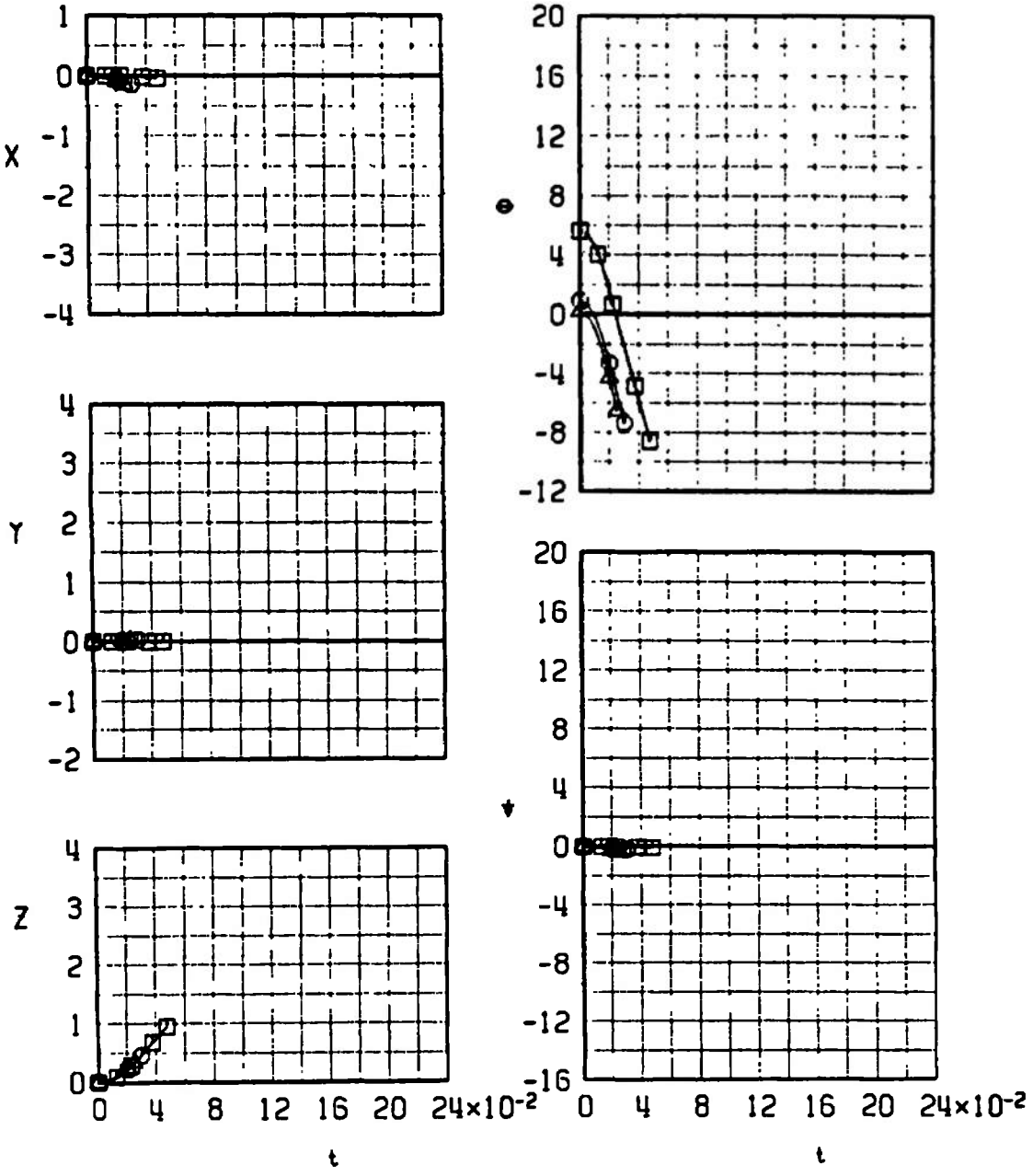

k. Configuration 8L, Ejector 16
Fig. 24 Continued

SYMBOL	CONF	M_∞	α
□	8R	0.407	8.6
○	8R	0.651	3.9

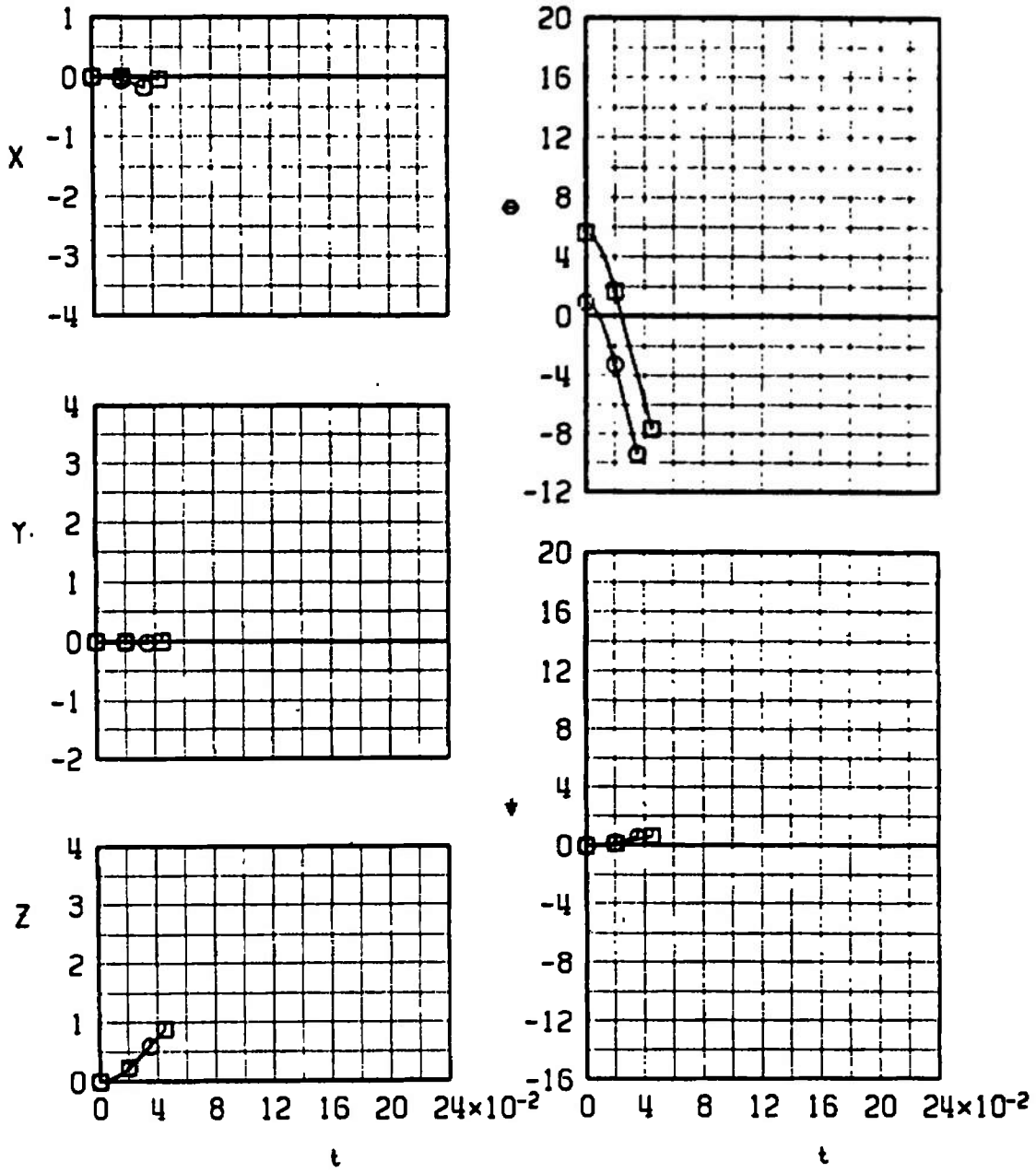

I. Configuration 8R, Ejector 16
Fig. 24 Continued

SYMBOL	CONF	M_∞	α
□	7L	0.407	8.6
○	7L	0.651	3.9
△	7L	0.773	3.2

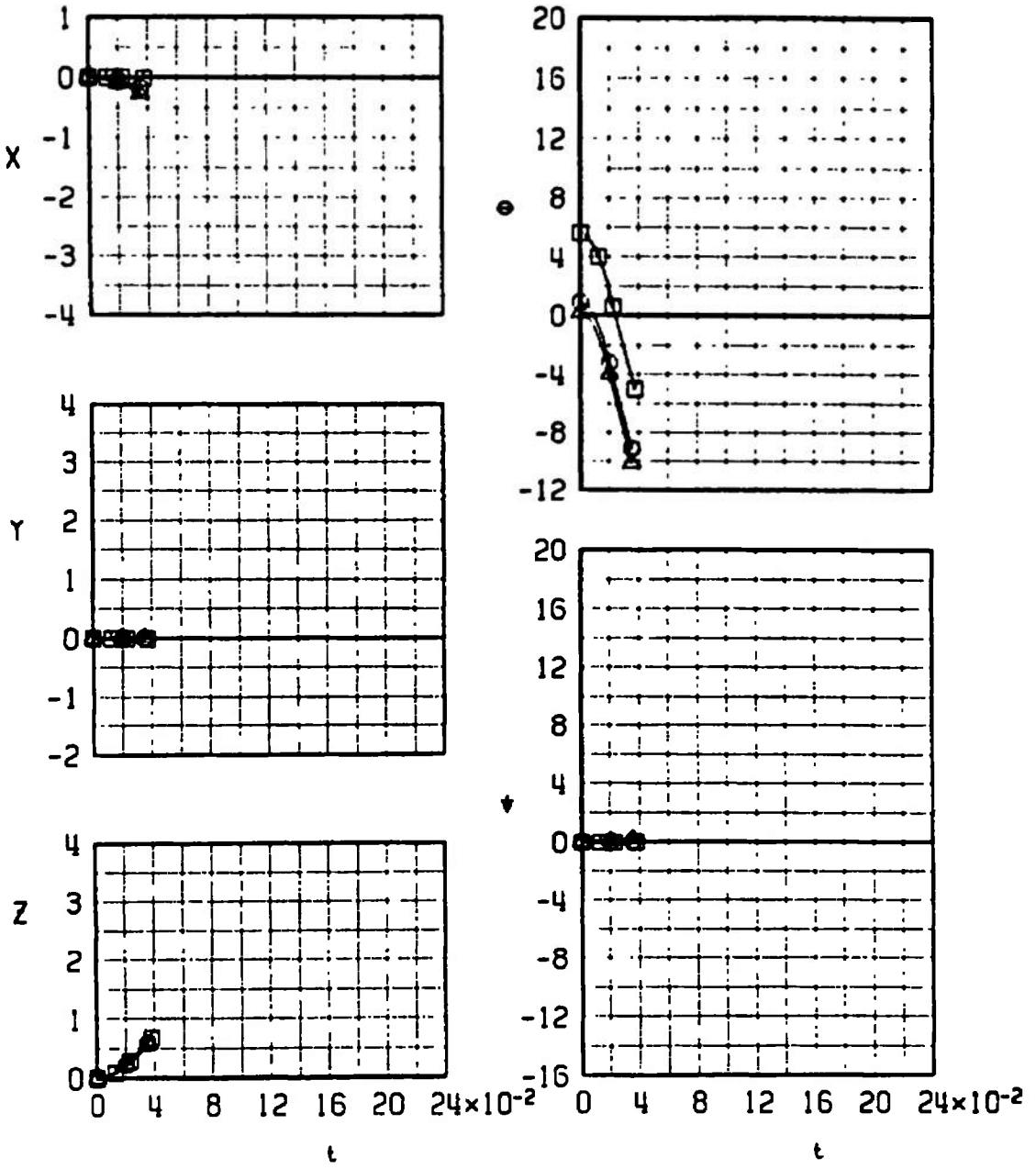

m. Configuration 7L, Ejector 16
Fig. 24 Continued

SYMBOL	CONF	M_∞	α
□	7L	0.407	8.6
○	7L	0.773	3.2

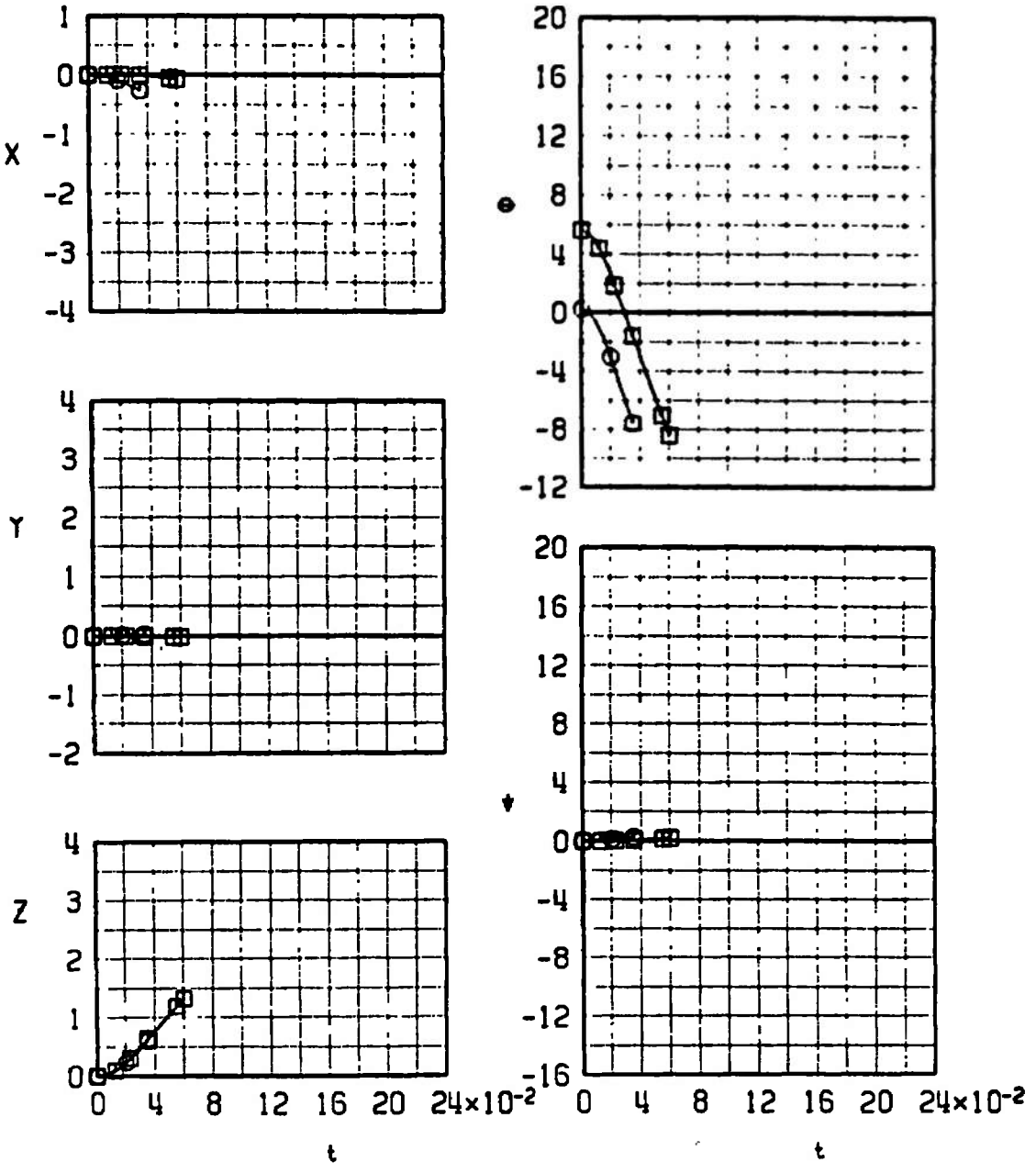

n. Configuration 7L, Ejector 18
Fig. 24 Continued

SYMBOL	CONF	M_∞	α
□	7R	0.407	8.6
○	7R	0.651	3.9
△	7R	0.773	3.2

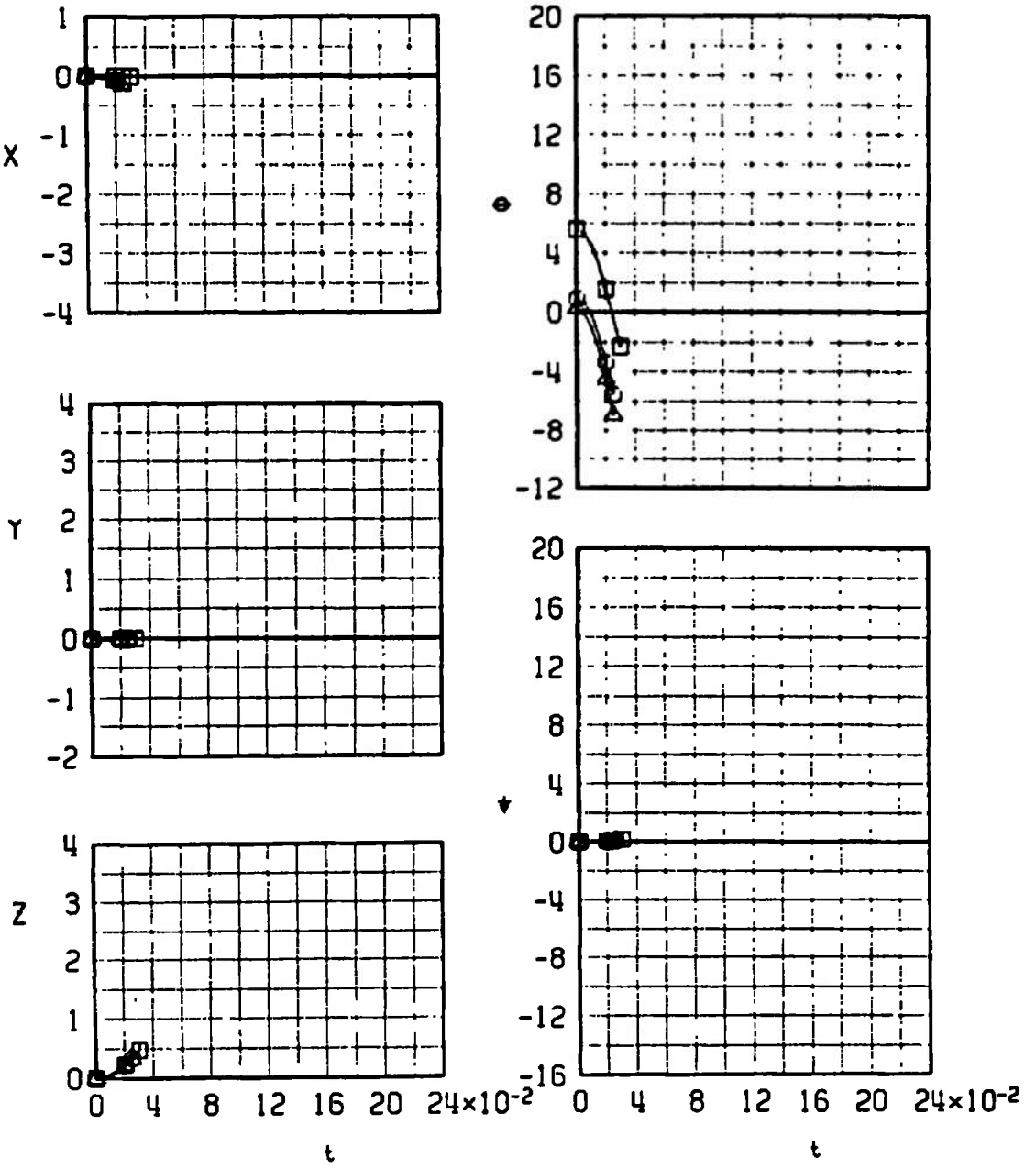

o. Configuration 7R, Ejector 16
Fig. 24 Continued

SYMBOL	CONF	M_∞	α
⊡	7R	0.407	8.6
⊙	7R	0.773	3.2

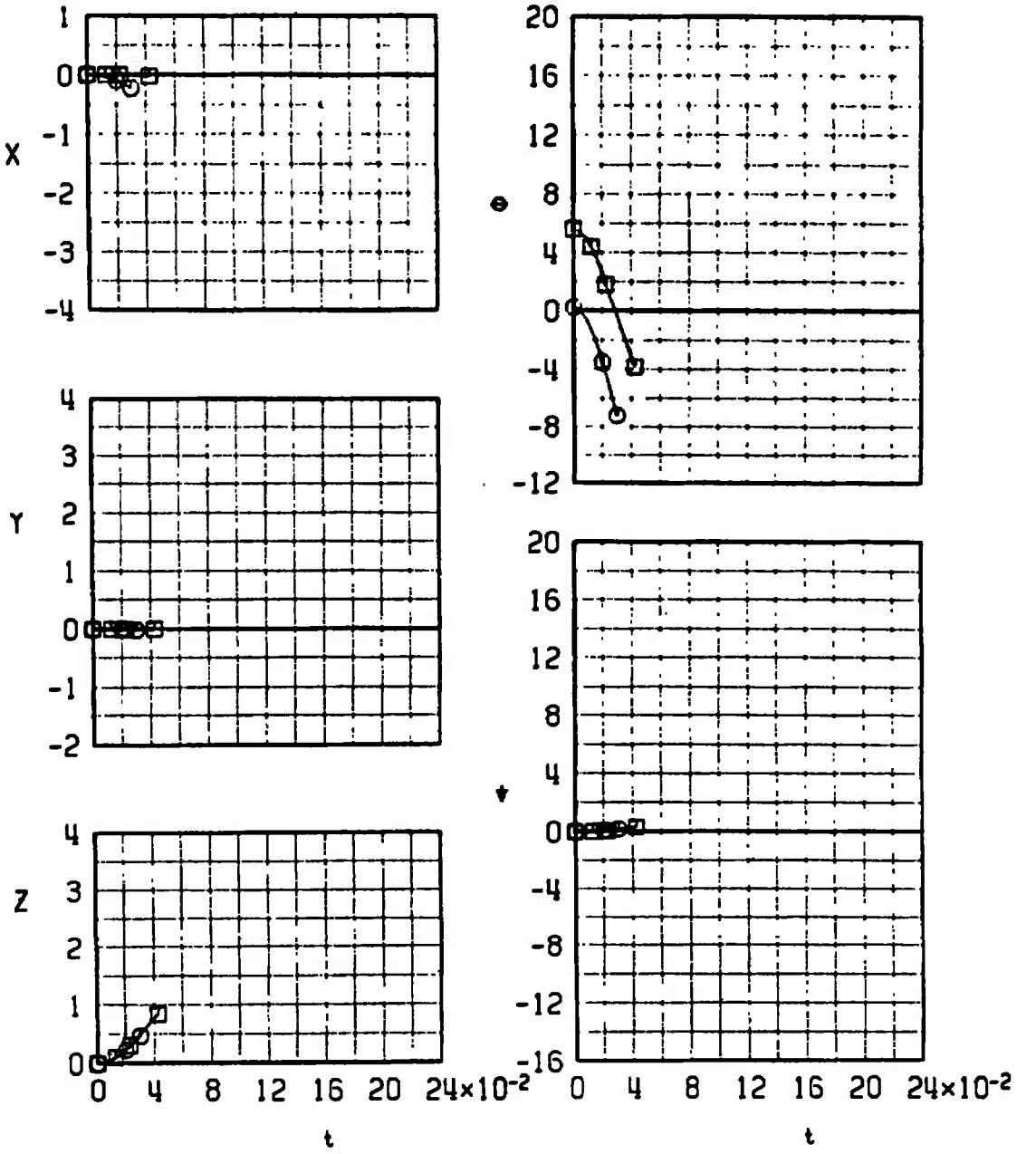

p. Configuration 7R, Ejector 18
Fig. 24 Continued

SYMBOL	CONF	M_∞	α
□	9L	0.407	8.6
○	9L	0.651	3.9

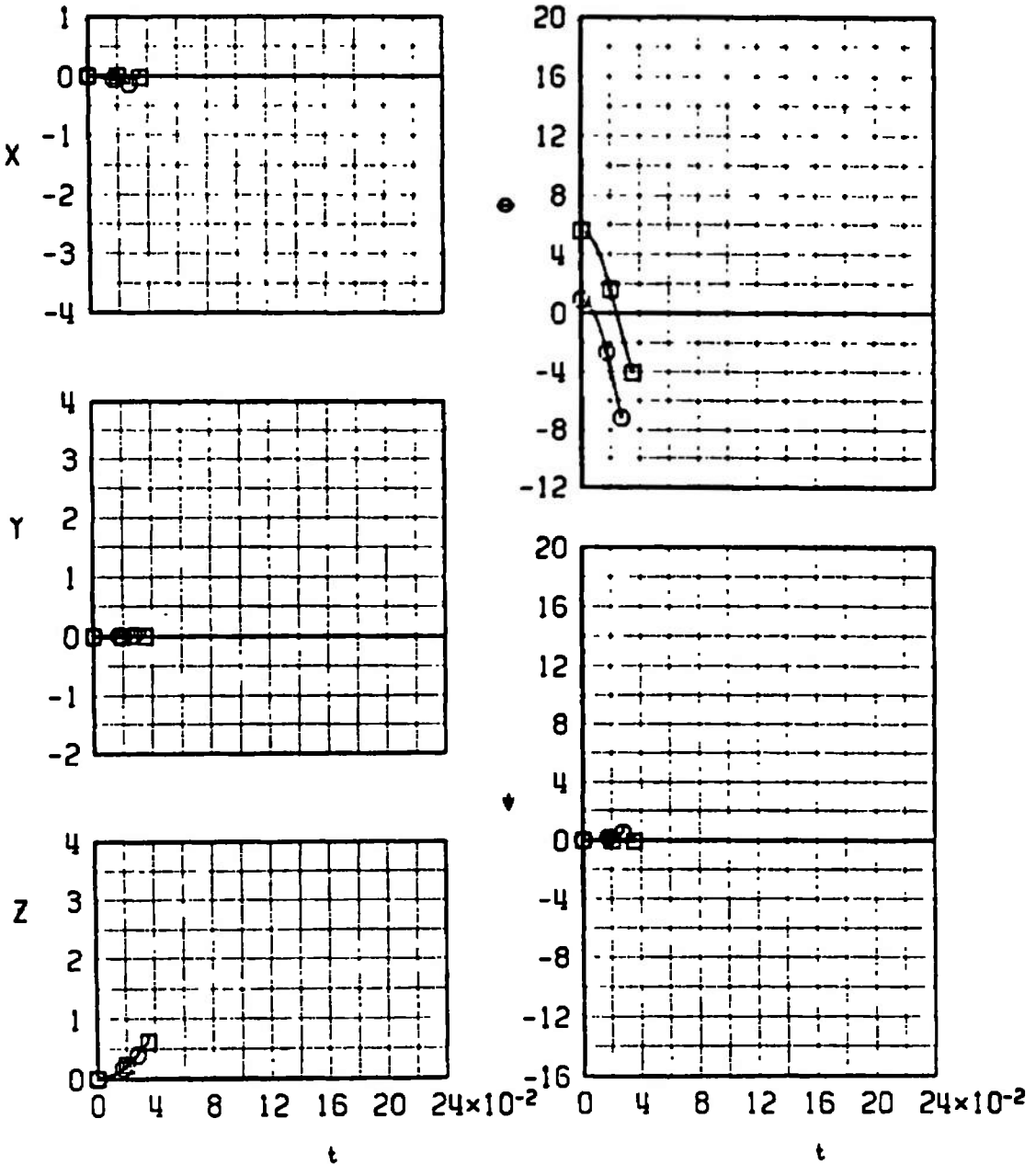

q. Configuration 9L, Ejector 16
Fig. 24 Continued

SYMBOL	CONF	M_∞	α
☐	9R	0.407	8.6
○	9R	0.651	3.9

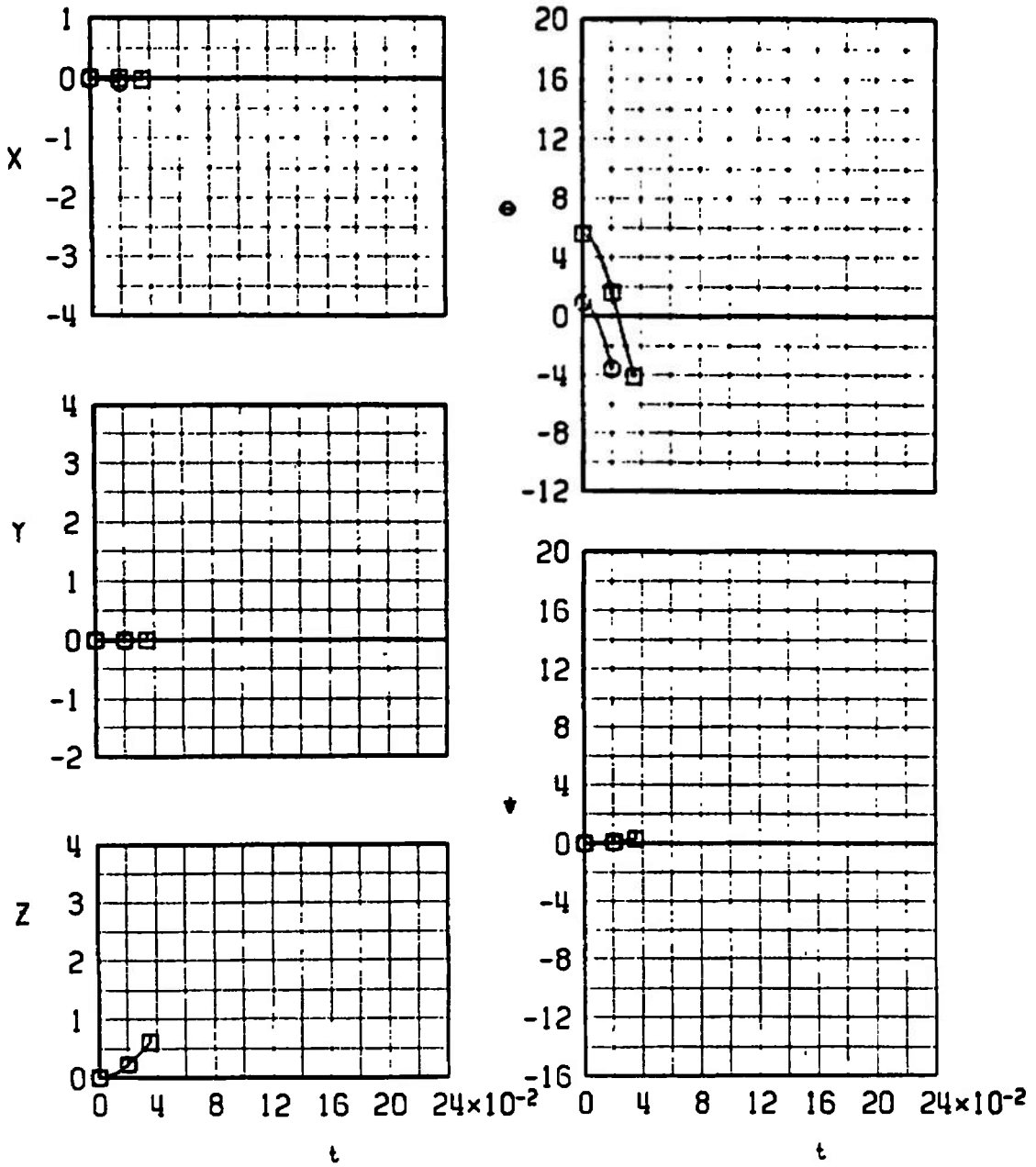

r. Configuration 9R, Ejector 16
Fig. 24 Concluded

SYMBOL	CONF	M_∞	α
⊡	17L	0.325	12.9
⊙	17L	0.732	3.4

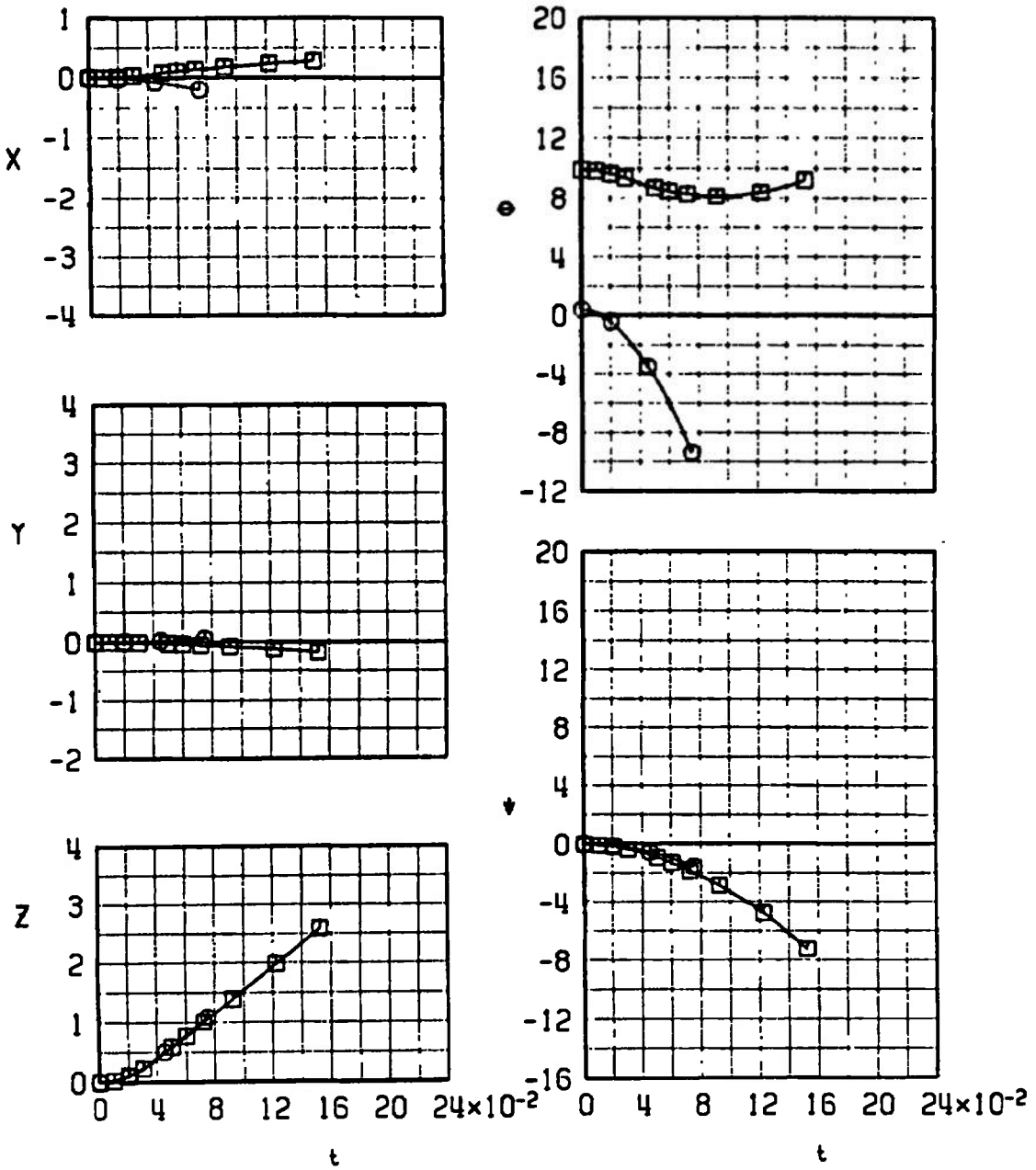

a. Configuration 17L, Ejector 20

Fig. 25 Trajectory Data for the Expended CBU-30/A Store

SYMBOL	CONF	M_∞	α
⊡	17R	0.325	12.9
⊙	17R	0.732	3.4

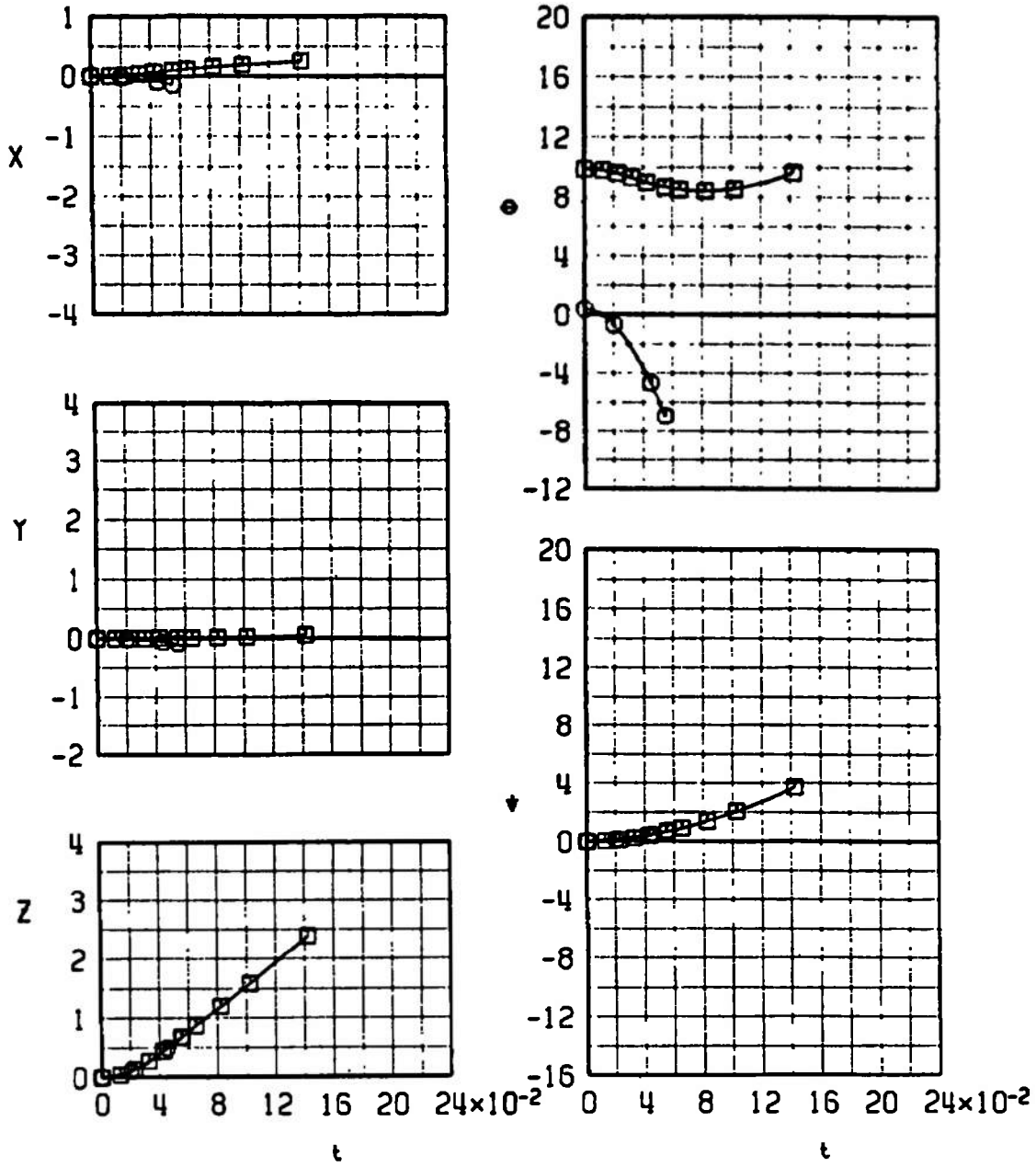

b. Configuration 17R, Ejector 20
Fig. 25 Concluded

SYMBOL	CONF	M_∞	α
□	23L	0.407	8.6
○	23L	0.569	4.9
△	23L	0.732	3.4

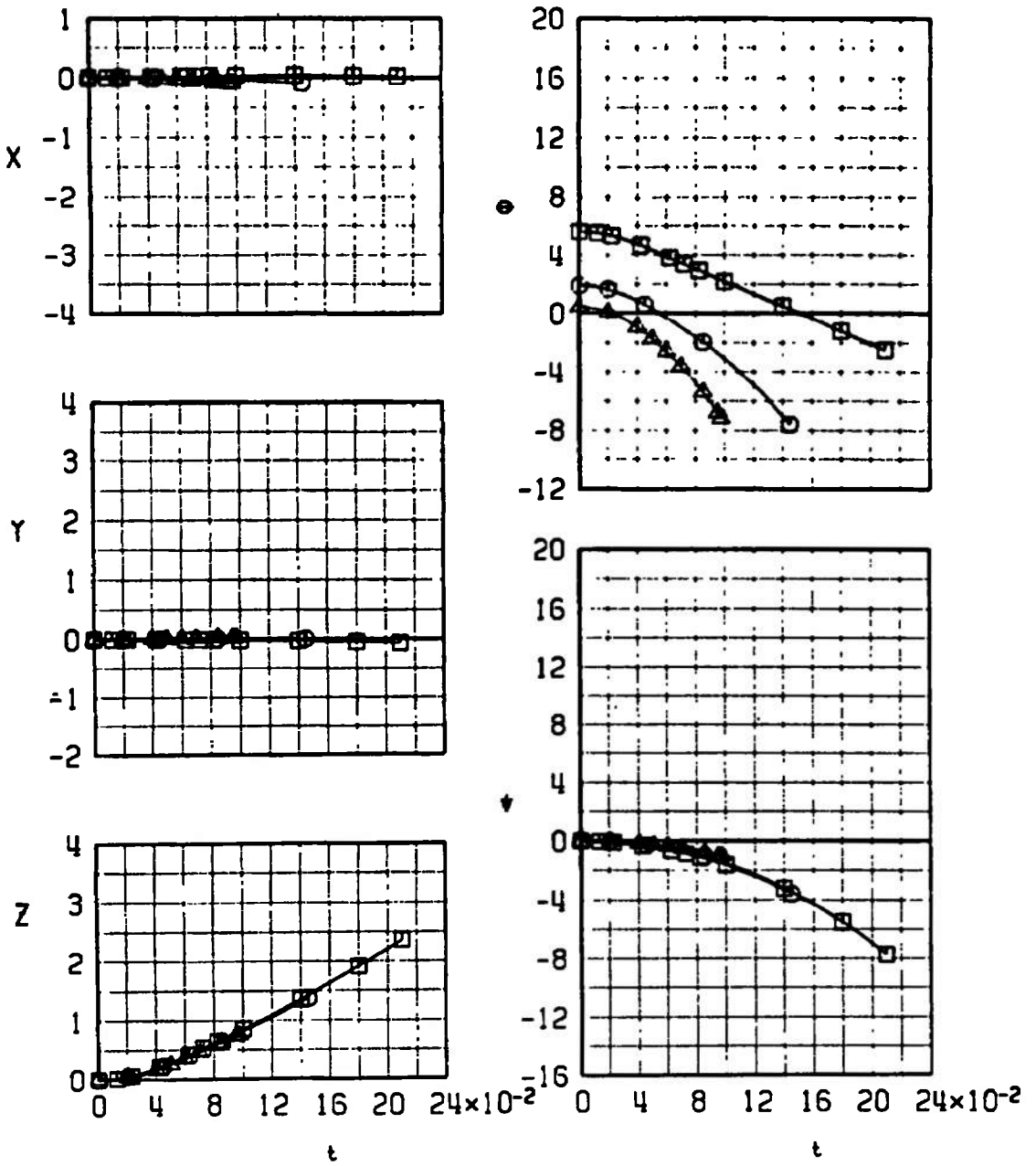

a. Configuration 23L, Ejector 23

Fig. 26 Trajectory Data for the Loaded LAU-68A/A Store

SYMBOL	CONF	M_∞	α
□	23R	0.407	8.6
○	23R	0.569	4.9
△	23R	0.732	3.4

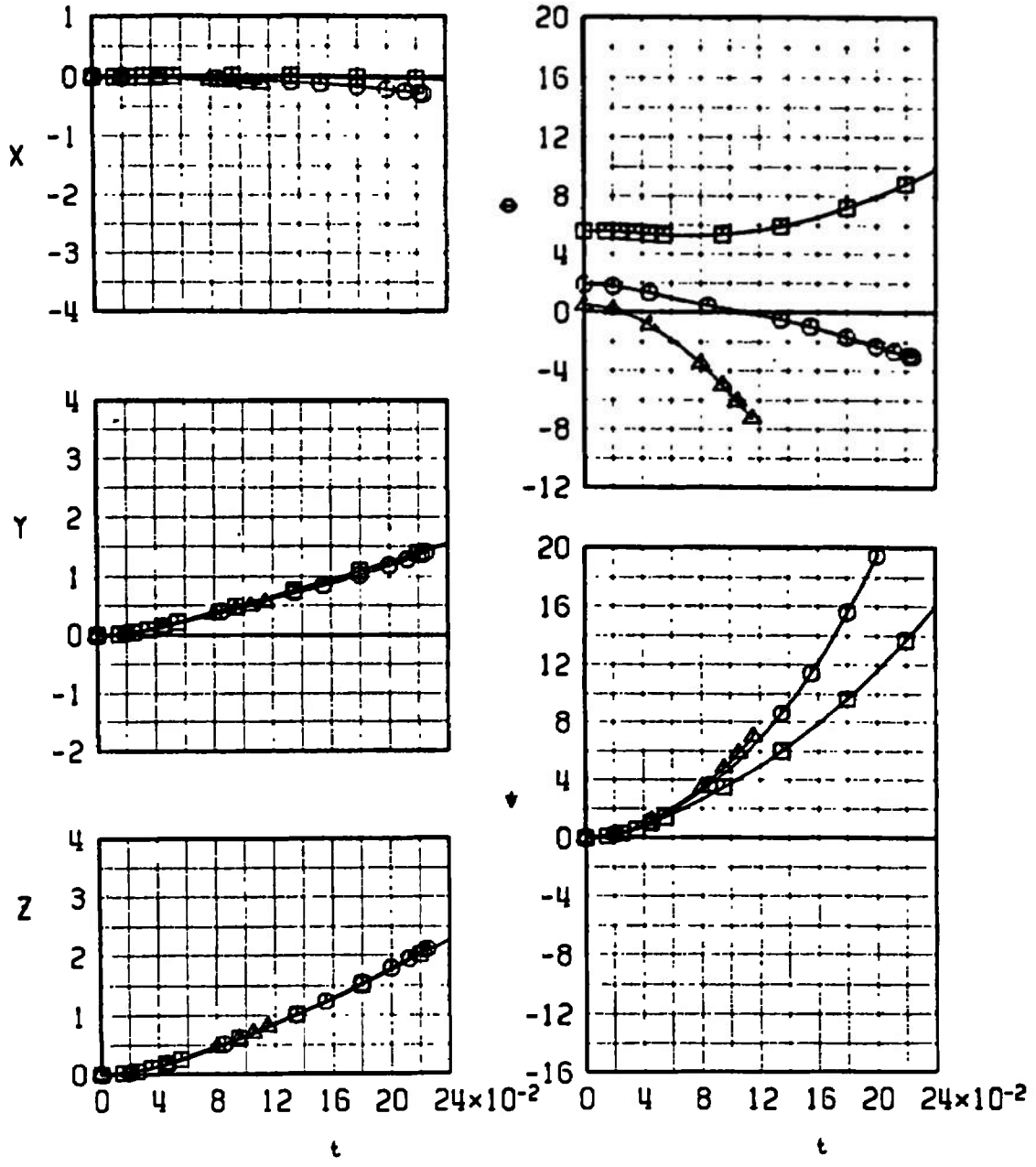

b. Configuration 23R, Ejector 23
Fig. 26 Continued

SYMBOL	CONF	M_∞	α
□	24L	0.407	8.6
○	24L	0.569	4.9
△	24L	0.732	3.4

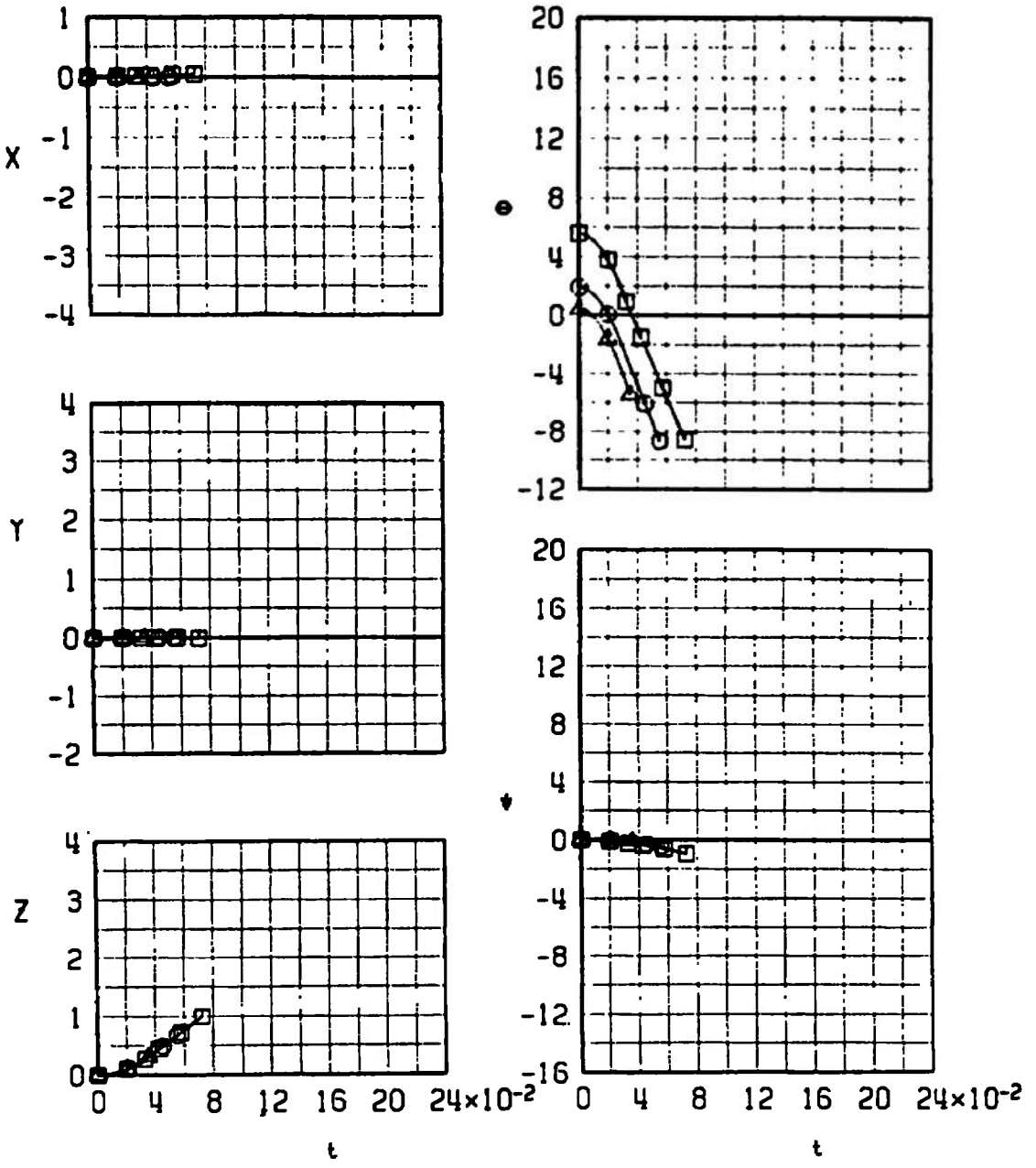

c. Configuration 24L, Ejector 24
Fig. 26 Continued

SYMBOL	CONF	M_∞	α
□	24R	0.407	8.6
○	24R	0.569	4.9
△	24R	0.732	3.4

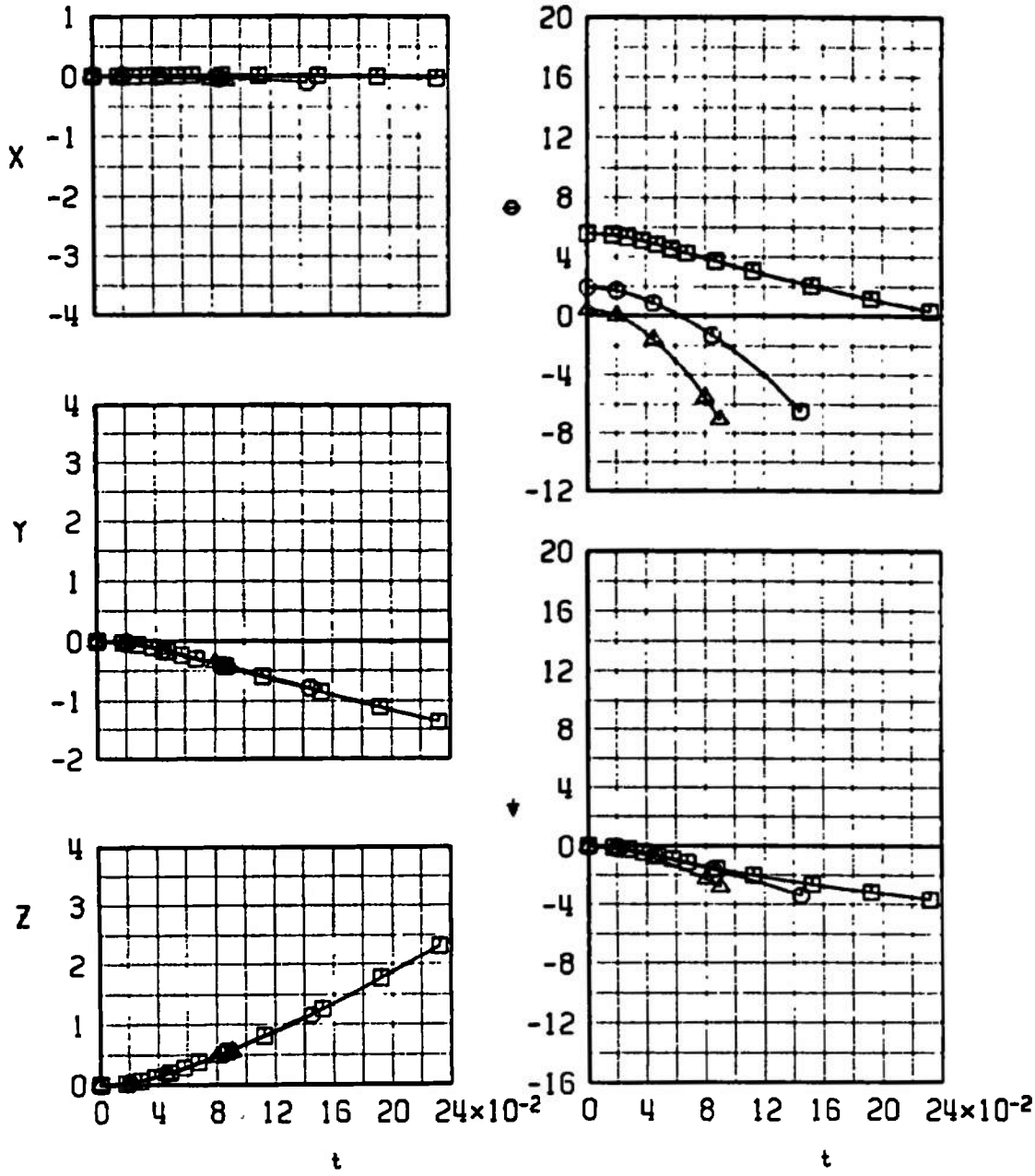

d. Configuration 24R, Ejector 23
Fig. 26 Concluded

SYMBOL	CONF	M_∞	α
□	21L	0.407	8.6
○	21L	0.569	4.9
△	21L	0.732	3.4

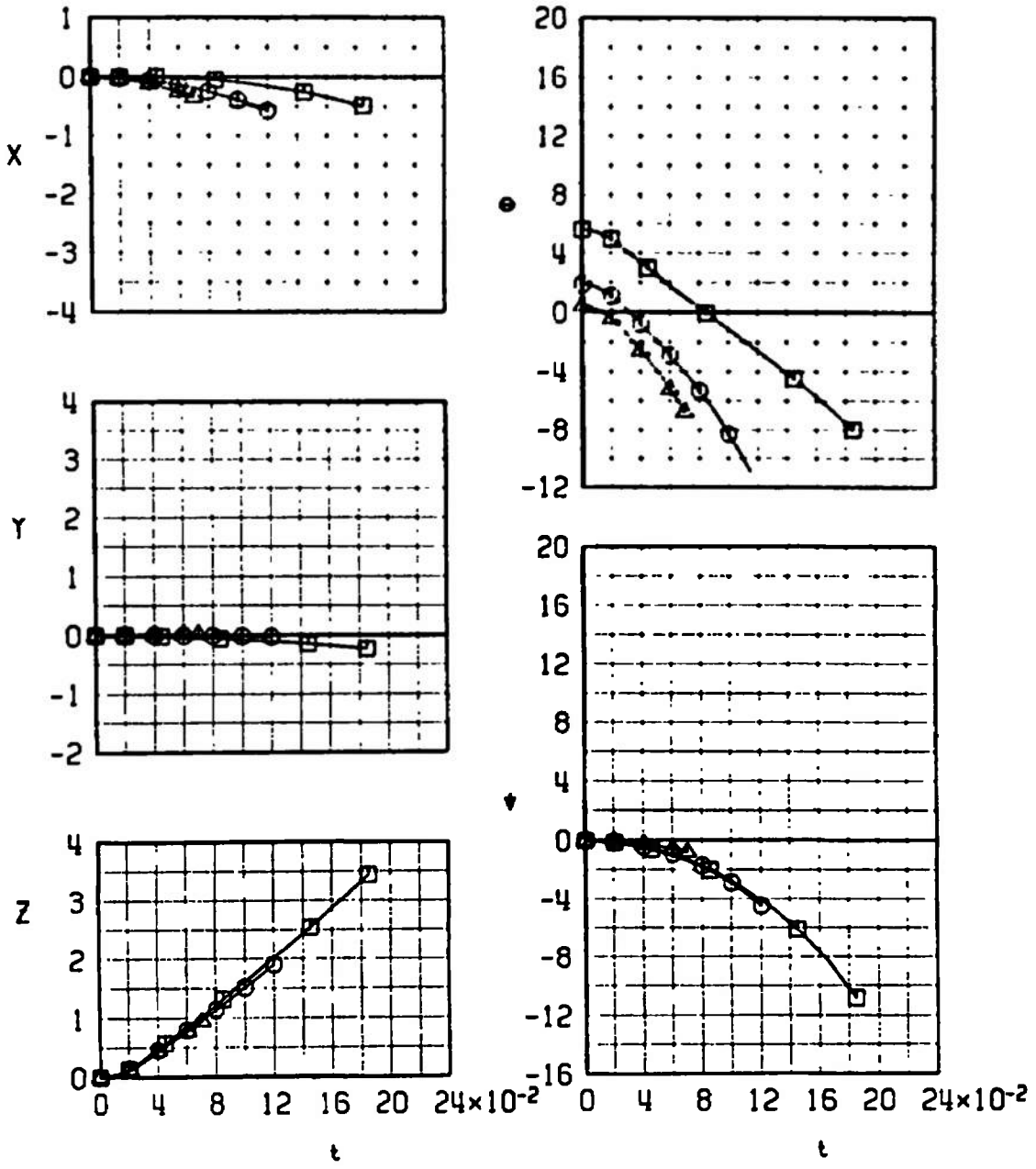

a. Configuration 21L, Ejector 21

Fig. 27 Trajectory Data for the Expended LAU-68A/A Store

SYMBOL	CONF	M_∞	α
□	21R	0.407	8.6
○	21R	0.569	4.9
△	21R	0.732	3.4

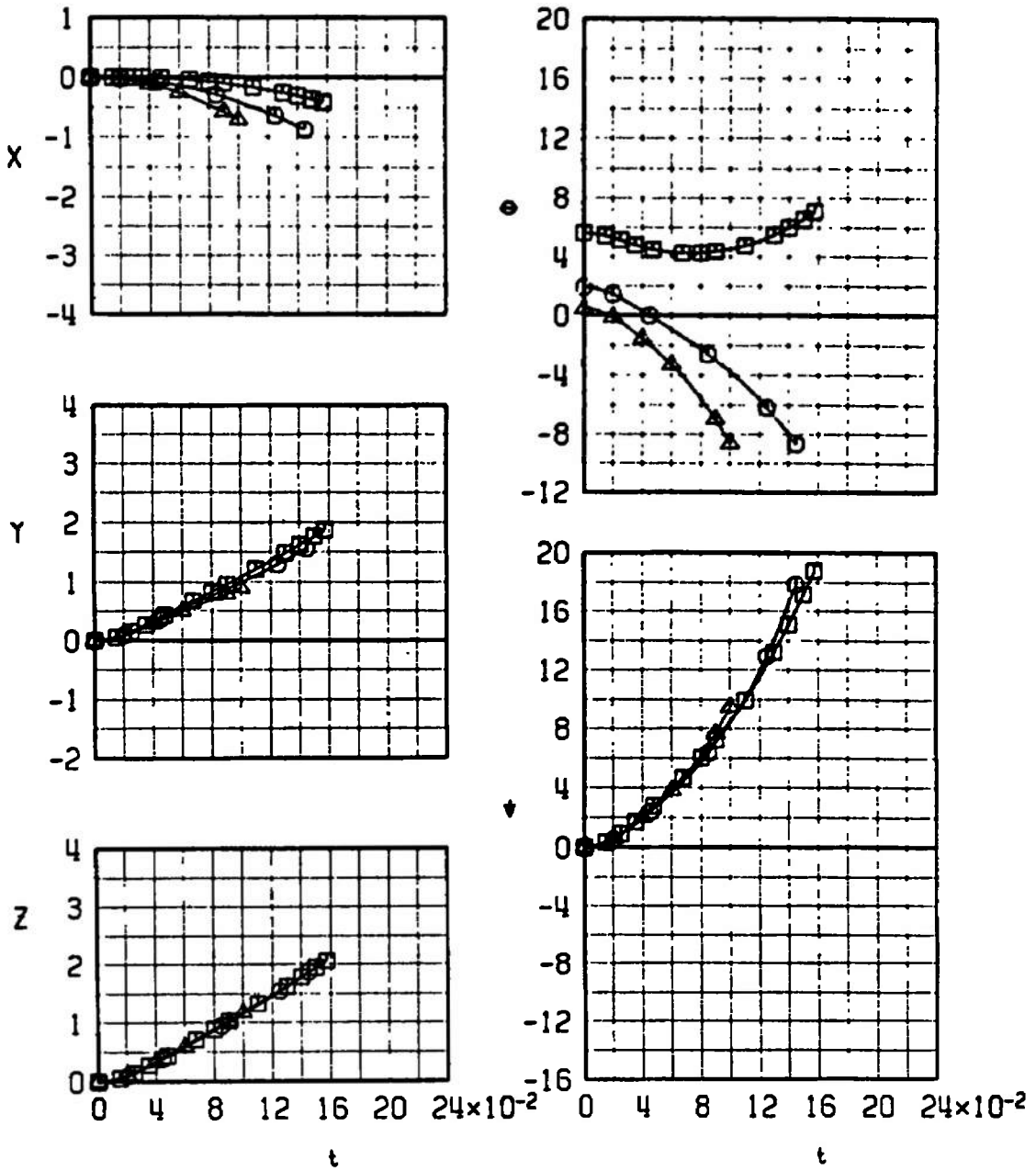

b. Configuration 21R, Ejector 21
Fig. 27 Continued

SYMBOL	CONF	M_∞	α
□	22L	0.407	8.6
○	22L	0.569	4.9
△	22L	0.732	3.4

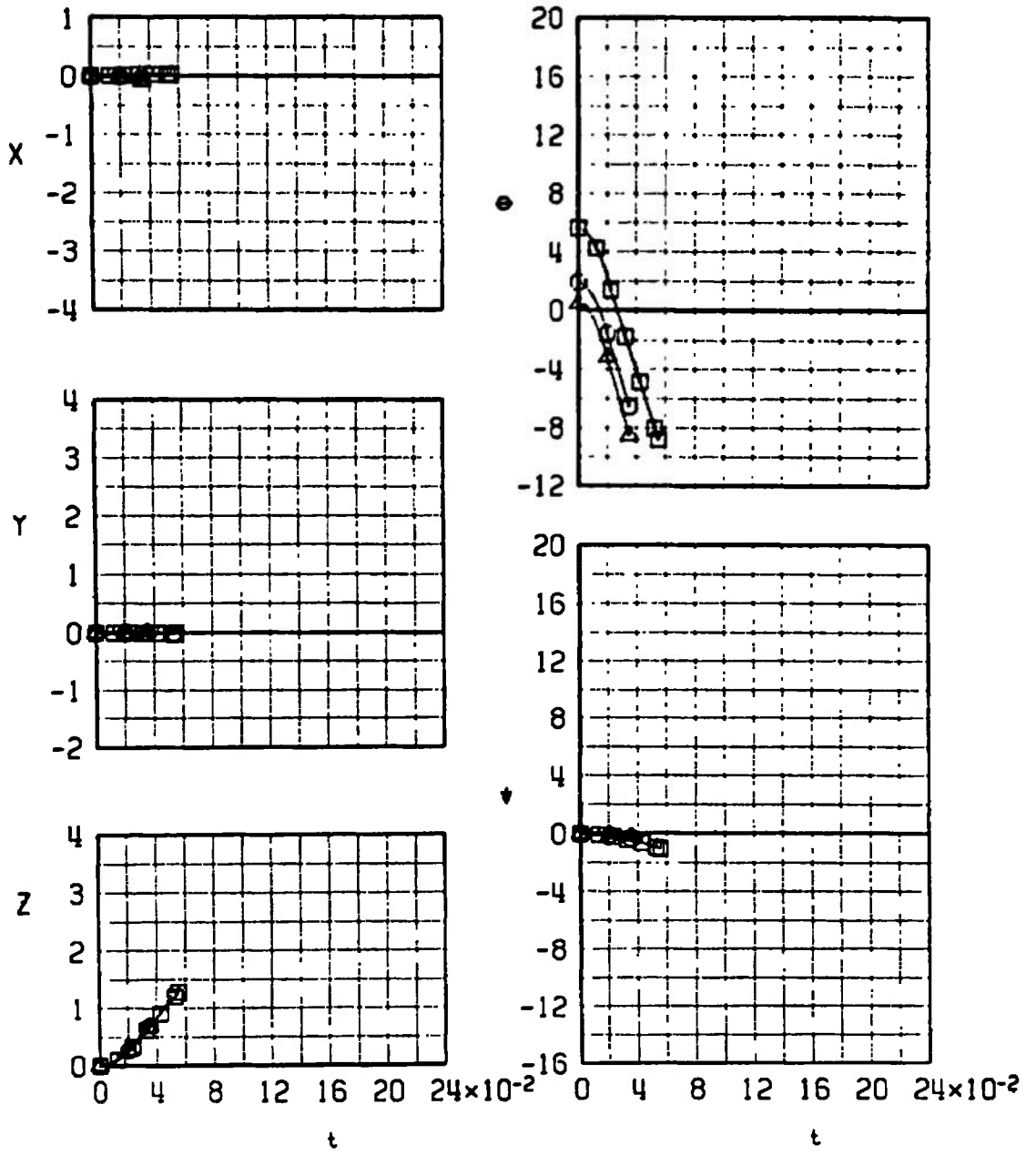

c. Configuration 22L, Ejector 22
Fig. 27 Continued

SYMBOL	CONF	M_∞	α
□	22R	0.407	8.6
○	22R	0.569	4.9
△	22R	0.732	3.4

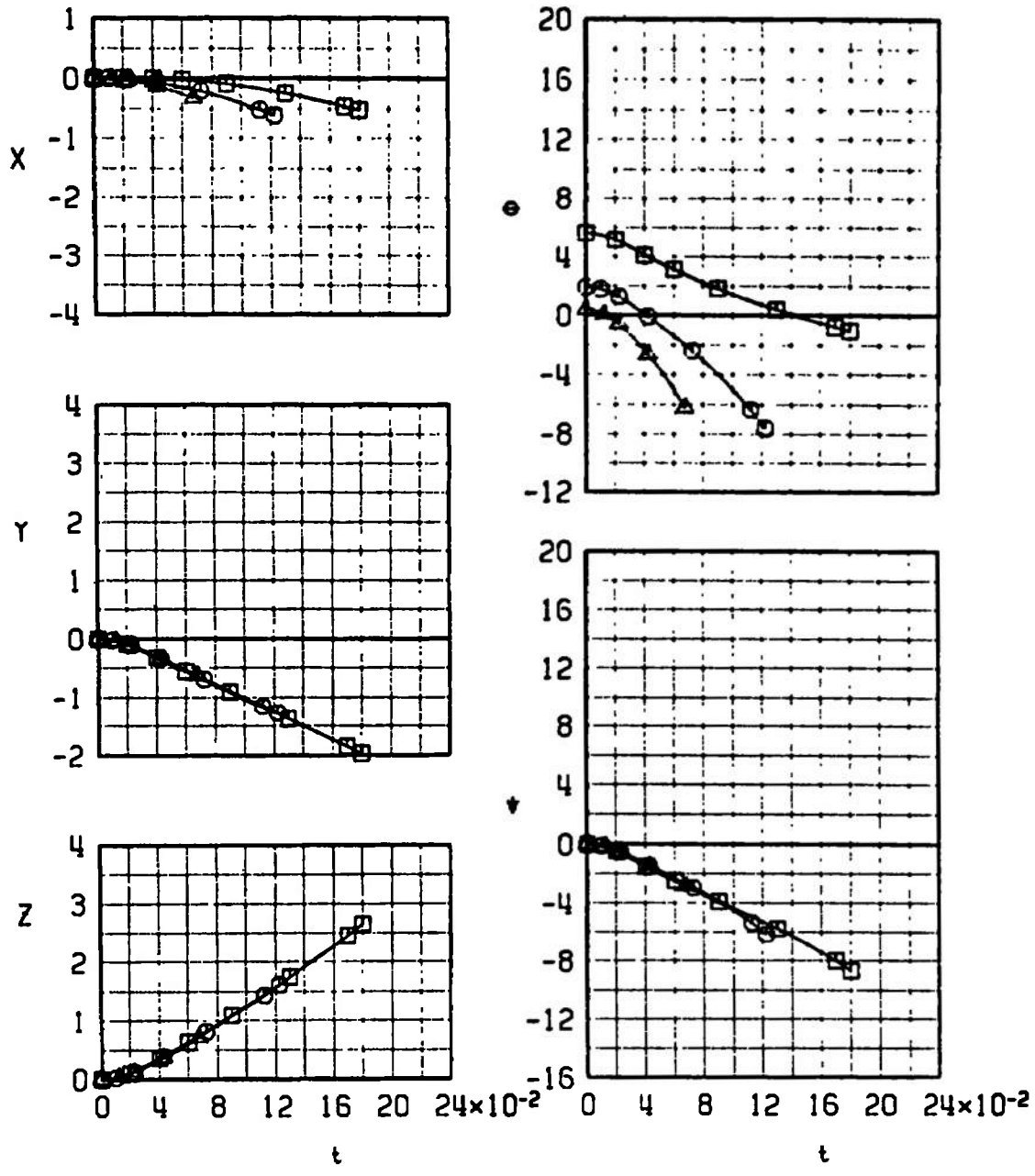

d. Configuration 22R, Ejector 21
Fig. 27 Concluded

TABLE I
IDENTIFICATION OF SIMULATED EJECTOR FORCES

Identification No.	Store	Rack	Orifice Combination Simulated, Fwd/Aft	F_Z or F_{Z_1}, lb	F_{Z_2}, lb
1	SUU-23/A (E)*	MAU-12B/A	No. 7/No. 6	2220	0
2	SUU-23/A (E)*	↓	No. 7/No. 5	1980	1440
3	SUU-23/A (L)**	↓	No. 7/No. 6	2500	0
4	SUU-23/A (L)**	↓	No. 7/No. 5	1980	1600
5	CBU-12A/A (E), CBU-46/A	TER	NA	1230	NA
6	CBU-12A/A (L)	TER	NA	1150	NA
7	CBU-46/A (L)	TER	NA	1150	NA
8	CBU-12A/A (E), CBU-46/A	MAU-12B/A	No. 7/No. 5	1750	1090
9	CBU-12A/A (L)	↓	No. 7/No. 5	2090	1400
10	CBU-46/A (L)	↓	No. 7/No. 5	2040	1410
11	CBU-12A/A (E), CBU-46/A	↓	No. 5/No. 5	1370	1410
12	CBU-12A/A (L)	↓	No. 5/No. 5	1860	1620
13	CBU-46/A (L)	↓	No. 5/No. 5	1800	1550
14	LAU-3/A (E)	TER	NA	1300	NA
15	LAU-3/A (L)	TER	NA	1170	NA
16	LAU-3/A (E)	MAU-12B/A	No. 7/No. 5	1500	1050
17	LAU-3/A (L)	↓	No. 7/No. 5	2140	1350
18	LAU-3/A (E)	↓	No. 5/No. 5	1300	1360
19	LAU-3/A (L)	↓	No. 5/No. 5	1890	1630
20	CBU-30/A (E)	↓	No. 5/No. 5	1390	1420
21	LAU-68A/A (E)	TER	NA	1300	NA
22	LAU-68A/A (E)	MAU-12B/A	No. 7/No. 5	1500	1050
23	LAU-68A/A (L)	TER	NA	1220	NA
24	LAU-68A/A (L)	MAU-12B/A	No. 7/No. 5	1750	1090

*(E) denotes expended

**(L) denotes loaded

NOTE: Z_E = 0.24167 ft for the TER

Z_E = 0.34167 ft for the MAU-12B/A

TABLE II
FULL-SCALE STORE PARAMETERS USED IN THE TRAJECTORY CALCULATIONS

Parameter \ Store	SUU-23/A		CBU-12A/A and CBU-46/A			LAU-3/A		CBU-30/A	LAU-68A/A	
	Loaded	Expended	-12A/A Loaded	-46/A Loaded	Expended	Loaded	Expended	Expended	Loaded	Expended
$\overline{m}$	53.770	33.412	20.420	27.351	5.128	15.385	2.362	5.843	5.937	2.083
X_{cg}	9.117	7.792	5.170	5.333	5.108	3.114	2.162	4.483	3.026	2.508
Z_{cg}	---	---	---	---	---	---	---	0.808	---	---
S	2.6397	2.6397	1.326	1.326	1.326	1.352	1.352	1.339	0.5346	0.5346
b	1.833	1.833	1.300	1.300	1.300	1.313	1.313	1.306	0.825	0.825
I_{xx}	12.90	8.10	3.3	4.3	1.0	2.6	1.1	1.1	1.0	0.4
I_{yy}	517	328	86.5	106	21	24	4.56	21.2	9.1	4.6
I_{zz}	517	328	86.5	106	21	24	4.56	21.2	9.1	4.6
C_{m_q}	-63	-63	-38	-38	-38	-18	-7.6	-25	-18	-14
C_{n_r}	-63	-63	-38	-38	-38	-18	-7.6	-25	-18	-14
X_L	---	---	0.057	0.220	-0.005	-0.297	0.282	---	0.120	0.203
X_{L_1}	1.217	-0.108	1.062	1.225	1.000	0.708	1.287	1.067	1.125	1.208
X_{L_2}	-0.450	-1.775	-0.605	-0.442	-0.667	-0.959	-0.380	-0.600	-0.542	-0.459
C_A	---	---	---	---	---	---	---	---	0.300	0.800

TABLE III
MAXIMUM FULL-SCALE POSITION UNCERTAINTIES RESULTING FROM BALANCE INACCURACIES

Store	M_∞	t	ΔX	ΔY	ΔZ	$\Delta\theta$	$\Delta\psi$
SUU-23/A Loaded	0.569	0.20	±0.004	±0.004	±0.003	±0.05	±0.09
SUU-23/A Expended	↓	0.20	±0.006	±0.006	±0.004	±0.08	±0.1
CBU-12A/A Loaded	↓	0.15	±0.004	±0.002	±0.002	±0.05	±0.08
CBU-46/A Loaded	↓	↓	±0.003	±0.002	±0.002	±0.04	±0.06
CBU-12A/A, CBU-46/A Expended	↓	↓	±0.02	±0.01	±0.008	±0.2	±0.3
LAU-3/A Loaded	↓	↓	±0.007	±0.004	±0.003	±0.2	±0.3
LAU-3/A Expended	↓	↓	±0.04	±0.02	±0.02	±0.8	±0.8
CBU-30/A Expended	0.732	↓	±0.03	±0.02	±0.01	±0.5	±0.8
LAU-68A/A Loaded	0.569	↓	---	±0.01	±0.02	±0.5	±0.2
LAU-68A/A Expended	0.569	↓	---	±0.05	±0.06	±0.9	±0.4

TABLE IV
AIRCRAFT WING LOADING CONFIGURATION IDENTIFICATION

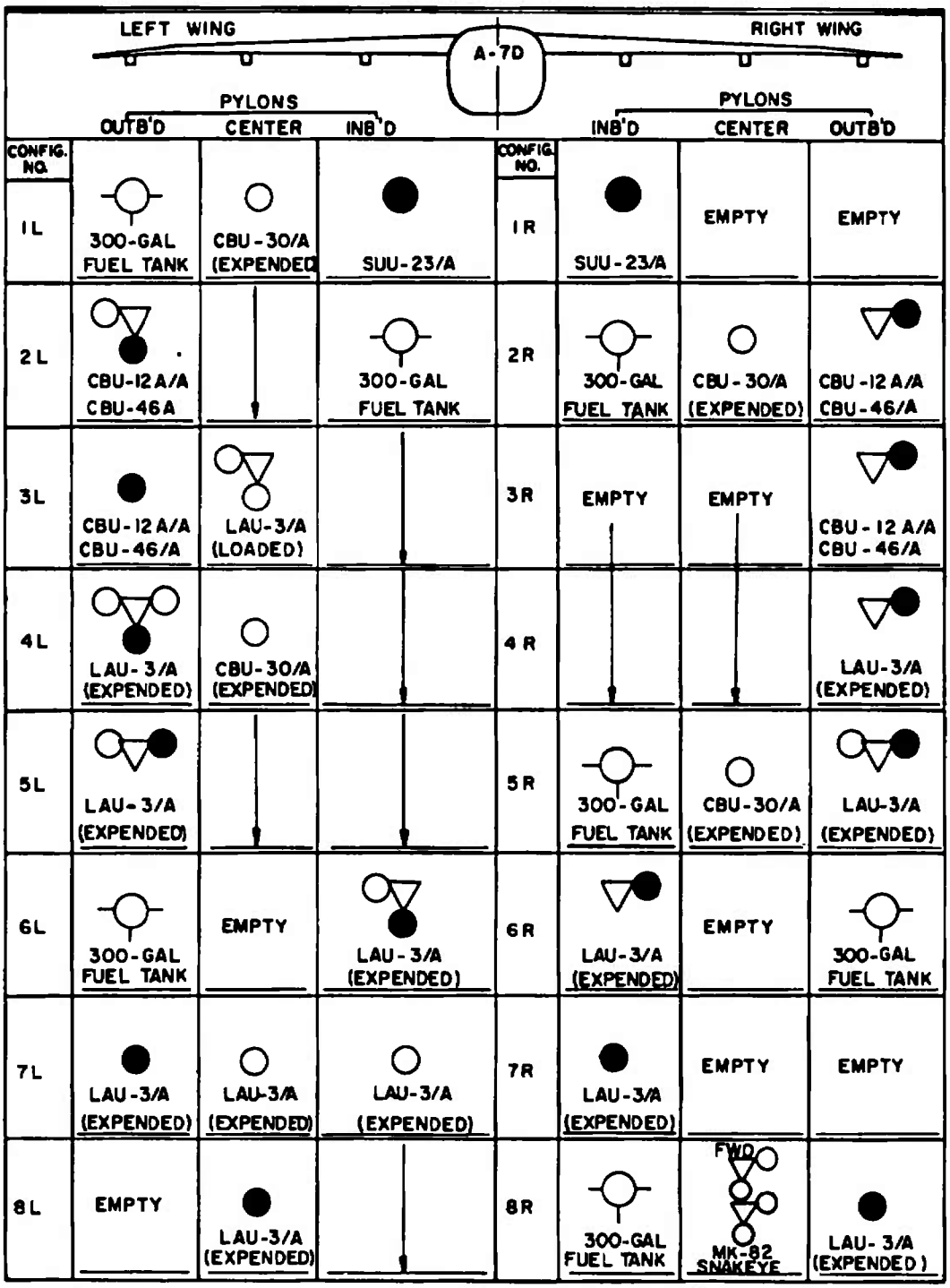

TABLE IV (Continued)

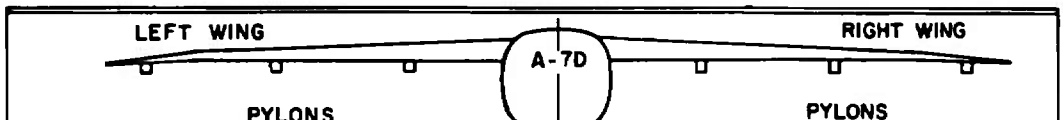

CONFIG. NO.				CONFIG. NO			
9L	LAU-3/A (LOADED)	LAU-3/A (EXPENDED)	300-GAL FUEL TANK	9R	SUU-23/A	LAU-3/A (EXPENDED)	300-GAL FUEL TANK
12L	LAU-3/A (LOADED)	LAU-3/A (LOADED)	LAU-3/A (LOADED)	12R	LAU-3/A (LOADED)	EMPTY	EMPTY
13L	300-GAL FUEL TANK	EMPTY	LAU-3/A (LOADED)	13R	LAU-3/A (LOADED)	EMPTY	300-GAL FUEL TANK
14L	LAU-3A (LOADED)	CBU-30/A (EXPENDED)	300-GAL FUEL TANK	15R	EMPTY	EMPTY	LAU-3/A (LOADED)
16L	LAU-3/A (LOADED)	EMPTY	EMPTY	16R			LAU-3A (LOADED)
17L	EMPTY	CBU-30/A (EXPENDED)		17R	300-GAL FUEL TANK	CBU-30/A (EXPENDED)	300-GAL FUEL TANK
18L	LAU-3/A (EXPENDED)	EMPTY		18R	EMPTY	EMPTY	LAU-3/A (EXPENDED)
19L	EMPTY	LAU-3A (EXPENDED)	300-GAL FUEL TANK	19R	300-GAL FUEL TANK	LAU-3/A (EXPENDED)	EMPTY

○ DENOTES DUMMY STORE
● DENOTES STING MOUNTED STORE
▽ DENOTES TER
▽▽ DENOTES MER

TABLE IV (Concluded)

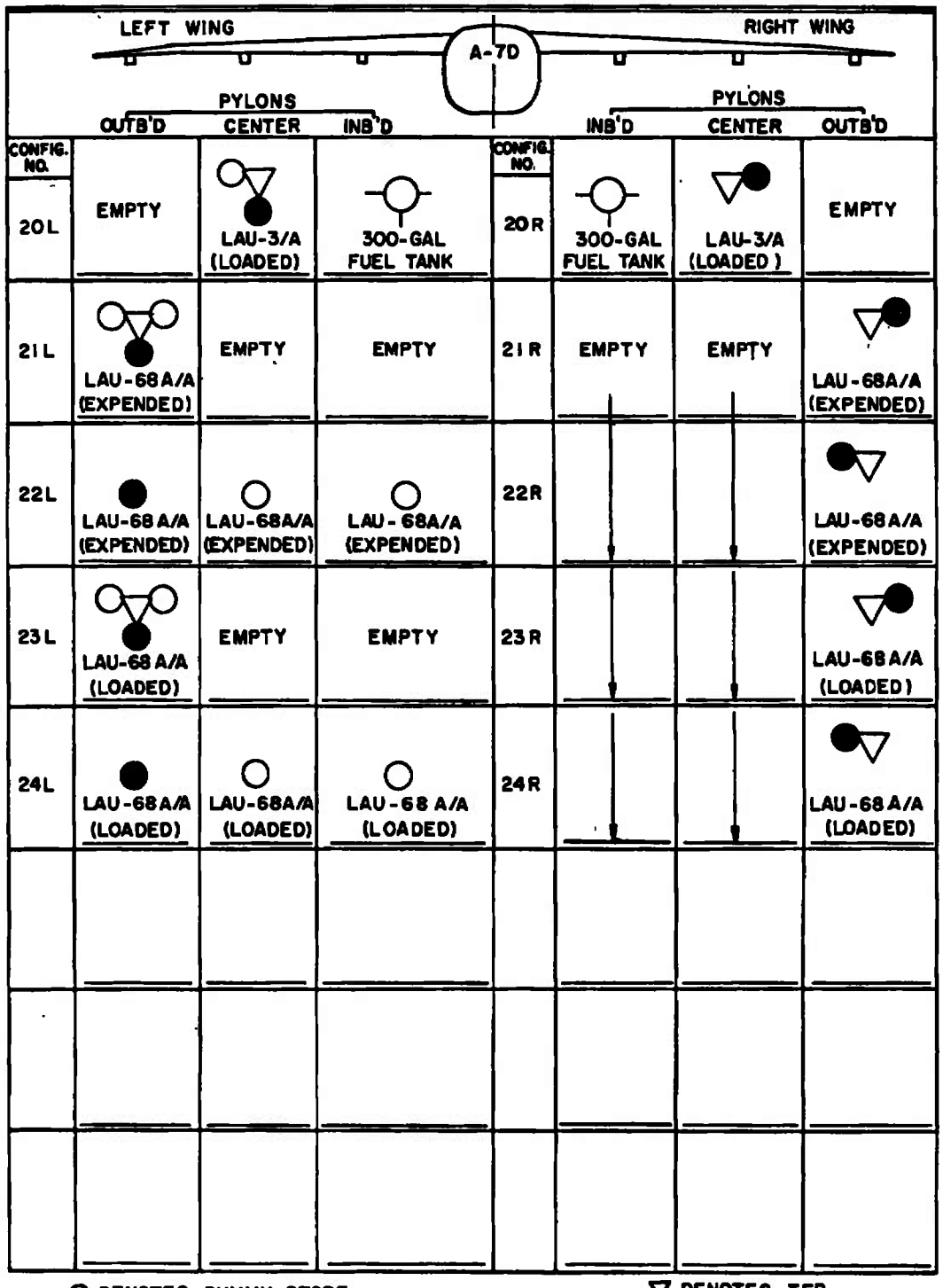

UNCLASSIFIED

Security Classification

DOCUMENT CONTROL DATA · R & D

(Security classification of title, body of abstract and indexing annotation must be entered when the overall report is classified)

1. ORIGINATING ACTIVITY (Corporate author)
Arnold Engineering Development Center
Arnold Air Force Station, Tennessee 37389

2a. REPORT SECURITY CLASSIFICATION
UNCLASSIFIED

2b. GROUP
N/A

3 REPORT TITLE
SEPARATION CHARACTERISTICS OF SIX STORES FROM THE A-7D AIRCRAFT AT MACH NUMBERS FROM 0.325 TO 0.814

4 DESCRIPTIVE NOTES (Type of report and inclusive dates)
June 21 to 27, 1972--Final Report

5. AUTHOR(S) (First name, middle initial, last name)
Willard E. Summers, ARO, Inc.

6 REPORT DATE	7a. TOTAL NO. OF PAGES	7b. NO. OF REFS
October 1972	103	1

8a. CONTRACT OR GRANT NO.

b. PROJECT NO.

c. Program Element 27121F

d. System 337A

9a. ORIGINATOR'S REPORT NUMBER(S)
AEDC-TR-72-146
AFATL-TR-72-193

9b. OTHER REPORT NO(S) (Any other numbers that may be assigned this report)
ARO-PWT-TR-72-120

10 DISTRIBUTION STATEMENT Distribution limited to U. S. Government agencies only; this report contains information on test and evaluation of military hardware; October 1972; other requests for this document must be referred to Air Force Armament Laboratory (DLGC), Eglin Air Force Base, Florida 32542.

11 SUPPLEMENTARY NOTES
Available in DDC

12. SPONSORING MILITARY ACTIVITY
AFATL(DLGC/Lt. S. C. Braud)
Eglin Air Force Base
Florida 32542

13 ABSTRACT Wind tunnel captive trajectory tests were conducted in the Aerodynamic Wind Tunnel (4T) to investigate the separation characteristics of six stores from the wing pylons and racks of the A-7D aircraft. The stores tested represented possible combinations of munitions to be carried by the A-7D when performing search and rescue missions. Separation trajectory data were obtained for the loaded and expended SUU-23/A gun pod, CBU-12A/A, CBU-46/A LAU-3/A, LAU-68A/A, and the expended CBU-30/A. Trajectories were obtained at Mach numbers from 0.325 to 0.814 with aircraft angle of attack corresponding to level flight at 4000-ft altitude. For selected configurations, data were obtained to assess the influence of changes in the applied ejector forces during separation from the MAU-12B/A pylon rack. The stores separated without contacting the aircraft with only two exceptions. Store-to-pylon contact occurred for the expended SUU-23/A at one Mach number ejector force combination, and the expended LAU-3/A contacted the triple ejection rack for one configuration at one Mach number.

Distribution limited to U. S. Government agencies only; this report contains information on test and evaluation of military hardware; October 1972; other requests for this document must be referred to Air Force Armament Laboratory (DLGC), Eglin Air Force Base, Florida 32542.

DD FORM 1 NOV 65 1473

UNCLASSIFIED

Security Classification

14. KEY WORDS	LINK A		LINK B		LINK C	
	ROLE	WT	ROLE	WT	ROLE	WT
external stores						
trajectories						
separation						
search and rescue						
scale models						
subsonic flow						
Mach number						
angle of attack						

AFSC
Arnold AFS Tenn